AN ABSTRACT OF THE THESIS OF

Luanne R. Ferrell for the degree of
Master of Arts in
Applied Anthropology presented
on October 17, 2006
Title: Prehistoric Patterns of Economic and Technological Behavior Reflected in the 2004 Lithic Assemblage of Site J69E, Espiritu Santo Island, Baja California Sur

Abstract approved: Signature redacted for privacy.

Loren G. Davis

The La Ballena #3 site J69E is a shell midden located on Espiritu Santo Island in Baja California Sur. Archaeological excavations conducted in the summer of 2004 investigated a midden containing lithic and shell artifacts as well as faunal and human remains. Analysis of the debitage and formed lithic tool assemblage collected from the surface of the site and from subsurface levels reveals a record of hunting and gathering practices associated with late Pleistocene to early Holocene age radiocarbon dates.

There are five research goals addressed in this thesis encompassing the characterization of technological behaviors from the 2004 lithic assemblage; evaluating patterns of technology through time; evaluating uses of raw lithic materials; evaluating logistical and economic patterns from the production of lithic tools; and evaluating whether the lithic materials indicate mobility within the island and/or the mainland.

Theoretical approaches that deal with the organization of hunter-gatherer subsistence practices are used in conjunction with the results of lithic analyses to determine patterns of past human behaviors. Determinations of lithic raw material types and provenance within the island landscape were conducted using microscopes and remote sensing techniques. Typological and aggregate analytical methods were used to determine tool production, hunter-gatherer mobility, and site function.

The results of the analyses show that the people inhabiting site J69E emphasized the production of flakes from a variety of core types that were made into expedient flake tools as well as groundstone manufacture. The remote sensing technologies show that the lithic raw materials were being collected from within the area of La Ballena Bay. Together, these data indicate that the hunter-gatherers living in this area practiced forager logistical and subsistence strategies but with relatively low mobility. The practices follow the expected patterns for marine adaptations in the late period Las Palmas culture, which may have had its roots among the early inhabitants of J69E. Adaptations to early maritime environments have not been significant in the New World; however, from this research we can see that the inhabitants successfully adapted to the environments very early.

Prehistoric Patterns of Economic and Technological Behavior Reflected in the 2004 Lithic Assemblage of Site J69E, Espiritu Santo Island, Baja California Sur

by
Luanne R. Ferrell

A THESIS

submitted to

Oregon State University

in partial fulfillment of
the requirements for the
degree of

Master of Arts

Presented October 17, 2006
Commencement June 2007

Master of Arts thesis of Luanne R. Ferrell presented on October 17, 2006

APPROVED:

Signature redacted for privacy.

Major Professor, representing Applied Anthropology

Signature redacted for privacy.

Chair of the Department of Anthropology

Signature redacted for privacy.

Dean of the Graduate School

I understand that my thesis will become part of the permanent collection of Oregon State University libraries. My signature below authorizes release of my thesis to any reader upon request.

Signature redacted for privacy.

Luanne R. Ferrell, Author

ACKNOWLEDGEMENTS

First and foremost I would like to thank my major professor, Dr. Loren Davis. Without all of your constant dedication to this project my work would have been much more difficult. Thank you for showing me all that archaeological research can entail and for allowing me to experience new things, like calamari and eel.

Next I would like to thank Harumi Fujita and all others with INAH for all of the hard work everyone put into allowing our crew to conduct an archaeological project on the island. Your love for archaeology shows through your dedication.

I would like to thank my committee members for helping me through the tough process; Anne Nolin, Carol Caughey, and Brian Tilt.

I would like to say thank you from the bottom of my heart to the crew for helping me to accomplish this project: Fred Anderson, Don Wright, Mike & Todd from the University of Alberta, and Raul.

I would like to thank Bob and Barbra for the cold drinks on the hot days.

I would like to thank my parents, Sam and Connie Houser, for all of your love and support. Without family to help you through the rough times what do you have?

I would like to thank my Grandma Baker for opening my eyes to the world of archaeology and for constantly checking in on me to make sure that I was doing what I was supposed to be doing. You are the best.

Last but not least I would like to thank my husband Keith for everything that you sacrificed to allow me to continue pursuing my dreams. I know that without you I would never have been able to accomplish the amount that I did. Thank you so much and I love you very much.

I would like to finish by saying thank you to all of the kitchen tables out there that lent themselves to me so that I could visit friends and families while keeping on track to finish this thesis.

TABLE OF CONTENTS

TABLE OF CONTENTS (Continued)

Page

LIST OF FIGURES

LIST OF FIGURES (Continued)

Figure Page

LIST OF FIGURES (Continued)

Figure Page

LIST OF FIGURES (Continued)

Figure Page

LIST OF FIGURES (Continued)

Figure Page

LIST OF FIGURES (Continued)

Figure Page

LIST OF TABLES

Prehistoric Patterns of Economic and Technological Behavior Reflected in the 2004 Lithic Assemblage of Site J69E, Espiritu Santo Island, Baja California Sur

Chapter 1: Introduction

People inhabiting the New World during the late Pleistocene and early Holocene are believed to be adapted to inland environments, but the presence of early coastal sites can offer valuable insights into the study of maritime adaptations in the New World. In the past, New World archaeology has not focused on maritime adaptations because of the lack of known early sites, most early coastal sites are beneath the ocean; but with more sites being recovered the idea of early coastal adaptations is being favored.

During the summer of 2004, a team of Oregon State University archaeologists led by Dr. Loren Davis conducted test excavations at site J69E to explore its potential for yielding a late Pleistocene cultural occupation (Davis 2004). During the excavation, various lithic technologies presented themselves. There are a limited number of known coastal archaeological sites with late Pleistocene aged lithic components; therefore, the analysis of this component will improve our understanding of how late Pleistocene to Early Holocene resource economies were organized.

Site J69E is located on Espiritu Santo Island and is a part of the La Ballena #3 Complex. Espiritu Santo Island (Figure 1.1) is approximately 30 km in length and 5 km in width. The latitudinal and longitudinal coordinates for the island are 24.60° N and 110.18° E, located in the Sea of Cortez. Site J69E was discovered during surveys of the island by archaeologists of the Instituto Nacional de Antropologia e Historia (INAH) in 1981. A sample of marine shell collected from the surface of J69E produced a radiocarbon date of 11,284 ±121 BP (Fujita 2002: Table 1) indicating the

potential presence of an early paleocoastal occupation at the site. If this date is correct, site J69E would be one of the earliest sites on the Pacific Coast of the New World.

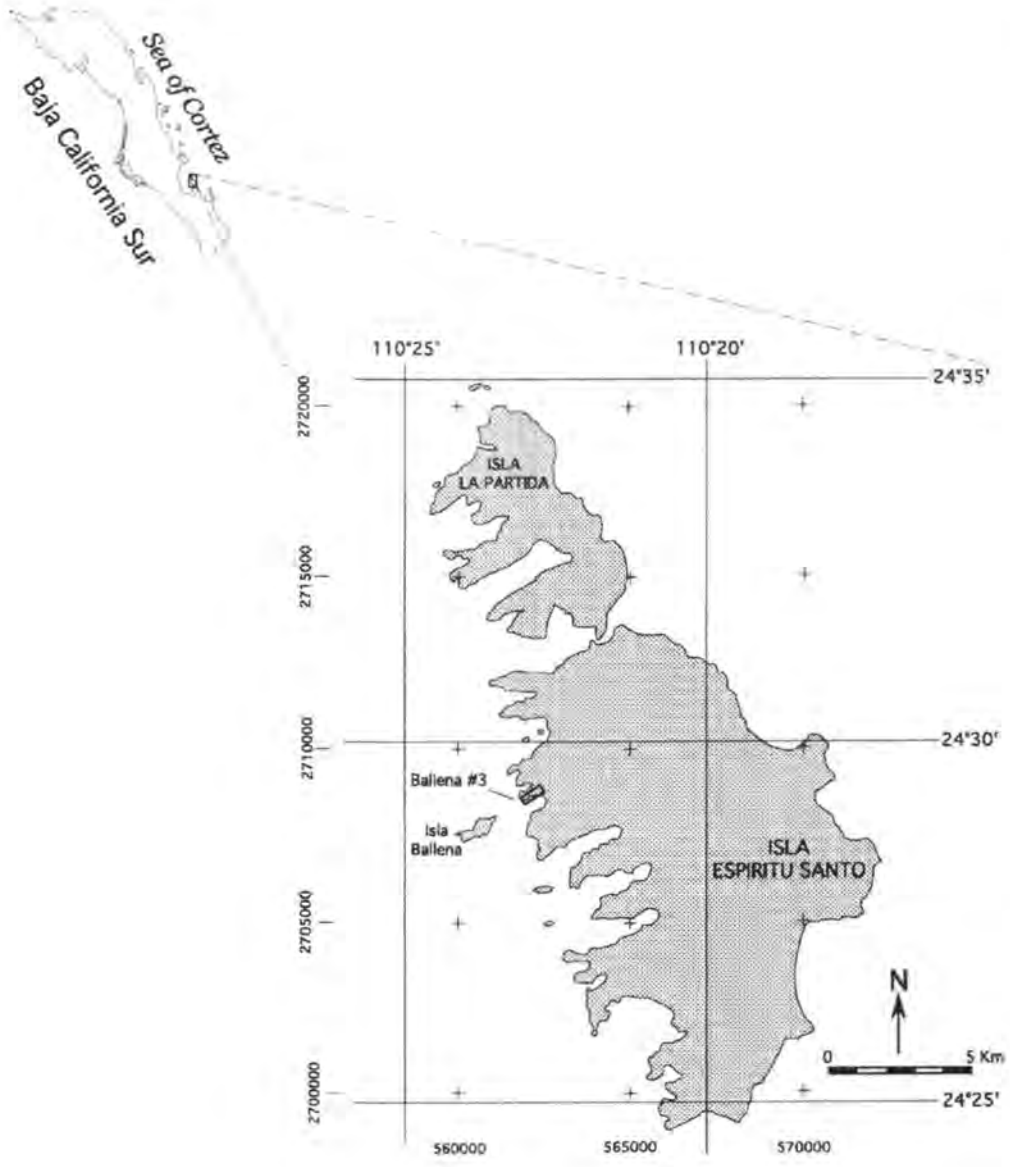

Figure 1.1: Location map of Espiritu Santo Island and the position of the Ballena Complex #3 where site J69E is located.

Additional radiocarbon dates were returned on shells recovered during the 2004 excavations at J69E, which range from 7820 ±70 BP to 8540 ±70 BP (Davis 2006).

This site is important for determining patterns of technology and economic strategies seen in early coastal settings.

Environmental Context of the Cape Region

The Baja California peninsula of NW Mexico includes the states of Baja California and Baja California Sur. The Pacific Ocean borders both states to the west and the Sea of Cortez lies to the east of the peninsula. The geography of the peninsula can be broken into three land surface types: mountains (62.9%), desert plains (21.6%), and coastal plains (15.5%) (INEGI 2004). Baja California Sur is dominated by extensive mountains and deserts containing two highland belts and three lowland areas (Hammond 1954).

The peninsula is mainly composed of different mountain ranges aligned in a northwest-southwest direction, with high basins and uplands. These ranges divide the hydrology of the peninsula towards two different marine systems, the Pacific Ocean and the Sea of Cortez. Due to several complex tectonic events associated with differential movements between the Pacific and North American plates there is a constant northwest trend in the migration of Baja California (Lee 2001).

Baja California Sur's bedrock consists of 42.1% sedimentary rock, 22.6% extrusive volcanic rock, 7.5% intrusive plutonic rock, 3.0% metamorphic rock, and 24.8% unconsolidated sediments (INEGI 2004). There are three series of surface geology units found in the mountain ranges of Baja California Sur, which contain the majority of these bedrock types. The pre-Tertiary basement complex covers the greatest area. It consists of granite and dioritic masses along with various

metamorphic rocks. The Tertiary series is the thickest of the three series and has two known formations. The first formation, known as the Comondu formation, is Miocene in age and consists of accumulations of lavas, tuffs, agglomerates, conglomerates, and sandstones. The second formation, The Salada formation, is Pliocene in age and consists of marine and continental sediments. The third series is comprised of Quaternary alluvium and coastal sediments. This series accounts for most of the unconsolidated sediments in Baja California Sur (Hammond 1954).

The native people of Baja California used a wide range of lithic materials, including rhyolite, basalt, andesite, granite, cherts, metasedimentary, and sedimentary rocks. Some of the materials were traded from other parts of the peninsula and North America while the rest of the lithologies reflect locally available materials (Davis 2005).

The coastal environments during the Pleistocene and Holocene epochs were largely controlled by the fluctuating sea levels. The terrestrial glaciations and subsequent meltwater release during interglacial times accounted for the sea level variation during the last glacial maximum ~18,000 BP. The sea level during this time was 120-135 meters below its modern levels. As the temperatures rose worldwide the terrestrial glaciers began to melt causing the oceans to fill with meltwater. The sea level reached modern levels by 5,000 BP. Unfortunately, most of the Pleistocene coastal environments were submerged under the rising sea levels.

The islands in the Sea of Cortez are comprised of the Comondu formation. This resilient bedrock material has allowed the islands to be a constant scene in the peninsula's coastal landscape during the late Pleistocene to early Holocene periods

(Davis 2005). There are three main types of islands situated in the coastal landscape which include islands that are extensions of the mainland but are separated by shallow waters, islands that are steep peaks of mountain ranges, and islands that are loose marine deposits not connected to any specific terrestrial feature (Johnson and Simian 1997). These island types express varying degrees of habitation of floral, fauna, and humans.

The sea level changes that would have occurred before 5,000 BP would have drastically changed the landscape as well. With little tectonic uplift occurring the rivers on the landscape would have rapidly aggraded their channel fill to compensate for the rising sea level. Because of this many early archaeological sites located in these riverine settings are now deeply buried under meters of river deposits (Punke & Davis 2005). Open sites near the coast are likely to be found in terrestrial deposits that overlie the last interglacial marine terrace and can occur up to 5 meters above sea level (Ortleib 1979).

Wind effects the movement of sediments in marine and terrestrial environments. During the winter, high pressure systems to the north travel down across the axis of the Sea of Cortez toward the equator causing the wind to blow from the north. During the summer months, southerly winds travel from the equator causing lighter, warmer air to be circulated. Currently, the transition between the southerly winds to the northern winds allows for *chubascos*, or tropical cyclones, to move up the Pacific coast of Mexico during late August and September (Carew 1967). Marine cores taken at the mouth of the Gulf of California show that the Gulf basin water began circulating after about 6,000 cal B.P. (Douglas et al. 2003). The presence

or absence of specific species of marine fauna, when seen in the fossil record, may indicate the conditions of the wave and wind actions through time.

The climate of the peninsula is currently hot and dry. Around 10,000 BP, the climate in North America had an overall drying trend. The intermittent glacial periods of the Pleistocene and the formidable rainshadows caused by uplift of the Peninsular Ranges allowed the peninsula to maintain a wetter cooler climate (Hammond 1954). The Cape Region of Baja California was wetter and cooler during the Pleistocene and was supported by populations of crocodiles, green iguanas, and boa constrictors as well as semi-aquatic elephants, green hares and large cats (Lee 2002). Plants found in a packrat midden near Sierra de San Francisco can be associated with cooler wetter climates. The California juniper and other plants such as laurel sumac found in the midden, require a climate that is cooler and wetter than the current climates (Rhode 2002). It is shown that woodlands expanded throughout the lower elevations during Pleistocene climatic conditions (Van Devender 1990).

The vegetation coverage in the coastal setting includes a variety of types. The salt flats contain mangrove thickets, saltbrush (*Atriplex sp.*), pickleweed (*Salicornia pacifica*), iodine bush (*Allenrolfea occidentalis*), and Suaeda (Ritter et al. 1994). Salt flats are areas of saltwater encroachment along the shores. These areas were vegetated with mangroves of varying size and shape growing progressively away from the seawater (Carew 1967). The alluvial soils just beyond the salt flats, allow growth of leguminous trees, cacti, spurge plants, and other vegetation (Ritter et al. 1994). These areas allow the vegetation to grow tall and in close stand with one another (Carew 1967).

The shift to Holocene climatic conditions has altered the landscape in at least four significant ways by: (1) permitting open growth vegetation that minimizes erosion; (2) affecting the nature and rate of the weathering process allowing grain by grain disintegration of bedrock rather than rapid breakdown of rocks into fine fractures; (3) permitting only intermittent streams with some torrential floods in the arroyos; and (4) producing occasional violent agitation of the sea causing shoreline modifications (Hammond 1954).

Like other areas of the New World, Baja California experienced a decline in Rancholabrean fauna at the close of the Pleistocene. Fossil localities in Baja California that have extinct Pleistocene fauna, including horse (*Equus caballus*), bison (*Bison antiquus*), camel (*Camelops hesternus*), mammoth (*Mammuthus columbii*), Ilama (*Hemiauchenia macrocephala*), and a locally extinct form of rabbit (*Sylvilagus bachmani*) (Davis 2005). During the Holocene epoch, the terrestrial fauna found in the records, including jackrabbits, deer, coyotes, mountain sheep, wildcats, squirrels, doves, quail, ducks, geese, vultures, puma, and rattlesnakes, indicates a change in the environment(Carew 1967). The marine fauna are distinctly different for the colder, nutrient rich waters of the Pacific Ocean then it is for the subtropical waters of the Sea of Cortez. Species that are known to inhabit both environment types include seals, sea turtles, sharks, whales, and sea birds (Davis 2005).

The native peoples that lived in the Cape Region of Baja California Sur adapted to the strenuous conditions imposed upon their daily activities. Plants and animals available for consumption were not present year round. The environment would have flourished when water would have been present but would have been

dormant during intense periods of heat and humidity. The people would have needed to move locations to follow food and water resources. Most of the archaeological sites in the Cape Region are found in close vicinity to fresh water areas (Carew 1967).

Previous Archaeological Research in the Cape Region

There are a limited number of studies that have been conducted in the Cape Region of Baja California Sur. There were three main archaeologists throughout the Twentieth century that dedicated their time and energy to the archaeological investigations of the Cape Region. These studies began with Kate's motivations to discover funerary sites along the coast. His fieldwork in Baja California in the early 1880s was regarded as the beginning of academic anthropological research on the peninsula (Hovens 1991:15). He excavated burials on Espiritu Santo Island, and the cities of San Pedro, Zorillo, Ensenada, and Los Martires (Figure 1.2). His investigations revealed a type of burial known as secondary burials, where the corpse was buried to allow the flesh to decompose and then the bones were exhumed, painted with red ocher, and then reburied. Kate sought out to determine the origins of the native peoples. He exhumed seven individuals from the Cape Region and determined them to all belong to a tribe speaking Guaycuruan dialects. After further investigations of the crania he was convinced that the people inhabiting Baja California had Melanesian features (Hovens 1991; Massey 1947). With the discovery of a curious burial system and the variation in skull morphology different from that of most North American populations, a great deal of attention was brought to the area of Baja California Sur.

Many years passed before the next well known archaeologist came to the Cape Region. Massey began studying the Cape Region in the 1940s, almost 50 years after Kate. His discoveries consisted of mapping out the coastal sites along the eastern side of the peninsula and examination of cave burials. During his investigations he discovered many different cultures residing in Baja California. The two cultures that tie closest to the Cape Region are the Las Palmas and the Comondu cultures. The Las Palmas culture was located in the mountainous Cape Region from the Isthmus of La Paz to Cape San Lucas, seen in Figure 1.2 (Massey 1961). This culture was characterized by its use of numerous burial caves. There are a few diagnostic artifacts associated with the Las Palmas culture, which include wooden dart-throwers with hooks carved above the distal end with single bark-loop grips, netting made with lark's head knots, coiled baskets, *Olivella* shell beads, oyster shell ornaments, and spatulate bone pins. The only stone artifacts in association with the Las Palmas burials were "crude percussion flaked core chopping tools" (Massey 1961). These choppers are only found in open coastal middens in the area surrounding La Paz. This stone tool is the only link between the burial caves and the open sites (Carmean and Molto 1991). The lack of lithic materials in the caves, again points to the need for lithic studies to be conducted in the Cape Region. Massey's work concludes with a determination that the people inhabiting the Las Palmas culture area originated from North America or mainland Mexico not Melanesia (Molto and Fujita 1995).

The second culture is the Comondu and they were located in central Baja California. This culture is known for its shallow basin and flat milling stones, along with single hand cobble manos. The lithic technologies present throughout the culture

include tiny triangular obsidian and tuff arrowpoints attached to hardwood shafts. The Comondu culture traits include square knot netting, tubular stone pipes, and woven tump-bands. There are burial caves associated with these artifacts unlike that of the Las Palmas culture where the burials were usually separate from the artifacts (Massey 1961).

Massey's work presented a new outlook into the types of archaeological sites present along the southern portions of Baja California Sur. He excavated shell middens along La Paz Bay and caves along Sierra de Las Cacachiles (Figure 1.2) where he made observations of deep shell deposits, bifaced cobble hammerstones, and plano-convex scrapers. The open air camps near Los Frailes and Cabo Pulmo (Figure 1.2) contained basin milling stones, cobble handstones, and crude flake tools. Projectile points were absent in these sites (Massey 1947).

Massey also noted the ethnographic distribution of the people. There were three aboriginal groups inhabiting southern Baja California: the Guaicura, the Pericu, and the Huchiti (Massey 1947). The Pericu are tied closest with the inhabitants of Espiritu Santo Island (Massey 1949: Figure 1). They are known for their use of spears when fishing.

Figure 1.2: Location map of Baja California Sur showing location of archaeological sites excavated by Massey (Massey 1949).

Missionaries recorded the lifeways of the cultural groups when they arrived in the Californias in the 1750s. Jacob Baegert (1982) described the area as being

equivalent to hell. It was extremely hot and humid with very little shade from the surrounding vegetation and the ground is covered with stones. The inhabitants lived in small bands of 100-200 people, where each group had their own language. The long physical distances between the language groups allowed the separation of the people to continue. Although the languages were different the lifeways seemed to be similar. Each of the groups wore clothes made of plants and animal skins. They hunted small and large game including birds, deer, and rabbit. The people did not farm but instead gathered plants from the local areas and fished using spears and nets. The people were described as being aboriginal because of their simple lifestyles.

Massey has allowed current researchers to reexamine his collections, looking for similarities in the lithic technologies of the various areas of Baja California. In the La Paz region there are three distinct projectile point types: Large La Paz, Medium High-Notched, and Small La Paz. The major difference in the points is in the structure of the stem. The Large and Small La Paz points have contracting stems and/or are tanged. The Medium high notched point contains a notch that is high on the body of the point (Carmean 1994). These are the only known projectile point comparisons for this area.

Harumi Fujita currently contributes to the archaeology of the Cape Region by exploring the adaptations of the people to the changing landscapes. Her investigations have built on the previous research of Massey's discovery that the pre-contact people that were living on Espiritu Santo Island were the Pericu. These people had an adapted life way to the semi-desert environment of the island (Figure 1.3) where they emphasized an economic orientation toward marine shellfish. There were

no permanent river systems on the island or even on the coast of the mainland. The water only flowed during the rainy seasons, which came but once a year and usually at the end of the very dry season. On the island and on parts of the coast there were some estuaries where the Pericu could acquire drinkable water. Most of the time they relied on cisterns to collect water during the rainy seasons. According to Massey the Pericu people had a wide range of food at their disposal. Although they relied heavily on marine resources they also supplemented their diets with terrestrial plants and animals such as pitahaya, antigonon, jojoba, and tubers, insects and grubs, larger mammals (i.e. deer) from the highlands, and smaller mammals (i.e. rabbit) in the lowlands. On Espiritu Santo Island there was a great emphasis on marine resources such as shellfish, fish, and marine mammals. There is evidence that their diets were also supplemented with plants and small mammals (Massey 1955).

Figure 1.3: Images of semi-arid environment and marine environment on Espiritu Santo Island.

The INAH surveys of the island indicate that there are 127 coastal sites (Fujita & Poyatos de Paz 1998). The sites consist of caves and rock shelters, open camps,

shell middens, funerary caves, rock paintings, and trails. The rock shelters are the most frequent of the site types. There are many caves on the west coast of the island. These caves show that the people that were living in them kept the floors flat and clean; however, shell remains, lithic debitage, ash, and charcoal were usually present at the exterior of the caves. This suggests that the people drew a distinction between where they made their tools, where they processed and cooked their food, and where they slept (Fujita & Poyatos de Paz 1998).

Artifacts and faunal materials found at open camp sites reflect behaviors associated with daily activities. The evidence for living areas are rock rings and areas cleared of rocks. Food preparation can be seen in the remains of metates, mortars, manos, and mano/hammers for grinding up seeds from plants, marine mollusks mark the area for preparation, and burnt shells, indicating that fire was used to cook the food. Shell remains along with faunal remains indicate that terrestrial and marine resources were being consumed. Each of the open camp sites are located near water sources; whether an estuary, a tinaja (natural water catchment), a stream, or lagoon. Open sites are located on the sandy beaches and on elevated terraces (Fujita & Poyatos de Paz 1998).

The next site type is termed shell middens. According to Fujita there are two types of shell middens: habitational and non-habitational (1998). Shell middens are located near sandy beaches or rocky beaches, on dunes, or on marine, fluvial, or lake terraces, always positioned close to a source of fresh water. There are 40 species of bivalves and 33 gastropods located around the island; however, not all of these species are found in the island's sites. The major shell species that are found in the sites are

the large rock oyster (*Ostrea fisheri*), the pearl oyster (*Pinctada mazatlanica*), and the *Chama frondosa*. The shell midden sites contain debitage and hearth features but rarely do they contain formed tools such as side scrapers, choppers, metates, and manos (Fujita & Poyatos de Paz 1998).

Four cave sites were found to contain human remains, two of which had human remains that were covered with red ochre. Items such as worked wood, fragmented sea lion bone, bone awls, a pelican whistle, and worked oyster shells were associated with the caves as well. There were various studies conducted on the human skull that was collected, including studies on the dental morphology of the burials revealing that the people of the island were ate foods other than animals due to the caries found on the teeth (Fujita & Poyatos de Paz 1998).

There are two rock painting sites located on the island. They contain geometric figures composed of straight and curved, vertical and diagonally intersecting lines. At both of the sites the figures are painted in red, but at one site the figures are on the outside of the cave while at the other they are on the inside of the cave. Both of the caves have evidence of human occupation (Fujita & Poyatos de Paz 1998).

Lastly an extensive trail system is present on the island's west coast. This system seems to connect each of the different site types to areas where resources were to be collected. The island's system of trails is unique in the Cape Region. Essentially, it connects the living areas to the water resources, the food resources, the caves, and the lithic resources. It is believed by some that the trails mark a race track for the island's prehistoric inhabitants (Fujita & Poyatos de Paz 1998).

The highest concentration of recorded site types, consisting of 19 sites connected by trails, including open camp sites, rock shelters, rock paintings, tinajas (water catchments), and funeral caves lies between the La Ballena Bay and the El Puertecito Bay. A large concentration of sites in this area is called the J69 La Ballena #3 complex, which includes site J69E (Figure 1.3). This complex consists of seven different open camps of varying sizes and contains archaeological evidence for different activities. Many of the camps contain rock rings that are believed to be wind breaks for simple single-family dwellings. There are numerous artifacts found on the surface of each of the open camps. These artifacts include grinding stones, choppers, end and side scrappers, cores, and lithic debitage related to tool manufacturing debris. The major shell species were found at each of the camp locations (Fujita & Poyatos de Paz 1998).

Figure 1.4: Site photo of La Ballena #3 complex, location of campsites A-D are circled. Site E is located beyond the image to the left. View is to the west.

According to Fujita and Poyatos de Paz's study (1998), there is little evidence on the surface of campsite E for sufficient determination of the activities that were taking place there. J69E is the closest site to the fresh water sources on the terrace (Figure 1.4). It is the furthest away from the La Ballena Bay but the first to be reached from the El Puertecito Bay. The trails connecting the sites in the complex pass by J69E but do not connected it to the other sites. It is believed that this site's function is tied closely with its proximity to the two bays.

Figure 1.5: Site photo of La Ballena #3 complex, location of campsite E is circled, tinajas are boxed. Figure 1.4 overlaps slightly on the right of this image. View is to the west.

There are very few early New World coastal sites with extensive lithic components. As a result, we know very little about the technology of early coastal peoples. The activities taking place on Espiritu Santo Island are not fully understood because only a few sites have been fully excavated. A full analysis of the lithic

technology associated with site J69E is greatly needed to develop the comprehension of the early coastal sites of Baja California Sur and to expand our understanding of paleocoastal cultural pattern in the New World.

Goals of the Research

The archaeological research that has been conducted in Baja California Sur has lacked specific details associated with lithic technologies. In order to better understand how people adapted to coastal settings, more research needs to be conducted. The research presented in this thesis will address three themes regarding: 1) the structure of prehistoric technology at J69E; 2) the nature of raw material provenance; and 3) the logistical organization of the sites inhabitants. Five research questions have been formed to examine the research themes. They are as follows:

1) What does a late Pleistocene to early Holocene age lithic assemblage look like in a Baja California Sur coastal setting? And, what can the assemblage tell us about technological behaviors? This question will be answered through typological and aggregate analyses of debitage along with formal and non-formal tool identification and analysis. Then, using middle range theory, conclusions will be drawn as to the behaviors associated with the lithic assemblage.
2) Do the lithic materials from site J69E reflect changes in technology through time? This question will be evaluated by comparing the character of the assemblage between excavation levels using a chi-squared test, distribution maps of tools, and examination of variations in tool counts between levels.

3) What are the distributions of the raw lithic resources on Espiritu Santo Island in proximity to site J69E? This question will be addressed using remote sensing techniques to create land coverage maps of Espiritu Santo Island.
4) What can the lithic assemblage of J69E tell us about the economy of the native inhabitants? This question will be examined by using economic theories in combination with the results from the analyses to determine the activities believed to be taking place at this site.
5) Is there any indication of mobility within the island and/or the mainland that can be seen in the lithic assemblage? This question will use the land coverage maps combined with the parent material analysis to determine locations of possible origins of raw materials for tool production, as well as a comparison of tool types found at the site with locally known tool types.

Chapter 2: Theoretical Background

Middle Range Theory and Hunter-Gatherer Studies

Lewis Binford's (1967) middle range theory is used to link the quantitative data collected from J69E and the human behaviors associated with the manufacture, use and discard of artifacts. Middle range theory follows the idea that analogies occur between the past and the present in the various theoretical contexts. An analogy is information that is derived in one context and used to explain data found in another context, present and past. Archaeologists frequently use analogies to make sense of the materials excavated during the archaeological investigations. For example an object's function may be revealed through modern experimental replication that reveals its best use. Middle range theory allows for arguments to be formed explaining the behaviors associated with materials found in the present. (Johnson 1999; Binford 1967)

Binford describes the middle range to be the area between the static archaeological present and the dynamic cultural past. His argument states that "giving meaning to contemporary patterns is dependent upon an understanding of the processes which operated to bring such patterning to existence" (Binford 1980:1). An analogy is not strictly a demonstration of formal similarities between entities but rather it is an inferential argument based on implied relationships between demonstrably similar entities (Binford 1967). Archaeologists need a solid understanding of the dynamics of cultural adaptations in order to demonstrate the statics that we observe in the archaeological record (Binford 1980).

There is no single clear definition of what middle range theory is and where it originated. Robert Bettinger (1991:63) describes Lewis Binford's theory as having two parts: "(a) how we get from contemporary facts to statements about the past; and (b) how we convert the observationally static facts of the archaeological record to statements of the dynamics". D.H. Thomas sees the middle range theory as a tool to "bridge the gap between the known, observable archaeological contexts and the unknown, unobservable systemic context... mid-range theory is necessary to provide relevance and meaning to the archaeological objects" (Bettinger 1991:62). Raab and Goodyear (1984:257) explain middle range theory "as providing a logical link between relatively low-order empirical generalizations and comparatively high-order theories".

In the practice of archaeology we make assumptions about the behavioral relationships between the static and the dynamic states. This theoretical concept serves as a bridge between the static facts of the archaeological record and the behavior that produced them. The middle range theory is intended to be used in conjunction with other theories. It was never meant to stand alone as a single theory but as a part of a larger theory building concept (Raab & Goodyear 1984). It is this reasoning that the middle range theory is used here with optimal theories for hunter-gatherers.

Binford uses middle range theory to explain hunter-gatherer organizational patterning based on environmental variables. In a study of Alaskan native cultures, Binford (1980) introduced a conceptual model of logistical organization among hunter-gatherers. In this model, hunter-gatherers logistical strategies range between

two extremes, occupied by *collectors* at one end and *foragers* at the other. Collectors and foragers organize their technological and settlement patterns in order to solve environmental pressures in different ways. If the environment was productive and contained resources that were both spatially and temporally homogeneous, widespread resources would be readily available for immediate consumption, requiring a technological and settlement system with relatively low complexity. In environments that include seasonal shortfalls in resource availability, more complex strategies are required of its hunter-gatherers. These challenges differentiate the foragers from the collectors. The best way to compare the organization of the collectors versus the foragers is by understanding the different environments associated with each adaptive strategy (Binford 1980; Bettinger 1991).

Foragers occupy environments with low interseasonal variability in subsistence resources producing a pattern wherein key resources are abundant and more or less continuously available throughout the year (Binford 1980). These strategies are typically associated with areas that are largely undifferentiated because resources are readily available; foragers do not store food in bulk quantities for delayed consumption but rather gather foods daily. Foragers maintain a high residential mobility and creating two site types in the process much include residential base camps and location sites. Residential base camps are places where the groups of people depart to obtain food and raw materials and then return to for processing, manufacturing, and maintenance of gathered materials and equipment. Location sites are places where people acquire food and raw materials (Binford 1990). The size of the foraging group in the residential camp is determined by the productivity of the

land. The greater the variety and density of resources, the more people can be supported at any given time. If the resources become exhausted or greatly reduced the group separates into smaller groups and creates new residential camps in areas that can supportive their new size (Binford 1980). Foragers consume resources that are within a few hours walk of the residential camp and therefore maintain a lifestyle without the need for storage.

The technology associated with the foraging system is typically termed "expedient". Expedient technology includes formal and non-formal tool types that are manufactured, used, and discarded according to momentary needs. They are technologically simpler and show a lower degree of complexity that formal tools (Bamforth 1986). Classifying a collection of tools as expedient is useful in describing important aspects of technological behavior. The tools are manufactured to be utilized for unknown activities and in varying situations. Some examples of expedient tools are modified flakes, unifaces, and bifaces.

Under a collector system, hunters and gatherers organize themselves into special task groups in order to exploit a particular resource at a specific time and place. Collectors differ from foragers in that they store their food for at least part of the year and they have organized food procurement parties where specific resources are acquired in bulk quantities (Binford 1980). Their resources are typically unevenly distributed across the landscape and vary seasonally causing the collectors to maintain high logistical mobility with low residential mobility. Collectors maintain the residential and location sites seen in the foraging pattern but add to it various field camps including: base camps for the task groups, caches for bulk resources and

equipment, and stations for gathering information regarding resources (Binford 1980). The specialized task groups that are sent out from the residential camps will seek to procure specific resources from a known resource area. Field camps are usually occupied for short periods of time and show evidence of specific tasks taking place such as hunting and processing of a single resource. The collector system has adapted to a continuously changing environment type where food and other resources for subsistence are not always readily available year round. Storing food allows people to deal with seasonal extremes throughout the changing years.

Technology associated with the collector system is more specialized than in the forager pattern. The collector toolkit contains items designed for use of specific resources by specialized task groups. Many of the tools are prepared ahead of time, often during the off-season, and stored for future use. This leaves more time and energy for hunting and gatherering practices during the peak seasons (Bettinger 1991; Binford 1980). Some archaeological patterns associated with collector systems are equipment caches, high quantities of late stage reduction debitage (pressure flakes), and high percentages of formal tools. Understanding how hunter-gatherers organize their subsistence practices and knowing how they interact with the surrounding environment allow for a greater understanding of the behaviors associated with the technologies presented in the archaeological record (Bettinger 1991).

Economic Anthropology

The study of economic anthropology is associated with the discipline of cultural anthropology. In the past two decades, archaeology has begun to play a role

in the development of new ideas and concepts in economic anthropology. Archaeology adds a temporal dimension to the study of economies in the present and in the past and provides the means to describe the economic structures of specific prehistoric communities and it enables us to understand the long term development of human economic behaviors. Technological and environmental data that are acquired through archaeological fieldwork most closely ties with the economy of the people. Materials that are most often found in an archaeological site are of a technological nature and usually aid in describing the cultural aspects of the people that once lived on the land. Many aspects of a culture can be discovered through the technological remains in an archaeological site, such as "how things were made, what raw materials were used, whether goods were obtained through trade, what people did for a living, how they were clothed and sheltered, whether there was craft specialization, and so on"(Gabel 1968:8).

A variety of site types tell different stories about the associated human behaviors. Quarry sites tell a different part of the story than do ceremonial burial sites. Generally speaking, the settlement sites of prehistoric people contain the majority of the data of economic interest because they are not specialty sites and therefore present a broader view of daily life. The idea of economic anthropology in archaeology means that the archaeologist must do more than just collect and analyze artifacts. They must go further into describing the patterns that are seen in the sites as well as the prehistoric climates, flora, and fauna.

According to Donald Mitchell and Leland Donald (1988:293), "the economic sector of a culture is taken to include all aspects of the production, distribution, and

consumption of goods and services". In their studies along the Northwest Coast of North America, Mitchell and Donald (1988) studied residential units, resources, units of production, and units of consumption to describe the economies of the various Northwest Coast tribes. Each one of the various units could be used as a single unit to describe one or two aspects of the economy but altogether they describe the entire economic basis for the region. The units of production section describes how families are separated to fulfill the production needs of the group, the gender differences within the division of labor for production, how slave labor played a role in production, and craft specialization. These four segregations for units of production help to describe how the production of the group was key to its economic basis. The economy of the individual families relied on the amount of people and the knowledge of those people to produce the items needed for survival. This can been seen in the archaeological record through such things as housing systems for sizes of families and the amount of families in each group, areas where specific activities were taking place such as tool manufacturing, and evidence of basketry and collecting materials needed for foraging. The interpretations of the materials that are left behind as the archaeological record are based on theories. These theories allow one to interpret the archaeological record. Once those interpretations have been made the economy of the culture can be determined (Mitchell and Donald 1988).

The next case study examines the intensification of hunter-gatherer economies. Paul Bouey (1987) examines the subsistence patterns of the Warm Springs region. He used these units to describe what would be seen in the archaeological record that would indicate that an intensification of the economy was taking place for the region.

He describes the idea of balancing out the currency expended (energy) with the reward (the amount of the currency a unit of the resource represents). The cost is based on the "search time" (the time required to find a resource) and the "handling time" (the time required to pursue, capture, and process the resource). The food resources that are at the top of the society's productivity list would be the ones that produce the least amount of currency expended. This is the same with the tools that are manufactured for the production of food products. The amount of energy that goes into tool manufacture must be less then the "search time" and the "handling time". There are three things that go into the making of a tool: 1) the raw material, 2) the energy, and 3) the knowledge of tool manufacture. The further the people were traveling to acquire the raw material the greater the energy they were planning on expending during the hunt. People used the resources that were close for short term uses and then disposed of them as soon as they broke. This economic basis for a subsistence pattern shows that people were willing to expend the needed energy when the outcome was greater then the original energy needed. An archaeologist might find a great deal of raw materials that are found close to the site in areas where the people didn't need to expend the energy to gather materials from further away. They might find nicely crafted stone tools made of materials from a great distance in areas where the materials are sparse or in areas where the materials were not suitable for hunting. The actual tool that is being crafted would depend on the amount of energy needed to acquire the raw material. The material that comes from the quarry around the corner might be suitable only for short term tools where as the material that comes from a great distance would be handled with much greater importance and nicely crafted tools

would be the product of the tool manufacture. It all comes down the currency expended, or the amount of energy needed to produce something (Bouey 1987).

Here I have discussed two different examples of how economic studies have encompassed archaeological studies. In both cases the authors have used more than one area of interest to examine the entire economic basis for a society. An area of interest will be used to answer the questions of determining economies or aspects of economies based on lithic technologies. These two examples shed some light onto the approach that is needed to answer such a question. The role that lithics play in an economy can be determined through energy expended and through units of production.

Chapter 3: Methodology

Field Methods

In 2004, a grid system was created over 25 square meters of site J69E to establish spatial control for excavations. The baseline for the grid system was oriented along and north-south axis on the eastern side of the site. A Cartesian system was used arbitrarily to determine that the southern most point of the line would have the designation of 100N 100E. Within this grid system we excavated five square meters and conducted surface collection in 16, 1 x 1 m^2 units. The location of these units was determined from two factors: soil depth and location of artifacts and human remains found in the previous surveys of the site. The excavation and collection units were confined to a 4 x 5 meter section located between 110N & 90E. These units were labeled A through T (units P, Q, S, & T were not sampled) (Figure 3.1). All of the surface materials were collected from the 16 units. Excavated sediments were screened through 3mm mesh and placed into bags labeled with the unit and level information. Within each level bag, materials were further separated into bags for shells, lithics, and bone. Each unit was excavated in arbitrary ten centimeter intervals of depth relative to a unit line level datum using brush and trowel.

Within the excavation processes, bones and formed artifacts were recovered in situ. The remainder of the materials were recovered in the screen and placed in their level bags. Unit sheets were filled out during and after all levels and units were completed and pictures were taken at the end of each level. Horizontal measurements were taken relative to the Cartesian grid. Due to the large quantities of marine shell

recovered, only those pieces that had diagnostic attributes (e.g. the hinge on a bivalve) were collected.

Unit A N113 E86	Unit B N113 E87	Unit C N113 E88	Unit D N113 E89	Unit E N113 E90
Unit F N112 E86	Unit G N112 E87	**Unit H** **N112** **E88**	**Unit I** **N112** **E89**	**Unit J** **N112** **E90**
Unit K N111 E86	Unit L N111 E87	**Unit M** **N111** **E88**	**Unit N** **N111** **E89**	**Unit O** **N111** **E90**
Unit P (not sampled)	Unit Q (not sampled)	**Unit R** **N110** **E 87**	Unit S (not sampled)	Unit T (not sampled)

Figure 3.1: Diagram showing the placement of the surface collection and excavation units at site J69E. Excavated units are in bold text.

Remote Sensing in Archaeology

The objective of acquiring the remotely sensed data was to create a land coverage map of the island for utilization in geologic mapping. This method creates a visual representation of the various geologic landforms present in the immediate area of site J69E and allows for interpretations of the landscape. The information acquired from these maps, such as locations of raw lithic materials, allows archaeologists to better understand site formation processes and site function.

Espiritu Santo Island is comprised of numerous igneous flows that trend in a southwesterly direction, originating from fault lines located near the center of the island. Remotely sensed data was acquired to determine the distribution of the

igneous flows and the locations of the lithic resources used in tool production at site J69E.

The remotely sensed data was acquired from the Advanced Spaceborn Thermal Emissions and Reflectance Radiometer (ASTER) sensor onboard the Terra satellite. The image that was acquired over Espiritu Santo Island was ASTER L1B registered radiance at the sensor. The satellite image was acquired on 07 June 2002 at 18:06:59.02 (Figure 3.2) from the ASTER website acquisition database. Even though ASTER has 14 bands available, nine bands, each associated with a different part of the visible and non-visible light spectrum, have been collected for this study. The purpose of this was to use only those bands that would be useful for this study and bands 10-14 contain information about the thermal part of the spectrum something which is not useful for this study. Bands 1-3 contain a spatial resolution of 15 meters. Bands 4-9 contain a spatial resolution of 30 meters. These bands are in 8 bit quantization (ASTER 2003).

The first step in this process was to create an image that allowed for examination of the distinction between the geology and the vegetation. The Normalized Difference Vegetation Index (NDVI) is used to map vegetation. The equation used to evaluate the image is:

$$NDVI = \frac{reflectance_{nir} - reflectance_{red}}{reflectance_{nir} + reflectance_{red}}$$

The brighter values in the image are vegetation and the darker values are the geologic formations. The NDVI image is the reference point for the remaining images created. All of the remaining images were linked to this image when choosing subset areas (Jensen 2005).

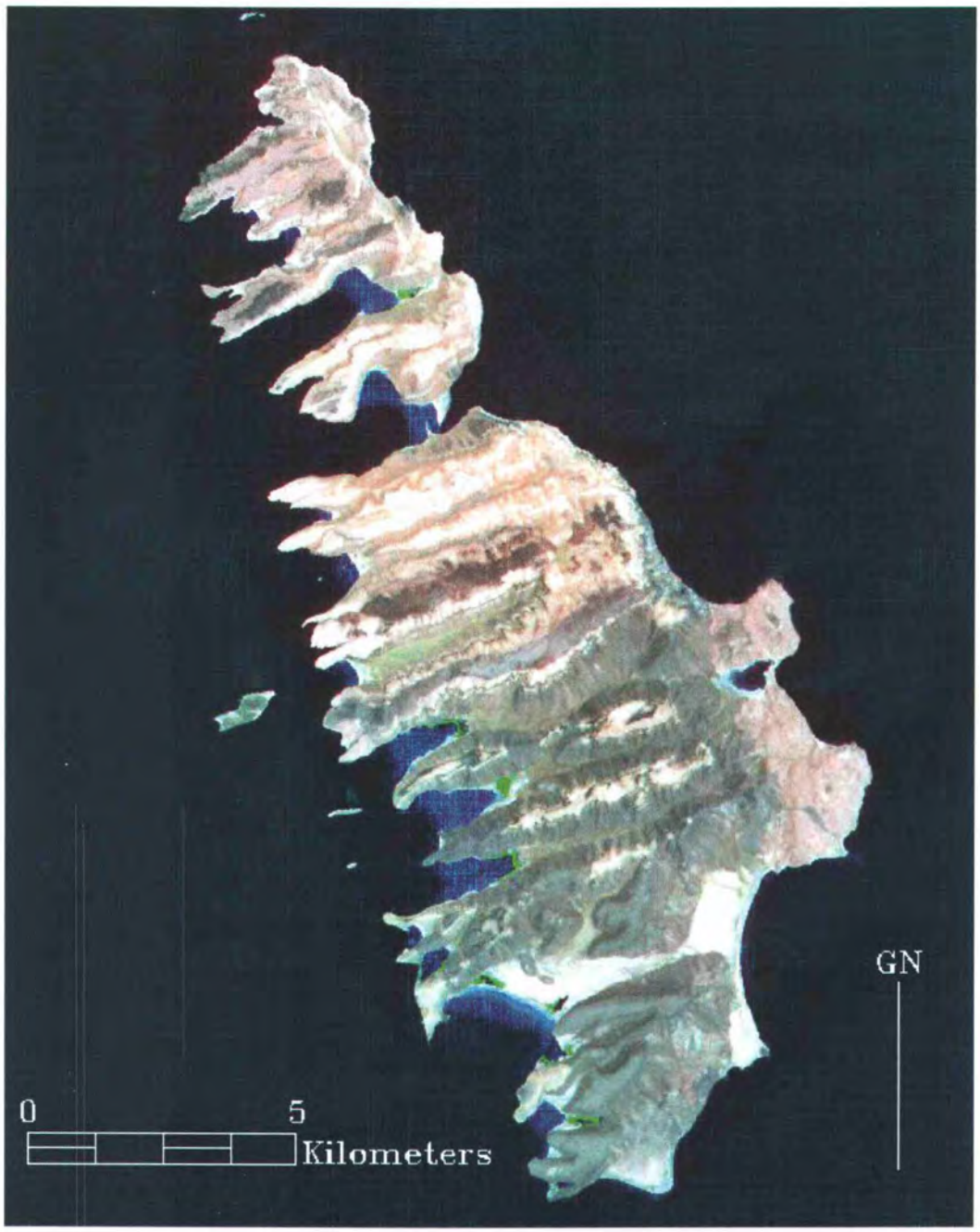

Figure 3.2: ASTER Satellite Imagery of Espiritu Santo Island. (*GN= magnetic north)

There were multiple steps in creating the final image for interpretation. Layer stacking was used to connect the two varying spatial resolution sets of bands together into 30 meter spatial resolution so that all of the bands could be used together as one

unit. The next step was to perform a relative radiometric atmospheric correction. This was accomplished using single-image normalization (Jensen 2005). This technique requires the analyst to determine the minimum values for the visible region of the desired scene using histograms. This was done by subsetting the image to eliminate the noise that was on the corners of the original image and then run the statistics function in the ENVI program to calculate the lowest brightness value for each band. The atmospheric effects correction algorithm (output $_{BVi,j,k}$ = input $BV_{i,j,k}$ – bias) is used to subtract the atmospheric noise out of the bands. This algorithm corrects the minimum values to zero, showing reflectance at the surface instead of the radiance at the sensor (Jensen 2005).

The next task was to classify the image. This method classifies all of the brightness values into categories. There are two methods for doing this: supervised and unsupervised. Both methods were used for this particular examination because each one uses a different selective style for the information (Jensen 2005).

The supervised method, termed Maximum Likelihood Classification Algorithm, uses probabilities to calculate useful land coverage maps. The algorithm calculates the probability of a pixel belonging to each of a predefined set of classes, and then assigns the pixel to the class for which the probability is the highest. The analyst chose the categories for the computer to classify based on their knowledge of the geologic coverage of the island and the NDVI image created to determine where the vegetation lies on the island. For this, eight probability classes are chosen in to which all of the pixels fall. These classes are andesite, light rhyolite, dark rhyolite, basalt, beach sand, Sea of Cortez, vegetation, and granite. Once pixels are chosen for

each class, the algorithm computes the probability of the mean values for each training area to determine placement of the remaining pixels based on the brightness values for the pixels that were chosen by the analyst. The specific supervised classification method used for this analysis takes the maximum likelihood of each brightness value and assigns the probability classes based on the mean values for each set of pixels (Jensen 2005).

The second method used was unsupervised classification where statistical clustering separates the categories. The method chosen for this classification was the Iterative Self-Organizing Data Analysis Technique (ISODATA). ISODATA is self-organizing because it requires little human input for it to run its calculations. There are a few criteria that the analyst must setup prior to running the calculations: maximum number of clusters, maximum percentage of pixels whose class values are allowed to be unchanged between iterations, maximum number of times ISODATA is to classify pixels and recalculate cluster mean vectors, minimum members in a cluster, maximum standard deviation, split separation value, and minimum distance between cluster means. The first iteration is made, where each pixel is compared to each cluster mean and assigned to the cluster whose mean is closest in distance. This process is repeated adding in the criteria setup by the analyst until meaningful mean vectors are established and a useful land coverage map is created. The maximum likelihood classification is different in that the computer puts the pixels into the classes that are predetermined by the analyst. Each one of these classifications produced a different land cover map. The maximum likelihood classification was used for the final interpretation based on the presumed accuracy of the classes (Jensen 2005).

The final step in this process was to spatially subset the image to the La Ballena Bay. Mapping out the land coverage of the bay in which the people living at the site would have inhabited, allows for a greater understanding of the economies associated with the land. Rock samples were collected from this cove in 2004. These samples were identified and classified. The geologic formation of the La Ballena Bay was then mapped out using the GPS longitudinal and latitudinal points that were acquired at the time of the gathering of the hand samples. Information acquired for this process allows land coverage maps of the island and the bay to be developed, along with distribution maps of the lithic materials that were found at the site, and draw some conclusions as to where the people were choosing to acquire the materials needed for hunting and gathering practices (Jensen 2005).

Remotely sensed images provide contextual data and help describe the landscape in areas that were not accessible while visiting the island. Using the techniques described above it was possible to determine where the different lithic types were present on the landscape and what their relationship to the site would be. These relationships are important to answering the questions of where are the lithic resources located on the landscape. Knowing how far away people were traveling to acquire the materials necessary for their cultural activities can help to explain the economic function of the site (i.e. foragers versus collectors).

Analytical Methods

Debitage Analysis

Debitage analysis is used in archaeological studies to understand past human behaviors. There are three main categories of debitage analysis 1) attribute, 2) typological, and 3) aggregate, all of which use statistical methods to characterize the assemblages (Andrefsky 2004). Only aggregate and typological analyses were conducted on this debitage assemblage due to time constraints.

Initially, debitage was sorted by parent material. Classification systems were set into place for determining lithic material types. There were 10 material classifications determined for the parent materials based on color and other morphological attributes (e.g. groundmass, crystal size). These classifications were: light rhyolite, dark rhyolite, glassy rhyolite, green rhyolite, red rock (rhyolite), quartz, quartzite, cryptocrystalline silica, basalt, and andesite. Hand samples were collected to represent each of these material types. These samples were analyzed by Brian Young, a graduate student at Oregon State University, using microscopes to determine exact material types. The remainder of lithic artifact analyses were conducted on each of the different raw material types.

In the manufacturing of stone tools there are many processes that take place. In order to identify which pieces in the assemblage connects with which process there are a few analyses that can be performed to classify the assemblage. In the process of manufacturing a stone tool there are four basic techniques that can be used to shape the stone into a desired form. The first is percussion flaking. This technique involves the removal of small chips of stone off the place that is being shaped into a tool by

hitting it with another object. The next technique is pecking which involves battering or pulverizing the stone with a hard object to remove portions of the piece surface until eventually the piece reaches the desired form. The third technique is grinding which involves the application of an abrasive material to gradually grind or wear away the unwanted portions of the lithic piece. The last technique is to use a sawing motion that uses sharp stone, abrasive stone, or even metal to cut off a large piece of stone to shape the piece. Most lithic materials cannot be subjected to all four of the techniques. Those materials that are flaked easily cannot usually be worked by pecking because they shatter rather than pulverize (Kooyman 2004).

Typological analysis is used to classify individual pieces of debitage into different technological or functional meanings. For instance, we have used the stage of reduction as the technological meaning of our typological classifications (Andrefsky 2001). Two typological analyses were used on the debitage assemblage. The first is termed triple cortex typology. This technique is based on stage reduction of the debitage where there are underlining assumptions that the technological origins of individual artifacts can be determined from combinations of key attributes alone. This analysis involves identifying the amount of dorsal cortex found on the debitage as a way of determining the reduction stages or sequence of reduction. Lithic tool production is a reductive process where cortex bearing flakes are associated with initial stages of lithic production and are absent in late stage tool manufacture. In this analysis the debitage was assigned to one of three categories: 1) interior- represents a flake that has no noticeable dorsal cortex remaining; 2) secondary- represents a flake that has 1-50% of the dorsal cortex remaining; and 3) primary- represents a flake that

has more than 50% of the dorsal cortex remaining. The total number of flakes in each category was noted. There are some methodological problems with the reduction stage approach to classifying a debitage collection in terms of its link to behaviors; therefore, the free-standing typology is used as another way of approaching the same individual artifacts (Sullivan & Rozen 1985).

The second typological analysis is the free-standing typology. This analysis seeks to classify individual flakes based on a hierarchical key. This key is based on three dimensions of variability observed on debitage pieces: the single interior surface; the point of applied force; and the margins. Based on these dimensions, debitage are assigned to one of four mutually exclusive categories (Figure 3.3). The first category involves determination of a discernable single internal (ventral) surface indicated by a positive percussion feature. This includes ripple marks, force lines, or a bulb of percussion. If the features are not reliably determined or if there are multiple occurrences of the features then a single interior surface cannot be determined and the debitage is therefore considered debris. Following the hierarchical key, the second step would be to examine if there is a point of applied force or platform. If there is no platform present on the surface then the flake falls under the category of flake fragment. Fragmented or complete platforms lead us to determining if the margins are intact. This is done by examining the flake to see if the distal end exhibits a hinge or a feathered termination. If there are no intact margins then the flake is considered broken. If the margins are intact then the flake is complete. These four categories are considered to be interpretation-free because they are not linked to a particular method

of technological production nor do they imply a particular reduction sequence (Sullivan & Rozen 1985).

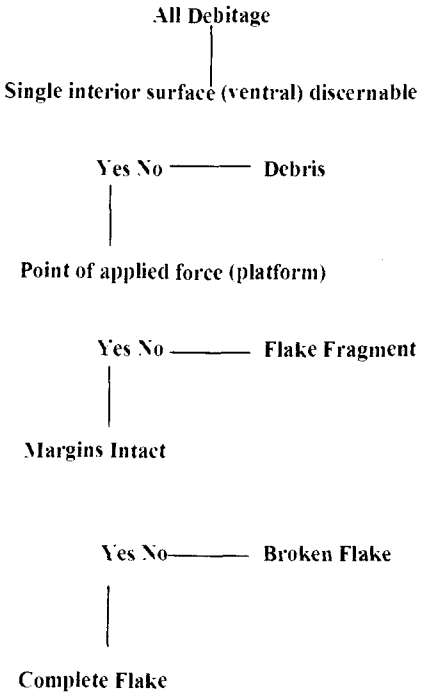

Figure 3.3: Technological attribute key used to define four debitage categories in Free-standing analysis.

Third and the last method of debitage analysis used here is called aggregate analysis. Aggregate analysis is used to stratify the entire assemblage of debitage by a uniform criteria, enabling a comparison of the relative proportions of debitage in each stratum (Andrefsky 2001:3). Aggregate analysis can be defined as "any technique that uses non-technological criteria to subdivide the entire assemblage before considering the technology of the assemblage as a whole" (Carr and Bradbury 2004:17). The debitage assemblage studied here was divided into stratified categories of size and weight. To separate aggregates of size, the size of each of the pieces of debitage were calculated using a series of concentric circles, which was used to divide the debitage

into seven size categories ranging from 1-6+ cm (Figure 3.4). The individual size of each piece was not noted but the amount of pieces that fall into each category was. These categories allowed us to examine the distribution of the debitage in relation to size. The size of the debitage is related to technology because artifact production is a reductive process where the size of the debitage produced from the process generally becomes progressively smaller as the artifact nears completion. Interpretations can be drawn from the amount of larger versus smaller flakes found in the assemblage (Andrefsky 2004:3).

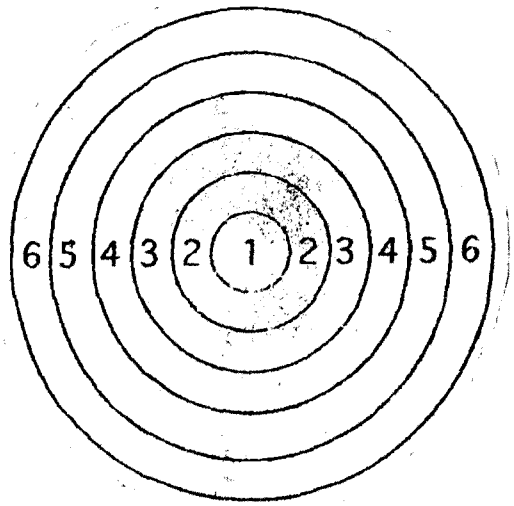

Figure 3.4: Set of concentric circles used for size categories in aggregate analysis.

The second part of the aggregate analysis involves separation of the debitage by weight categories. In this method each piece of debitage was weight and placed into one of 11 categories of weight (g) ranging from 0.1-0.2, 0.3-0.4, 0.5-0.6, 0.7-0.8,

0.9-1.0, 1.1-1.2, 1.3-1.4, 1.5-1.6, 1.7-1.8, 1.9-2.0, 2.1+. Size and weight aggregates were established for debitage by unit, level, and parent material. This information is useful in determining differences and similarities within the population and can be used to make interpretations about the mode of lithic reduction. The aggregate analyses are conducted for three reasons based on: "replicability, effectiveness in examining large assemblages, and the reductive nature of stone tool manufacture" (Carr & Bradbury 2004:21) to which they can be related.

Formal and Non-formal Tool Analysis

Analyses of the formed lithic tools examined many of the same features as the debitage analyses but with an emphasis on technological production and tool function. The tools were broken down into five forms: biface, uniface, cores, modified flakes, and ground stone. There is a recognizable morphology for each major type of tool. Descriptive attributes were used to describe and greater classify the tools within there forms (Kooyman 2004).

The biface analysis describes basic attributes of the tool but with more details. A biface also has manufacturing flaking that extends over all or almost all of both faces of the tool (Kooyman 2004). A flow chart was used to identify each specimen into biface types (Figure 3.5). There are four types of bifaces: 1) blank, 2) perform I, 3) perform II, and 4) finished. Once a determination of the biface type is made all of the specimens were measured, with calipers to the nearest millimeter, for their maximum length, maximum width, and maximum thickness. Then the weight was

measured to the nearest tenth of a gram. The edge angle was measured by tracing the slope of the modified edge and then using a protractor to determine the angle of that line. The material type was determined and comments were identified such as the flaking pattern (collateral, random), the cross-section, the presence of edge grinding, the presence of breakage and the location, and the presence of heat treatment.

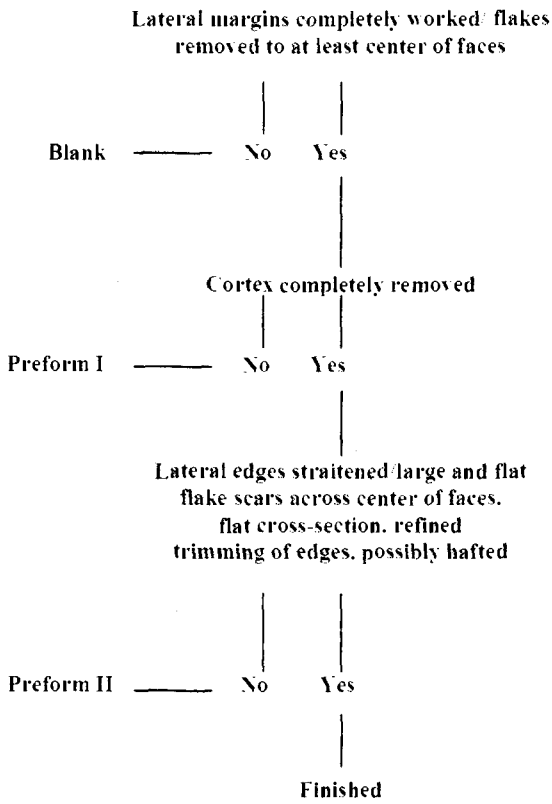

Figure 3.5: Flow chart for determining biface placement in manufacturing process (Andrefsky 2001).

The uniface analysis was used to describe the basic attributes of the tool. A uniface has manufacturing flaking extending over all or almost all of one face (Kooyman 2004). Data on the maximum length, maximum width, and the maximum thickness were collected for the analysis; again this was done using the calipers to the nearest millimeter. The weight was noted to the nearest tenth of a gram. Then the

angle of the worked edge was also determined. For this we used a range of values because the edge that was worked had a variety of angles present on the continuous surface so the smallest and the largest angles were determined. The material that the tool was made of was noted. Lastly, a descriptive analysis of the uniface was conducted by noting the flaking pattern on of the tool (e.g. collateral, random), the cross-section shape, the presence of edge grinding, the presence of breakage and location, and the presence of heat treatment.

Cores are pieces of lithic material from which flakes have been removed which the intention of using those flakes as the starting point for tools. We collected information about the maximum length, maximum width, and the maximum thickness to the nearest millimeter. Then we measured all of the artifacts to the nearest tenth of a gram. Anything that weighed over 200 grams was labeled as 200+. The direction to which flakes were driven off of the core was noted as unidirectional or multidirectional. The amount of cortex that remained on the core was noted as falling in a range of values between <5-50+ percent. Then we noted if there was a presence of platform grinding and finally the material type was noted. There are two basic categories for the cores. The cores from J69E can be classified as prepared or unprepared and as unidirectional or bidirectional. These classifications can indicate the use of the cores and their relationship to other parts of the technological system.

Modified flakes are flakes removed from a core that have been utilized for some function and can be classified into two basic forms: utilized and edge modified. The difference between the two is that the utilized flakes are those that basically are an unmodified flake or piece of shatter that has a naturally appropriate edges used for

some task. The edge modified flakes have been retouched or shaped for some task (Kooyman 2004). The edge modified flake analysis consisted of taking measurements and classifying flake attributes into typologies. The first section of this analysis was to measure the maximum length, the maximum width, and the maximum thickness. The measurements were taken using calipers to the nearest millimeter. Once this was done then the weight was measured in tenth of a gram. The triple cortex analysis was conducted on each modified flake by placing them into the categories of primary, secondary, or interior flakes. Then the free-standing typology was conducted on the modified flakes. This placed all of the flakes into the categories of complete, broken, fragment, or debris flakes. The next step determined the number of worked edges and the location of the worked edge on the flake. To do this, the flake is placed with the dorsal side facing up and the proximal end oriented away. The tool edge shape was classified as concave, convex, or straight. Close examination reveals whether the flake had been modified on one surface (uni-marginal) or both surfaces (bi-marginal). The angle formed by the two converging faces is of major functional significance. The angle is measured between 0 and 90°. A scraping tool would have a steep edge while a cutting tool would have a sharp edge. Based on Wilmsen's (1968) study on angles of lithic tools it was found that scrapers have angles between 66-75°, knives have an angle between 26-35°, and saws have an angle of 46-55° (Kooyman 2004). The form of the retouched edge was described as either continuous or clustered. A continuous surface has modified edges that extend along the side of the flake. The clustered surface has modification in separate sections down the side of the flake. Lastly, a classification of parent material type was made.

Morphological aspects of groundstone artifacts were also analyzed. Here we measured the maximum length, maximum width, and maximum thickness of each piece with calipers to the nearest millimeter. Then we measured the weight of the stone to the nearest tenth of a gram. The material type was noted. The location of the utilization was also noted. Any characteristics about the groundstone item that made it different from all the rest were described. The presence and form of abrasive surfaces or crushed areas were noted and largely form the basis for determining the function of the groundstone item. If the material has a surface that is battered or crushed then it was previously used as a fabricator (e.g. hammerstone). If the utilized surface is smoothed and discolored then it would have probably been used as a food processor (e.g. metate). The absence of a comfortable holding surface on any of the groundstone indicates that the tool was not intended for intensive use. The predominantly expediently design, lightly worn, and has only one utilized surface indicates a short term settlement (Adams 2002).

Chapter 4: Results

Raw Materials

Of the 10 types of lithic raw material identified from the site assemblage, rhyolite was the most abundant lithology, comprising 89% of all materials by count (Figure 4.1). The remaining lithic resources accounted for less then 3% each of the sample and include quartzite, quartz, cryptocrystalline silicate, basalt, andesite, and unidentified red rock.

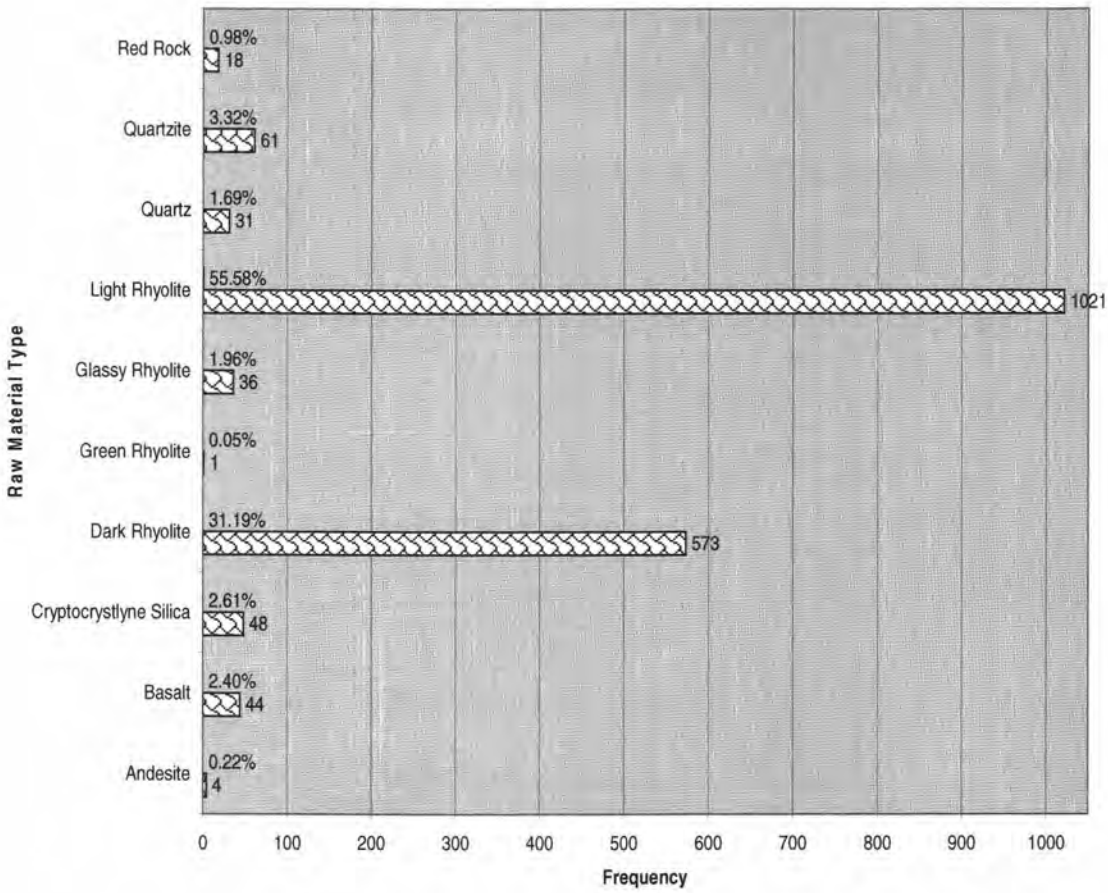

Figure 4.1: Parent material frequencies and percentages determined for J69E.

The main lithic resource type is rhyolite. There are five categories of rhyolite that were seen at the site: light, dark, glassy, red, and green. The light rhyolite was of major importance in the lithic technology at J69E. This material usually appears in a white to pinkish color and contains medium sized crystals of quartz and sanidine, and higher temperature potassium feldspar (Sen 2001: 247). Rhyolites are typically very fine grained and can have excellent flaking qualtities. In this case the rhyolites, all of the different types, have larger crystals within the finer base structure. This is due to the way that the lava cooled. It is believed that the lava began to cool within the earth's surface and then was forced to the surface without time to reheat and melt the crystals that had already formed. The different colors indicate different flows of lava. These various flows have different appearances because they contain varying amounts of trace elements. This causes them to have different strengths within their structures. In other words because of the mineral variations the light rhyolite seems to hold up better in the tool manufacturing than the other rhyolites but this does not exclude the other material types from being used (Sen 2001).

The next resource is basalt. This material was found most frequently as fire-cracked rock and secondarily as groundstone. Basalt is made of plagioclase, silica, and pyroxene. Basalt consists of fine grained minerals with a fine grained matrix creating a rock that is fairly solid but contains minerals that weather easily. This weathering process naturally breaks down the rock and creates talus slopes, making it easier to acquire for tool manufacture (Sen 2001).

The next set of resources is formed from a single mineral. Quartz, quartzite, and ccs all form in subsurface locations. The materials would have to be dug for or

found in an outcrop or acquired through trade from a distant source. The minerals are solid and can be used to create strong tools (Sen 2001).

The last rock is andesite, which is made up of plagioclase feldspar, amphibole, silica, and pyroxene. The matrix is usually lighter in color with darker phenocrysts. This rock would be weaker in strength and less desirable for flaking because of the phenocrysts. It could be used as an expedient tool but would not create strong formal tools. (Sen 2001)

Remote Sensing Data

The classification of the 12 rock samples that were collected from the area surrounding La Ballena cove were used to plot the distribution of the lithic material types observed on the satellite image (Figure 4.2). The majority of the cove is composed of varying types of rhyolite. The satellite image shows a dark red rhyolite near the water with a color change gradually transforming up the slope. The colors change from a dark red or maroon rhyolite to a much lighter almost gray rhyolite. This color variation is probably due to different volcanic flows of rhyolite heat treating the landscape and changing the composition of the materials. Basalts are found in the form of talus slopes on the northern most terraces in the bay. The quartz was always found in veins running in the cracks of the lighter rhyolites. The andesite material was found in conglomerates on the top most portions of the terraces. Table 4.1 shows the distribution of the lithic hand samples that were collected from the cove. This information was used to map out the locations of the lithic materials in Figure 4.3.

The variation in locations of the resources in Figure 4.2 and Figure 4.3 are attributed to the variation in spatial resolutions. There are many more pixels in the Figure 4.2 to which the computer program statistically places into the categories. Figure 4.3 is much smaller of an area and therefore more accurate to the specific location of the lithic raw material resources. Figure 4.2 is used to visually represent the layout of the island and its distribution of the resources. Figure 4.3 is used as a tool in specifying the locations of the resources.

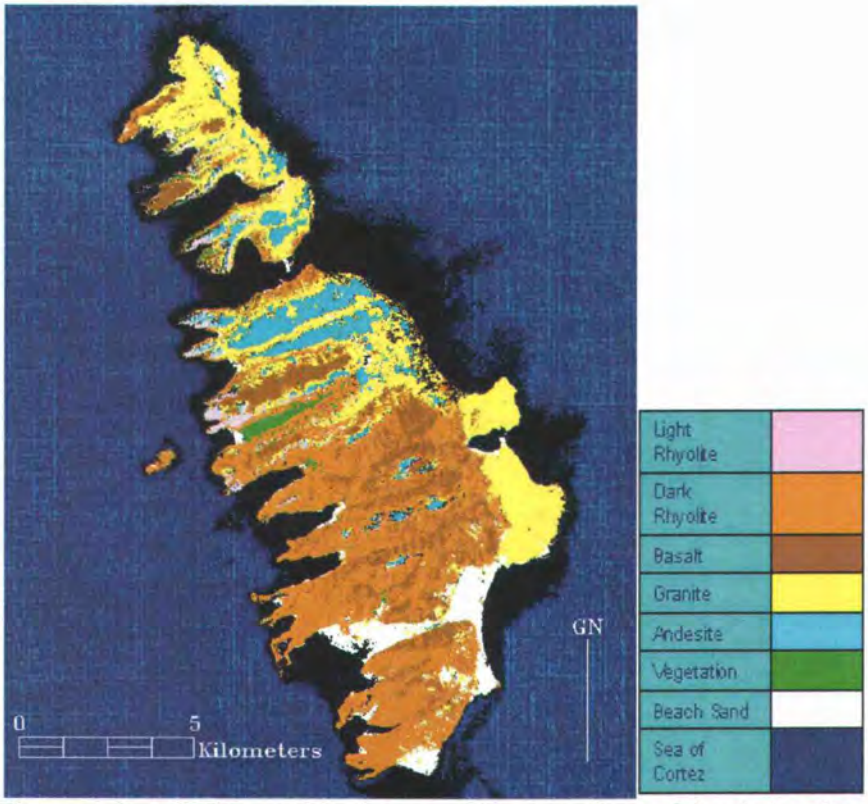

Figure 4.2: ASTER satellite image of Espiritu Santo Island showing the lithic distribution of the raw materials.

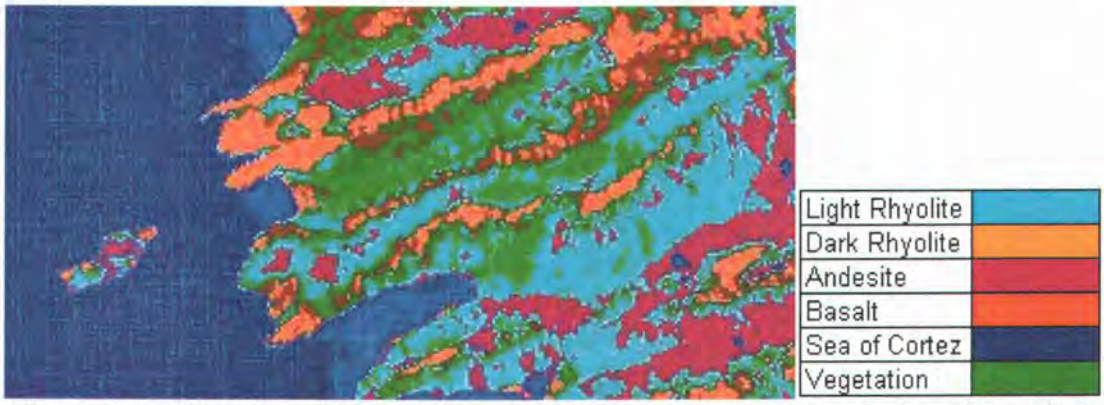

Figure 4.3: ASTER satellite imagery of La Ballena cove showing the locations of raw lithic resources

The visual distribution of the raw material is important for the determination of resources available to the inhabitants. The actual distance to the materials can determine cost-benefit (e.g. energy expenditure) contributions to the site. The analyzed ASTER imagery has mapped out the lithic resources in La Ballena Bay.

Table 4.1: Location of each of the lithic hand samples taken from La Ballena Bay.

Parent Material	Color	Northing	Easting
Rhyolite	Dark purple	24°29'13.08"	110°22'58.68"
Rhyolite	Light gray	24°29'12.36"	110°22'58.62"
Rhyolite	Light gray	24°29'9.24"	110°22'59.94"
Quartz and Pumice Rhyolite	Dark purple	24°29'10.14"	110°22'59.46
Andesite	Red	24°29'2.04"	110°22'59.28"
Basalt/Basaltic Andesite	Dark gray	24°29'1.44"	110°22'59.16"
Applelite	White	24°29'9.24"	110°22'59.94"
Rhyolite	Light gray	24°29'51.84"	110°22'51.18"
Andesite	Dark gray	24°29'51.60"	110°22'57.24"
Rhyolite	Light gray	24°29'31.44"	110°23'4.32"
Rhyolite	Dark gray	24°29'31.86"	110°23'5.52"
Rhyolite	Dark purple	24°29'29.40"	110°23'3.42"

Inserting this image into the ArcGIS 9.1 allows maps to be drawn for visual representation and determination of the exact distances from the site to the hand samples that were collected. Figure 4.3 and Table 4.2 show the results of the raw

material distributions. The basalt is the closest material to the site but is used the least. The rhyolites varieties are the next closest and are found at locations around the cove closest to where marine and terrestrial food sources would be gathered.

Table 4.2: Distances to parent material from J69E

Parent Material	Distance in Meters
Light Rhyolite	420
Basalt	388
Dark Rhyolite	427

Individual Units Debitage and Tool Analysis Results

Unit A

Debitage Analysis

Unit A contained cultural materials from its surface and produced one formed lithic tool and 31 pieces of lithic debitage analyzed. Figure 4.4 and Table A1 (all subsequent tables with an "A" are presented in Appendix A) show the results of analysis using the triple cortex typology. The surface assemblage of unit A had mainly interior flakes (74.2%) whereas secondary flakes accounted for 19.4% and primary flakes made up the remaining 6.4%.

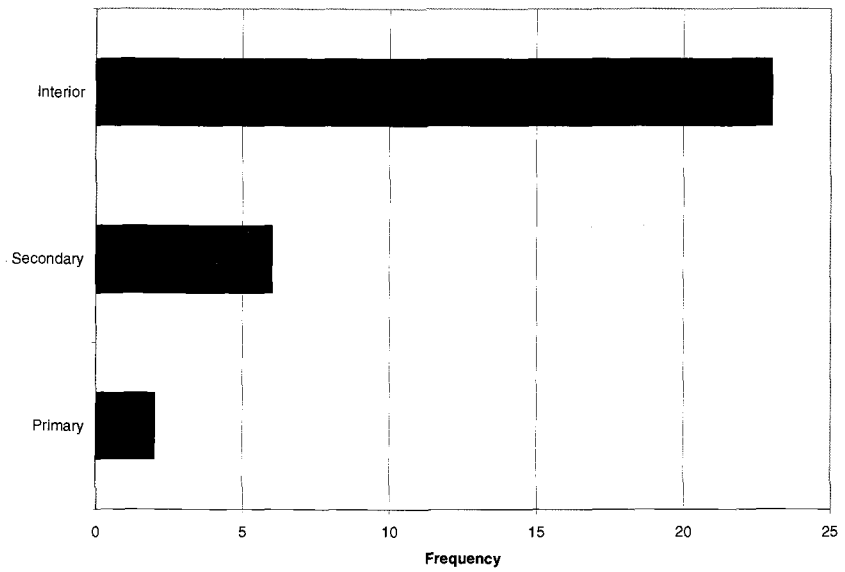

Figure 4.4: Barchart showing the triple cortex typology results for the surface assemblage of Unit A.

The results of the free-standing typology shown in Figure 4.5 and Table A.2 illustrate a trend towards early stage reduction. The majority of the flakes were in the broken flake category (51.4%) followed by 28.6% being complete flakes. The fragment flakes accounted for 11.4% and debris made up the remaining 8.6%.

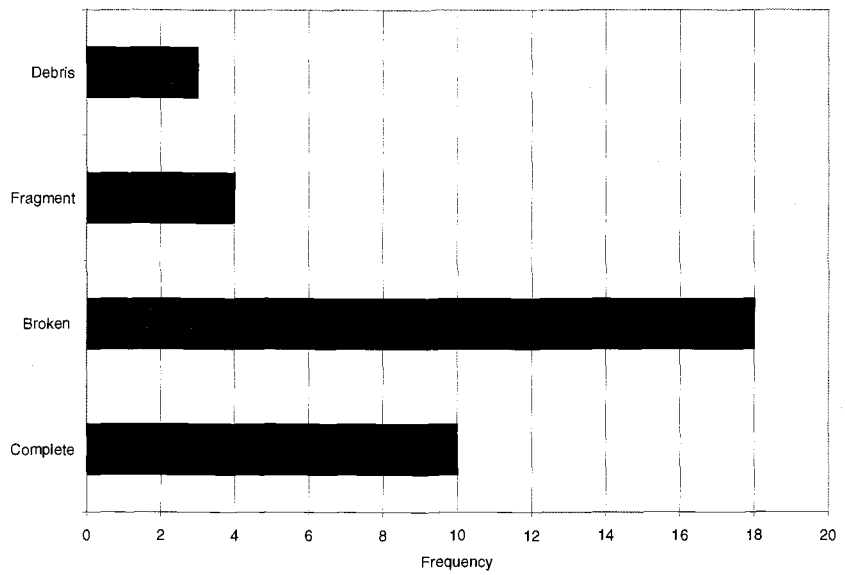

Figure 4.5: Barchart showing the free-standing typology results for the surface assemblage of Unit A.

Results of size and weight aggregate analyses for unit A are presented in Tables A.3 and A.4. A cumulative frequency plot (Figure 4.6) shows that 78.1% of the flakes fall within the three middle size classes (3-5 cm). The first two size classes contain 12.5% of the debitage and the remaining 9.4% are in the two largest size classes. Weight analysis (Figure 4.7) for the surface shows 80% of the assemblage falls in the highest weight class. The remaining 20% is evenly distributed among the other weight classes.

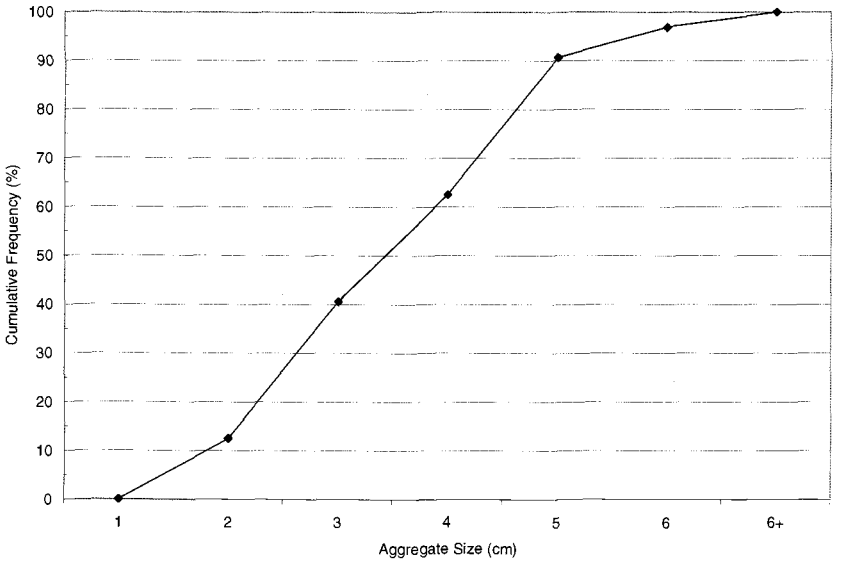

Figure 4.6: Cumulative frequency graph showing aggregate size class results for the surface assemblage of Unit A. (cumulative frequency plots that trend toward the upper left-hand side of the plot frame represent a debitage assemblage produced primarily through early stage reduction and plots that trend toward the bottom right hand corner indicate late stage lithic reduction) (Davis 2006)

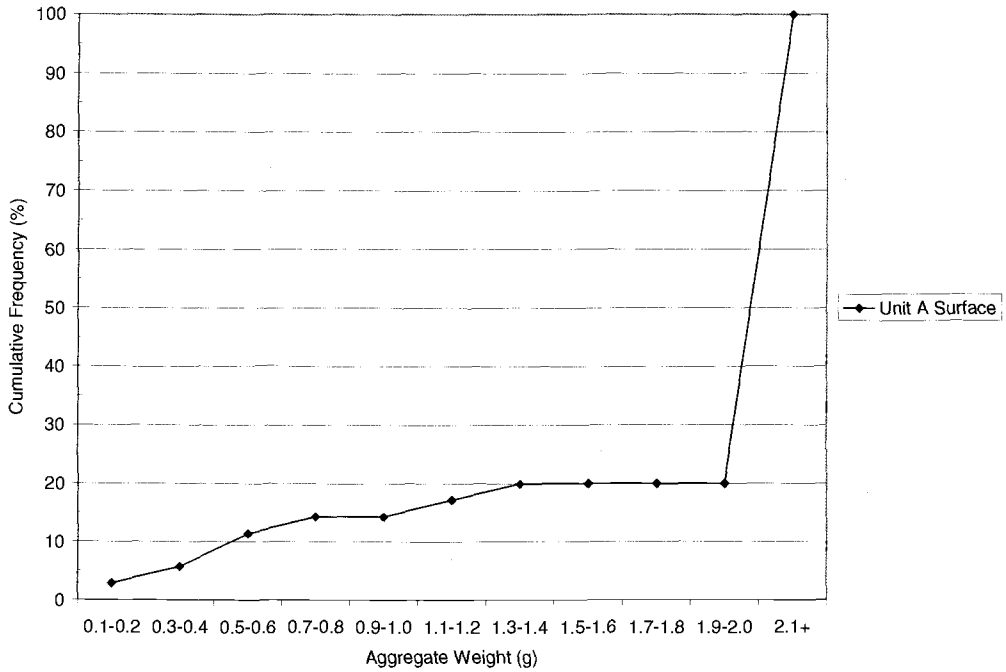

Figure 4.7: Cumulative frequency graph showing aggregate weight class results for the surface assemblage of Unit A.

Tool Analysis

Core (n=1)

Specimen 172, surface level (Figure B.31) (all subsequent figures with a "B" are presented in Appendix B): The flake removal characteristics of the surface of the specimen suggest a multidirectional core technology. Platform grinding is evident on some of the surfaces of the core. There is 5% of the cortex remaining on the specimen. The core is made of light rhyolite.

*(mm/g) MxL	MxWDT	MxTHK	WGT	DIR	COR%
46.4	40	32.8	51.8	multiple	5

(*MxL= maximum length; MxWDT= maximum width; MxTHK= maximum thickness; WGT= weight in grams; DIR= direction of flake removal; COR%= percentage of cortex remaining on specimen)

Unit B

Debitage Analysis

Unit B also contained lithic materials only found on the surface including three formed lithic tools and 48 pieces of lithic debitage. Figure 4.8 and Table A.1 shows the results of the triple cortex typology for unit B. Contrary to the findings for unit A, the debitage was evenly distributed throughout the three typological categories. The surface assemblage had 29.2% primary flakes, 31.3% secondary flakes, and 37.5% interior flakes.

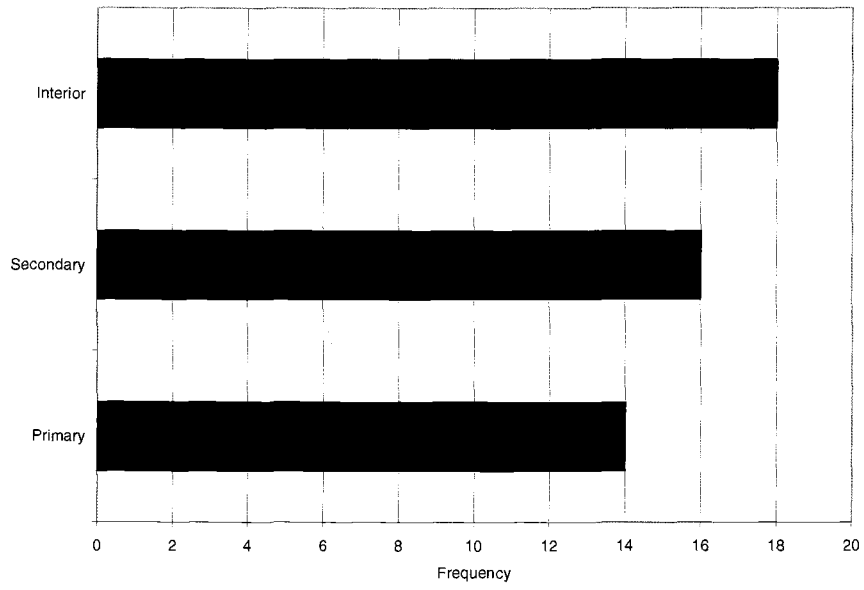

Figure 4.8: Barchart showing triple cortex typology results for the surface assemblage of Unit B.

The results of the free-standing typology are shown in Figure 4.9 and Table A.2. The majority of the assemblage was fragmented flakes (47.2%) followed by

24.5% broken flakes. The complete flakes accounted for 18.8% and the remaining 9.4% was debris.

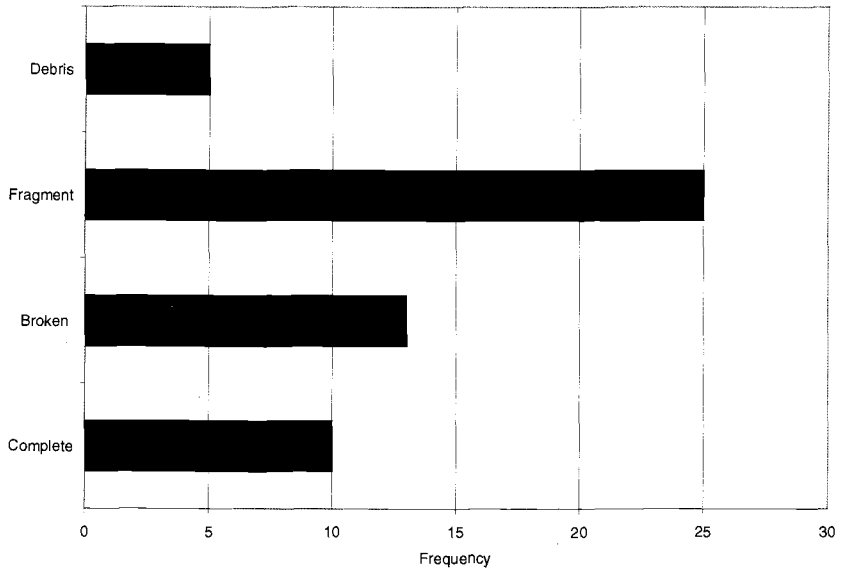

Figure 4.9: Barchart showing free-standing typology results for the surface assemblage of Unit B.

Size and weight aggregate analyses for Unit B show a trend towards middle stage size and early stage weight classes. Figure 4.10 shows a similar trend to that of Unit A, and other units to follow. Only 15.7% of the debitage falls in the lowest two size classes, while 64.7% remains in the middle three size classes (3-5 cm). The remaining 19.6% of the assemblage falls in the two highest size classes. The weight aggregate analysis (Figure 4.11) shows that 78.8% of the assemblage falls in the highest weight class with the remaining 21.2% distributed among the other weight classes.

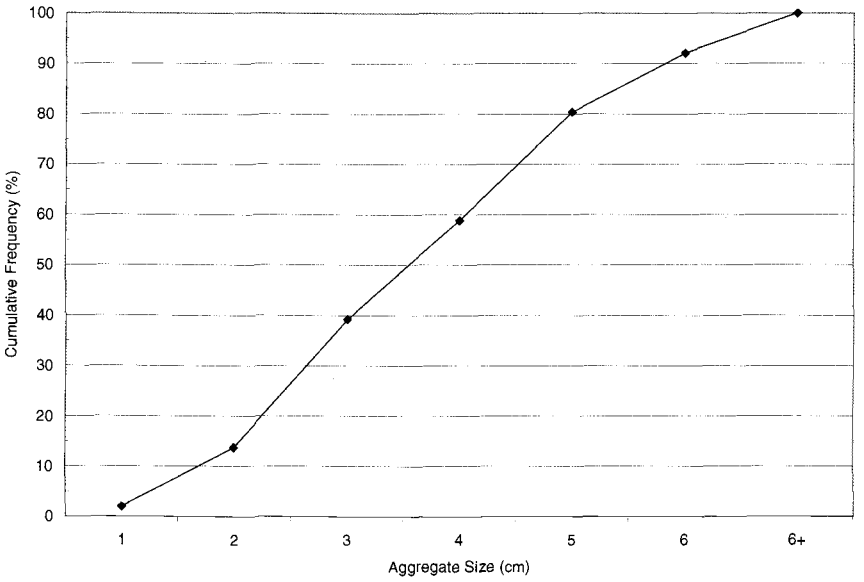

Figure 4.10: Cumulative frequency graph showing aggregate size class results for the surface assemblage of Unit B.

Figure 4.11: Cumulative frequency graph showing aggregate weight class results for the surface assemblage of Unit B.

Tool Analysis

Groundstone (n=1)

Specimen 217, surface level: This specimen is a grinding stone based on its smoothed and flattened end. The specimen has a flake removed from one side and is made of dark rhyolite.

(mm/g) MxL	MxWDT	MxTHK	WGT
64.9	51.	32.4	129.9

Non-formal Modified Flake Tool (n=1)

Specimen 111, surface level: This modified flake is an interior flake fragment. The right lateral edge has been modified uni-marginally in a convex shape. The wear pattern is continuous and the edge angle is 70°. The raw material is light rhyolite.

*(mm/g) MxL	MxWDT	MxTHK	WGT	Edge°	TCT	FST	Edge#
34.4	24	8.1	7.5	70	interior	Fragment	1

RT Loc	TEC	RTA	RTD
right lateral	convex	uni-marginal	continuous

(*TCT= triple cortex typology, FST= free-standing typology, Edge°=modified edge angle, Edge# = number of modified edges, RT Loc= modified edge location, TEC= tool edge characteristic, RTA= retouch attribute, RTD= retouch distribution)

Biface (n=1)

Specimen 158, surface level (Figure B.4): This biface fragment appears to be a perform 1. The biface was broken near the midsection. There is evidence of grinding on the worked edges. There is also cortex remaining on the surface. The raw material is dark rhyolite.

(mm/g) MxL	MxWDT	MxTHK	WGT	Edge°
52.2	39	22.1	36.8	45-75

Unit C

Debitage Analysis

Unit C contained one formed lithic tool and 58 pieces of lithic debitage recovered from the surface. The results from the triple cortex typology, seen in Figure 4.12 and in Table A.1, show that the majority of the assemblage falls in the interior flakes category (70.7%). The secondary flakes account for 19% and the primary flakes make up the remaining 10.3%.

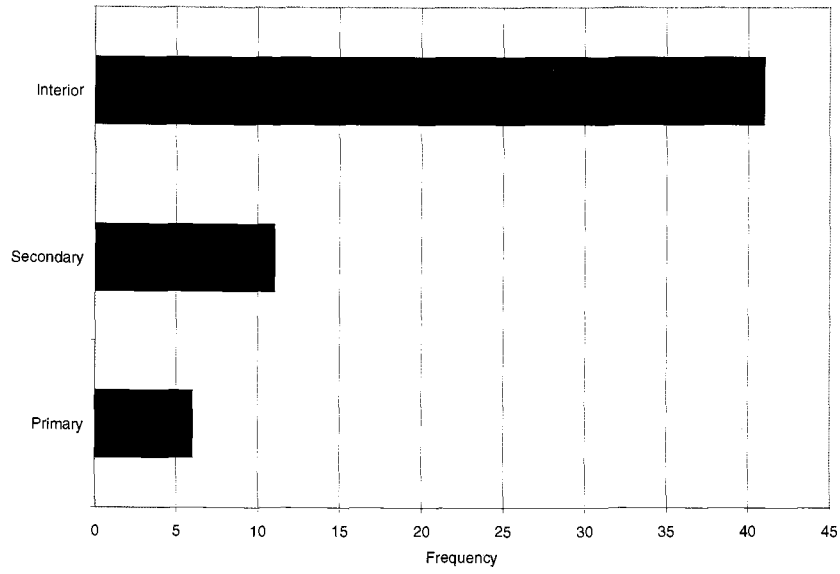

Figure 4.12: Barchart showing triple cortex typology results for the surface assemblage of Unit C.

The results of the free standing typology analysis are shown in Figure 4.13 and Table A.2 . The majority of the assemblage falls within the broken flake category, consisting of 52.9% of the population. The remainder of the assemblage is distributed evenly among the three other categories: 17.7% complete flakes, 16.2% flake fragments, and 13.2% debris.

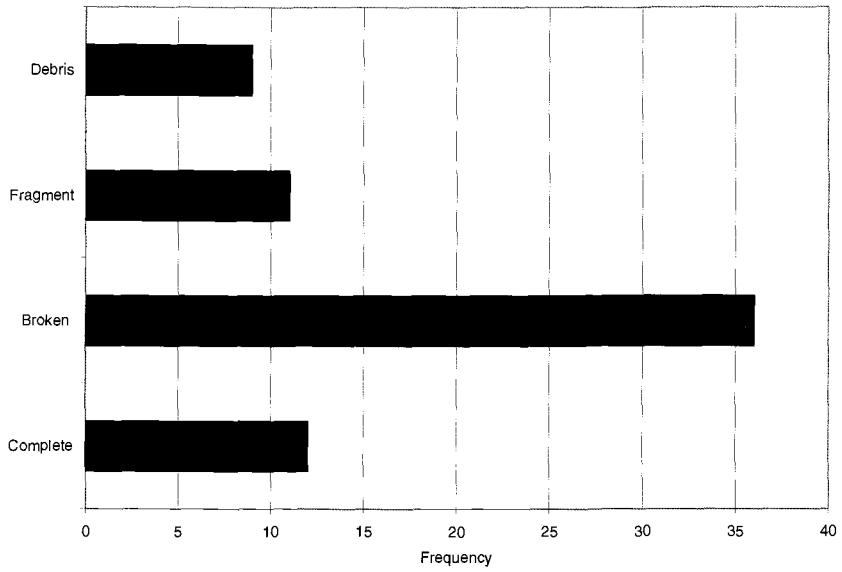

Figure 4.13: Barchart showing free-standing typology results for the surface assemblage of Unit C.

The aggregate size analysis shows a trend in late to middle stage reduction while the aggregate weight analysis shows a majority trend in early stage reduction with a slight peak in the late stage reduction classes. Figure 4.14 and Table A.3 illustrate the results of the aggregate size analysis. .

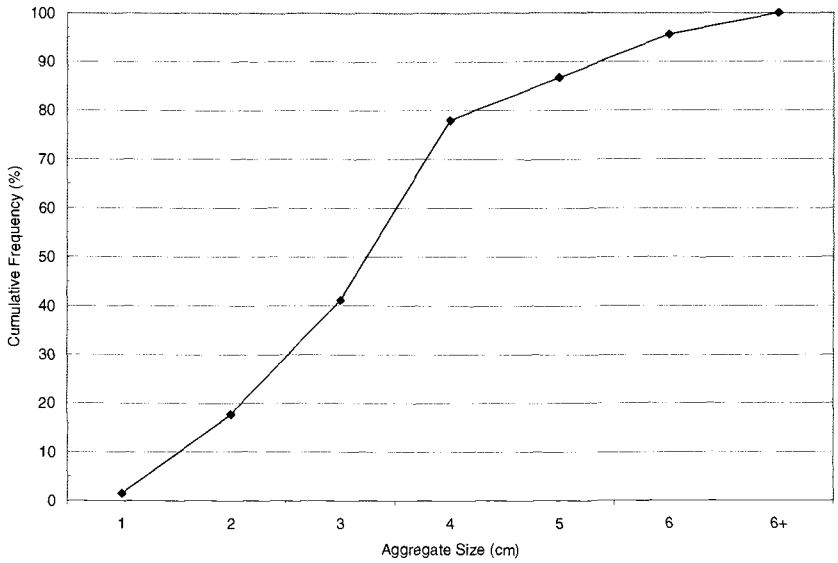

Figure 4.14: Cumulative frequency graph showing aggregate size class results for the surface assemblage of Unit C.

Size classes 2-4 cm accounts for 76.4% of the total assemblage. The smallest size class contains 1.5% of the population and the larger size classes account for the remaining 22.1%. The largest weight class dominates the population with 73.5% of the assemblage (Figure 4.15). The smaller weight classes (0.1-1.0 g) contain 17.6% of the population leaving the remaining 8.9% to be distributed evenly between 1.0 and 2.0 g.

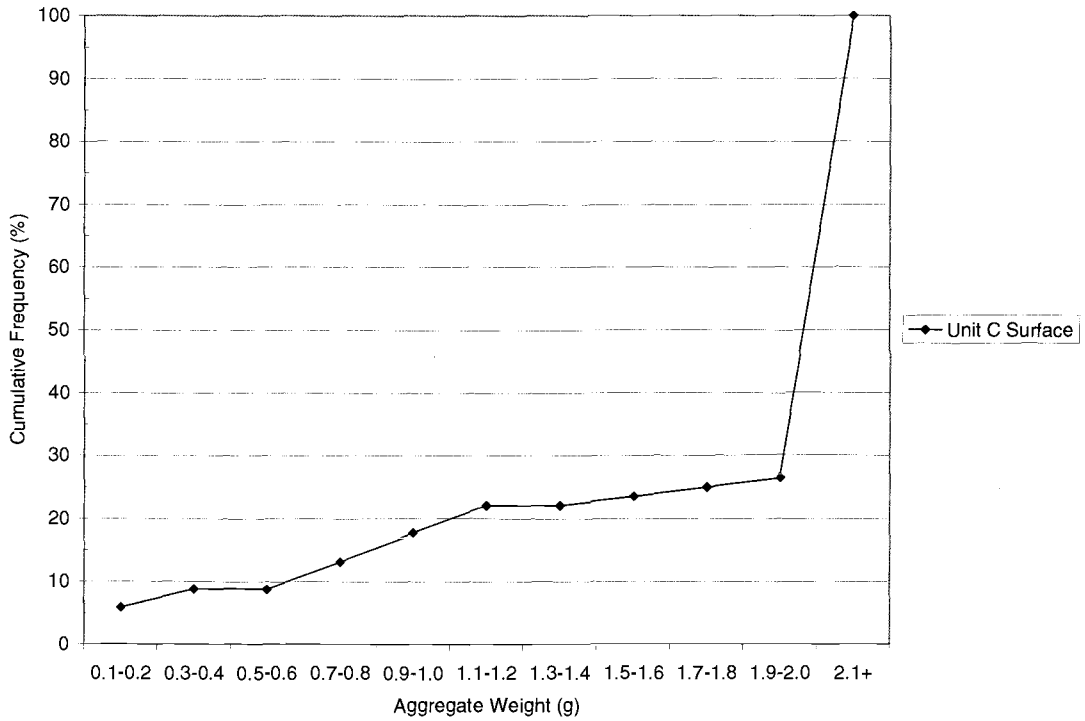

Figure 4.15: Cumulative frequency graph showing aggregate weight class results for the surface assemblage of Unit C.

Tool Analysis

Groundstone (n=1)

Specimen 218, surface level: This specimen is considered to be hammerstone due to the battered appearance on either end of the stone most likely due to impact. The specimen is complete. The raw material is light rhyolite.

(mm/g)	MxL	MxWDT	MxTHK	WGT
	64.3	54.1	27.2	133.2

Unit D

Debitage Analysis

Unit D only contained materials from the surface collections. The assemblage consists of 46 pieces of lithic debitage. The results of the triple cortex typology are shown in Figure 4.16 and Table A.1. The interior flakes accounted for 58.7% of the assemblage, while the secondary flakes contained 28.3%. The primary flakes made up the remaining 13% of the population.

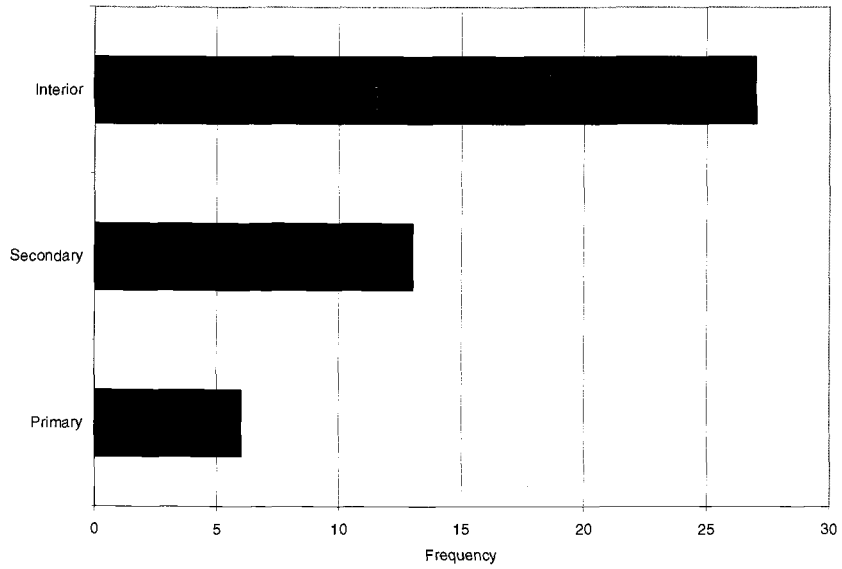

Figure 4.16: Barchart showing triple cortex typology results for the surface assemblage of Unit D.

The results of the free-standing typology are shown in Figure 4.17 and Table A.2. The surficial debitage assemblage includes 32.7% of the population being complete flakes, 28.8% being flake fragments, 23.1% being broken flakes, and 15.4% being debris.

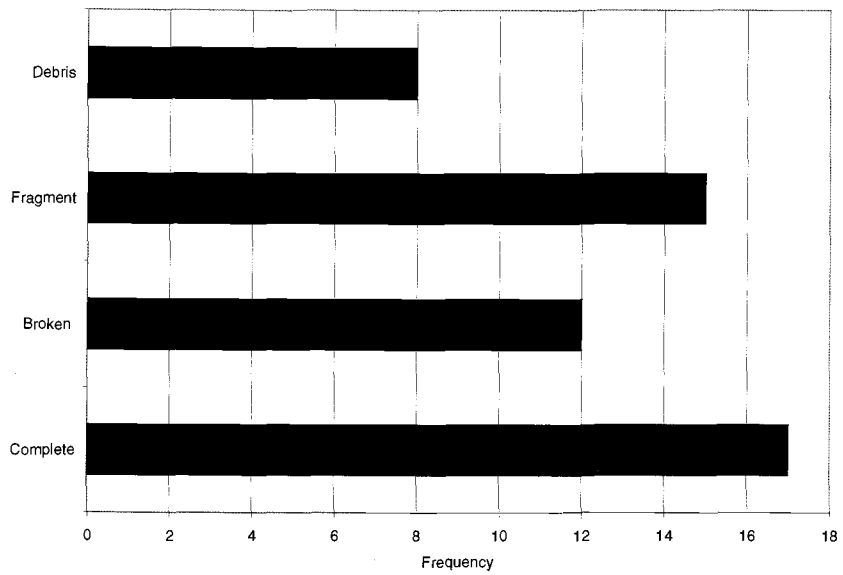

Figure 4.17: Barchart showing free-standing typology results for the surface assemblage of Unit D.

Results for the aggregate analysis for unit D show a trend towards middle stage reduction for the size and early stage reduction for the weight. Within the aggregate size analysis (Figure 4.18 and Table A.3), 89% of the population falls within the 2-5 cm size classes.

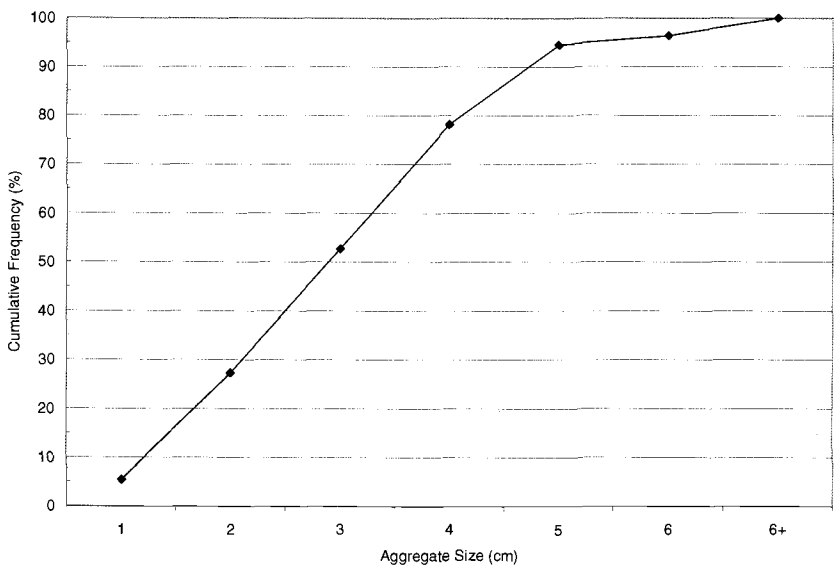

Figure 4.18: Cumulative frequency graph showing aggregate size class results for the surface assemblage of Unit D.

The smallest size class contains only 5.5% of the population and the 6 and 6+ cm classes account for the other 5.5%. The results of the weight class (Figure 4.19) vary slightly from the size class. The weight results show that 72.7% of the assemblage is greater than 2.1 g. There is also a slight trend, 22.7%, in the less than 1.0 g classes. The remaining 4.6% is in the 1.9-2.0 g class.

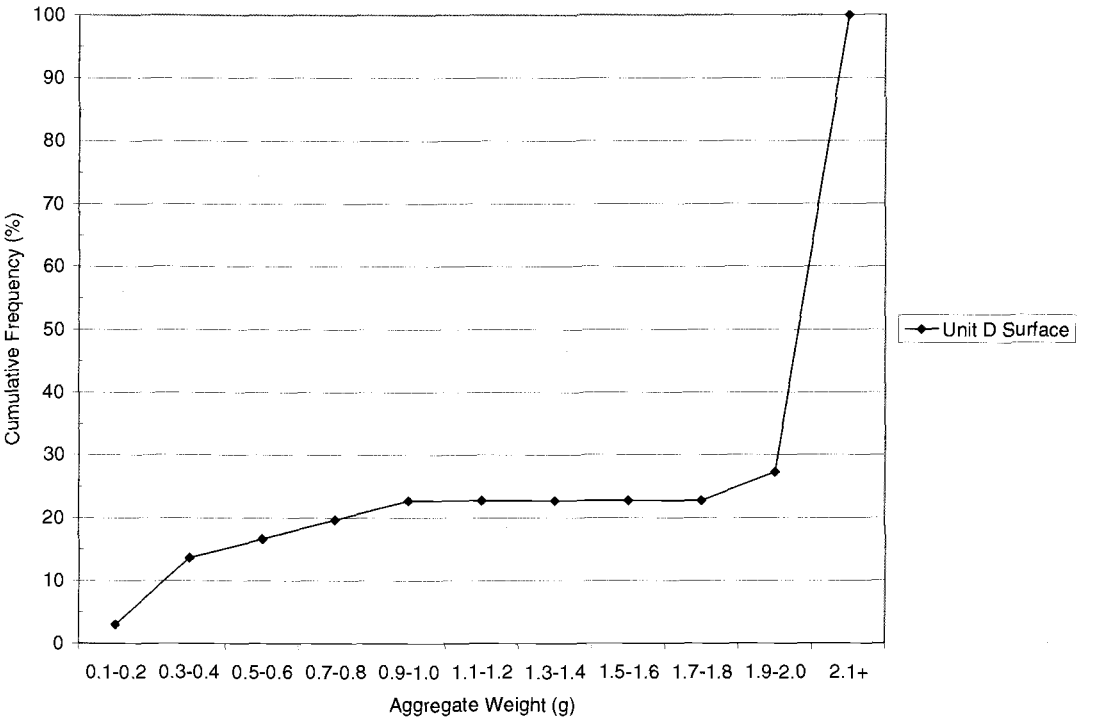

Figure 4.19: Cumulative frequency graph showing aggregate weight class results for the surface assemblage of Unit D.

Unit E

Debitage Analysis

The surface assemblage for unit E includes two formed lithic tools and 31 pieces of lithic debitage. Figure 4.20 and Table A.1 give the results of the triple cortex typology analysis. Interior flakes account for 48.4% of the population and secondary flakes make up 29%. The primary flakes account for the remainder of the 22.6%.

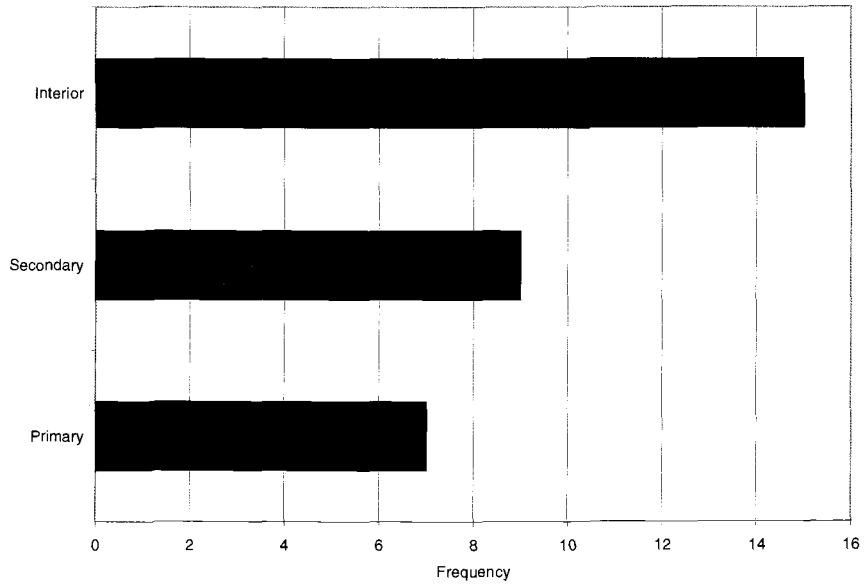

Figure 4.20: Barchart showing triple cortex typology results for the surface assemblage of Unit E.

The results of the free-standing typology are illustrated in Figure 4.21 and Table A.2. The majority of the flakes are fragments (40.6%).

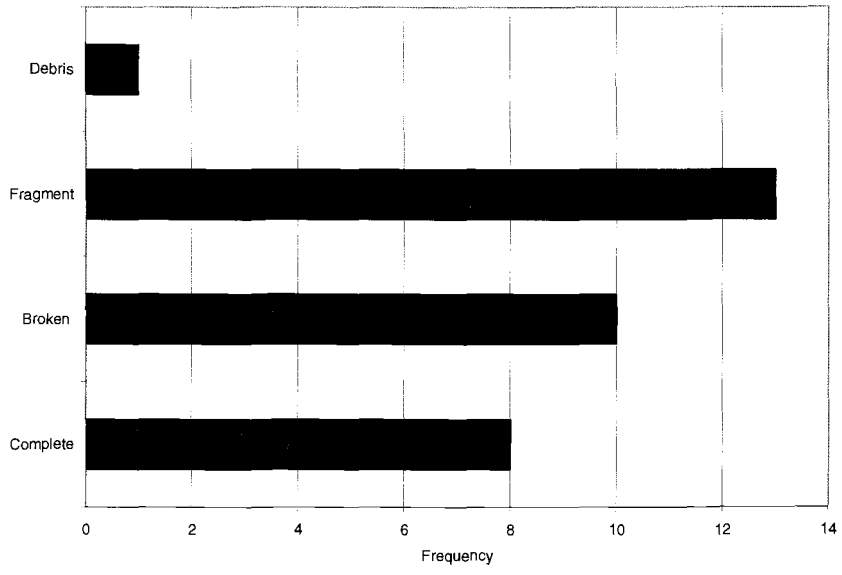

Figure 4.21: Barchart showing free-standing typology results for surface assemblage of Unit E.

The broken flakes account for 31.3% while the complete flakes make up 25% of the population. The remaining 3.1% of the assemblage is debris.

The aggregate analysis for unit E follows the same pattern as all of the other units discussed previously. The size analysis shows a trend towards middle stage reduction and the weight analysis shows a trend towards early stage reduction (Figure 4.22 and Table A.3). All of the assemblage falls within size classes 2-5 cm.

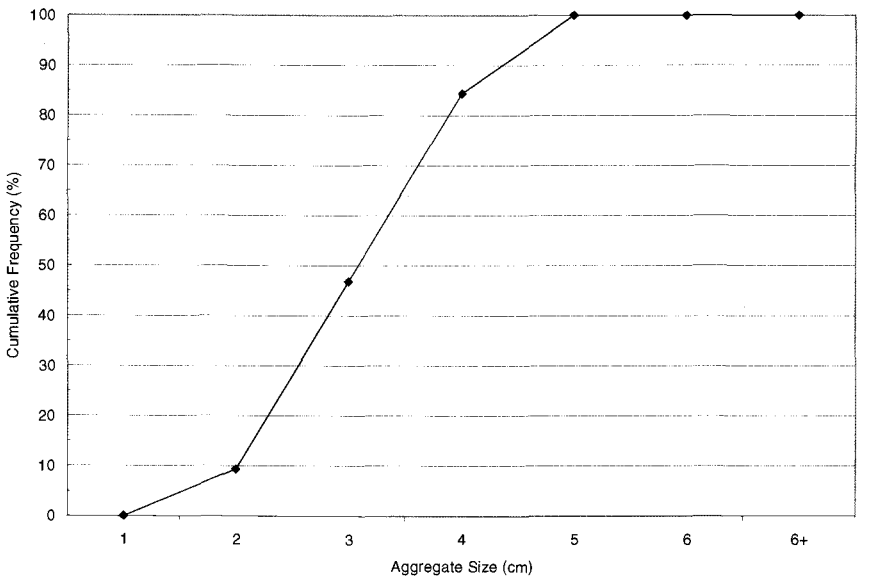

Figure 4.22: Cumulative frequency graph showing aggregate size class results for the surface assemblage of Unit E.

There are no pieces of debitage that fall in the smallest and two largest size classes. The weight class analysis (Figure 4.23) contains 75% of the assemblage falling in the highest weight class. The remaining 25% is unevenly distributed among the remaining weight classes with no major clustering of classes.

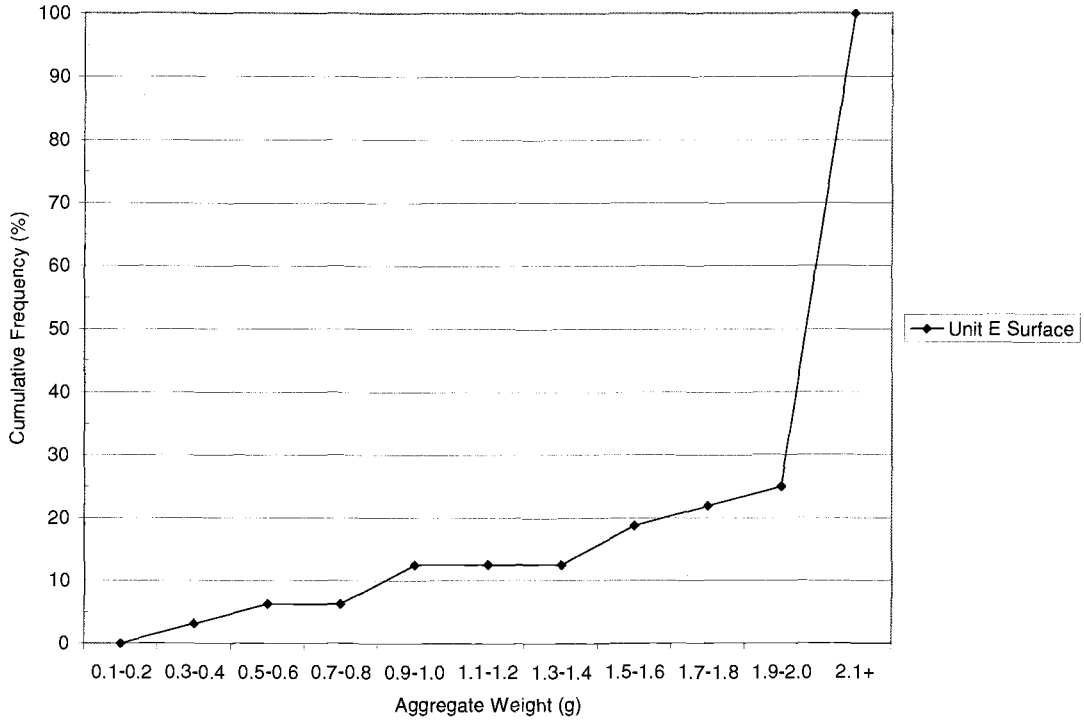

Figure 4.23: Cumulative frequency graph showing aggregate weight class results for the surface assemblage for Unit E.

Tool Analysis

Non-formal modified flake (n=2)

Specimen 112, surface level: The specimen displays modifications on the right and left lateral edges and on the distal end. The modified flake is made of an interior flake fragment. Flake removal characteristics include continuous use wear with a range in edge angles, 45-70°. The raw material is light rhyolite.

(mm/g)	MxL	MxWDT	MxTHK	WGT	Edge°	TCT	FST	Edge#
	38.3	34.4	17.7	29	45-70	interior	Fragment	3

RT Loc	TEC	RTA	RTD
right & left lateral/distal	straight/concave	tri-marginal	continuous

Specimen 113, surface level: The specimen displays modifications on the right proximal edge. The modifications are on a secondary broken flake. The flake removal characteristics include a straight, uni-marginal, and continuous use wear pattern. The edge angle is 33°. The raw material is light rhyolite.

(mm/g)	MxL	MxWDT	MxTHK	WGT	Edge°	TCT	FST	Edge#
	31	37.3	14.3	15.1	33	secondary	broken	1

RT Loc	TEC	RTA	RTD
right proximal	straight	uni-marginal	continuous

Unit F

Debitage Analysis

The surface level of unit F contained one formed lithic tool and 20 pieces of lithic debitage. The results of the triple cortex typology (Figure 4.24 and Table A.1), show the majority of the assemblage is made up of interior flakes (64.7%).

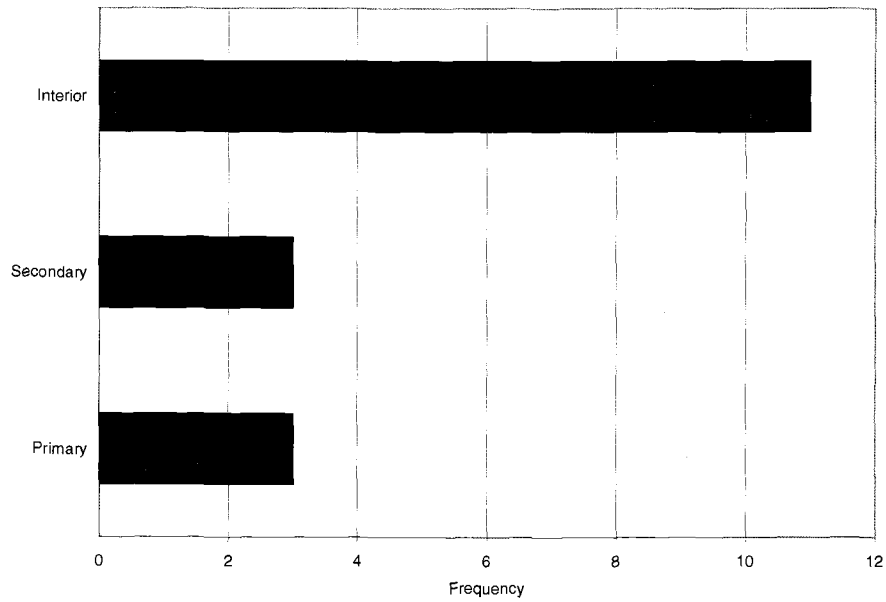

Figure 4.24: Barchart showing triple cortex typology results for the surface level of Unit F.

The primary and secondary flakes each contain 17.7% of the population. The surface collections from unit F maintain the patterning that has been seen so far in the assemblages; the interior flakes reserve the majority of the population.

The aggregate analyses show a trend in middle stage reduction. Figure 4.25 and Tables A.3 and A.4 show the results of the analyses conducted on the assemblage.

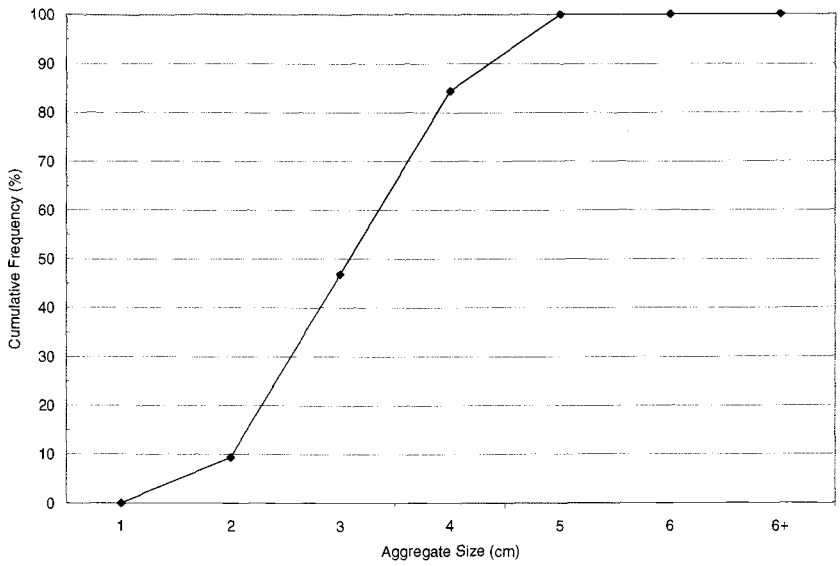

Figure 4.25: Cumulative frequency graph showing aggregate size class results for the surface level of Unit F.

The size analysis shows that 75% of the population falls within size classes 2-4 cm. The smallest size class contains 10% of the assemblage, sizes 5-6 cm contain the remaining 15%, and the largest size class contains no lithic materials. The weight analysis (Figure 4.26) shows that 80% of the assemblage falls in the largest weight class. The remaining 20% of the population falls within 0.5-1.4 g.

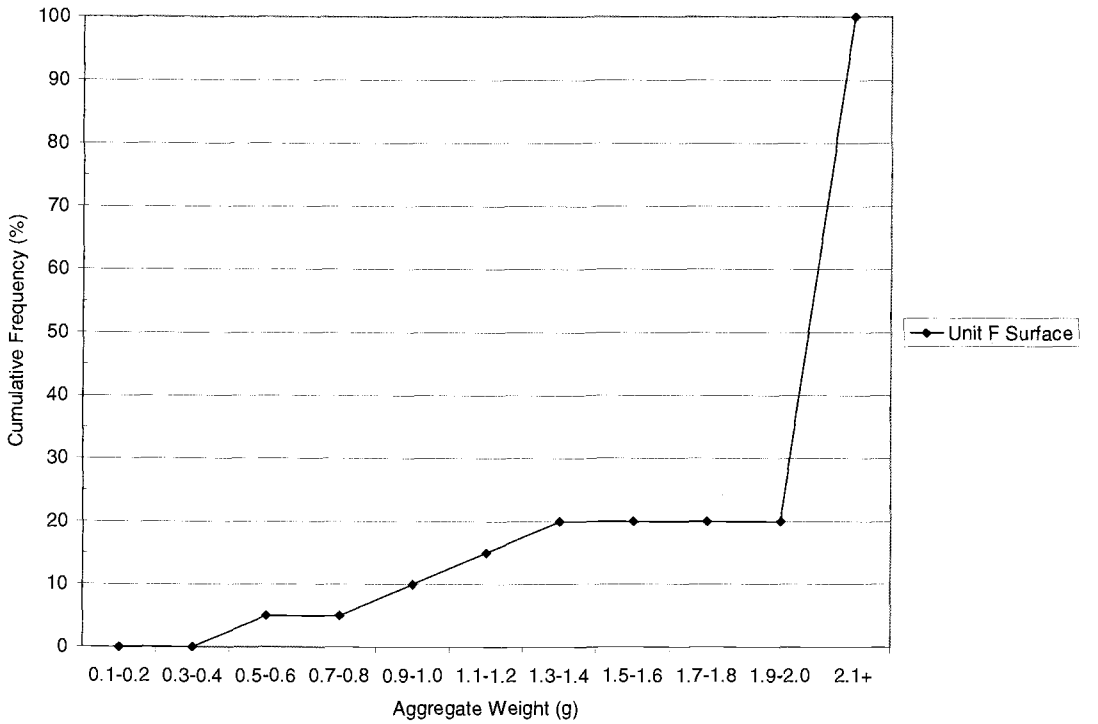

Figure 4.26: Cumulative frequency graph showing aggregate weight class results for the surface assemblage for Unit F.

Tool Analysis

Biface (n=1)

Specimen 171, surface level, Blank (Figure B.10): The specimen is a blank based on the lack of lateral margins being completely worked and the flakes that were removed didn't extend over half of the edge. It has a considerably thick cross section and is broken in the center of the biface. Flake removal is collateral with an edge angle range of 50-60°. The raw material is light rhyolite.

(mm/g) MxL	/ MxWDT	/ MxTHK	/ WGT	/ Edge°
42.5	25.5	11.4	10.4	50-60

Unit G

Debitage Analysis

Unit G contained two formed lithic tools and 28 pieces of lithic debitage. Figure 4.27 and Table A.1 illustrate a summary of the results of the triple cortex typology. The majority of the assemblage is composed of interior flakes (66.7%), and primary flakes (22.2%), and secondary flakes (11.1%).

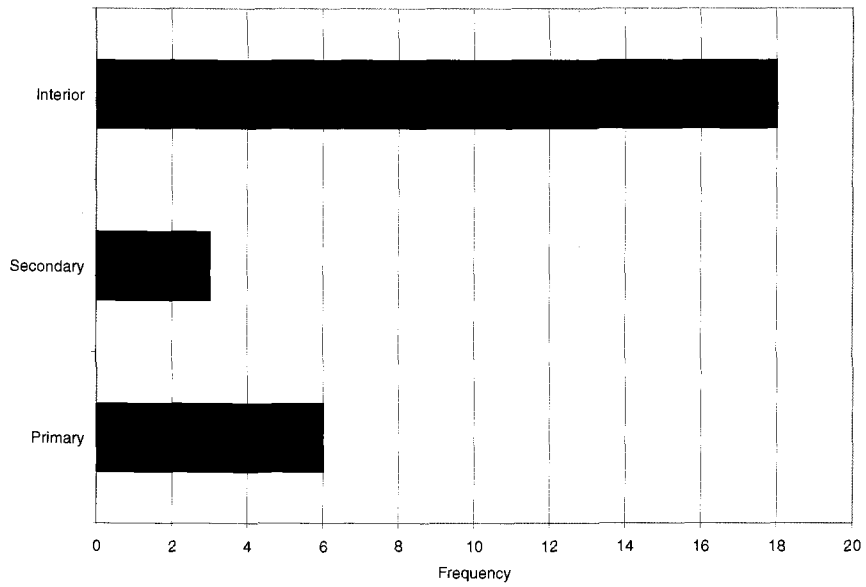

Figure 4.27: Barchart showing triple cortex typology results for the surface assemblage of Unit G.

The free-standing typology analysis shows 39.2% of the assemblage is broken flakes. The complete and fragmented flakes each account for 28.6% of the assemblage. The debris accounts for the remaining 3.6% of the population. Figure 4.28 and Table A.2 show the results of the free-standing typology.

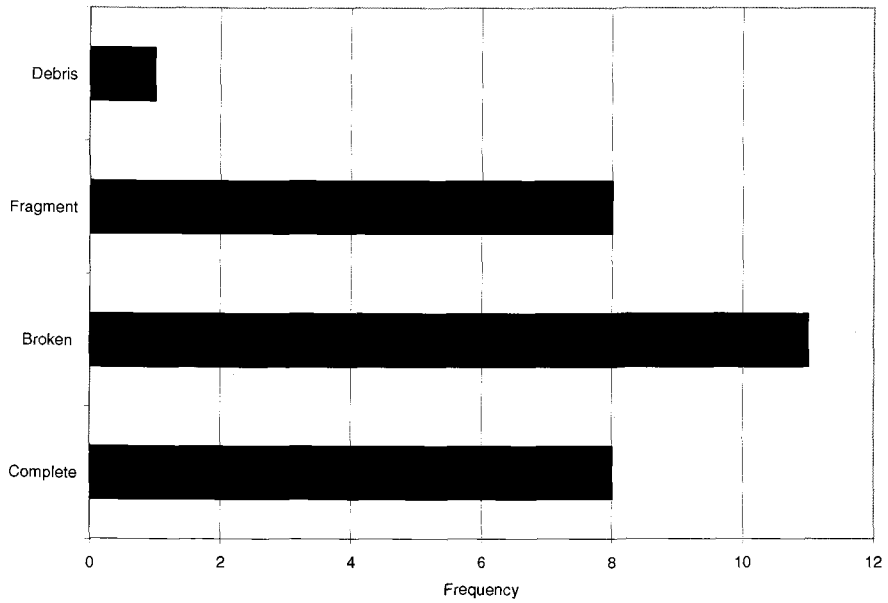

Figure 4.28: Barchart showing free-standing typology results for the surface assemblage of Unit G.

The size and weight aggregate analyses for unit G show similar trends towards early-middle stage reduction. Figure 4.29 and Table A.3 illustrate the results from the aggregate size analysis.

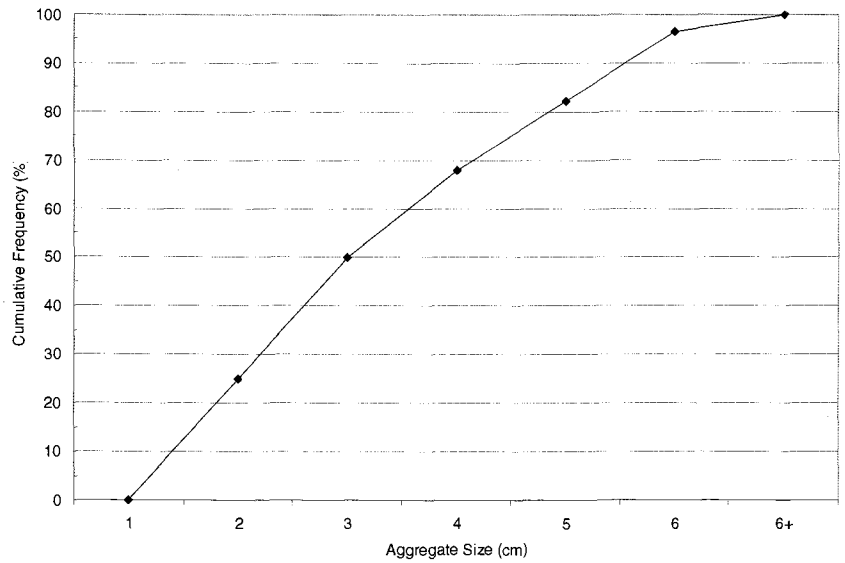

Figure 4.29: Cumulative frequency graph showing aggregate size class results for the surface assemblage of Unit G.

The middle size classes (2-5 cm) account for 81.2% of the assemblage. The remaining 18.8% of the population falls in the upper two size classes. The aggregate weight analysis (Figure 4.30) shows 57.1% of the assemblage falls in the two heaviest weight classes (1.9-2.1+ g). The smaller weight classes (0.1-0.8 g) accounts for 35.7% of the assemblage. The remaining 10.7% falls in the weight classes of 1.1-1.4 g. Table A.4 illustrates the results of the aggregate weight analysis.

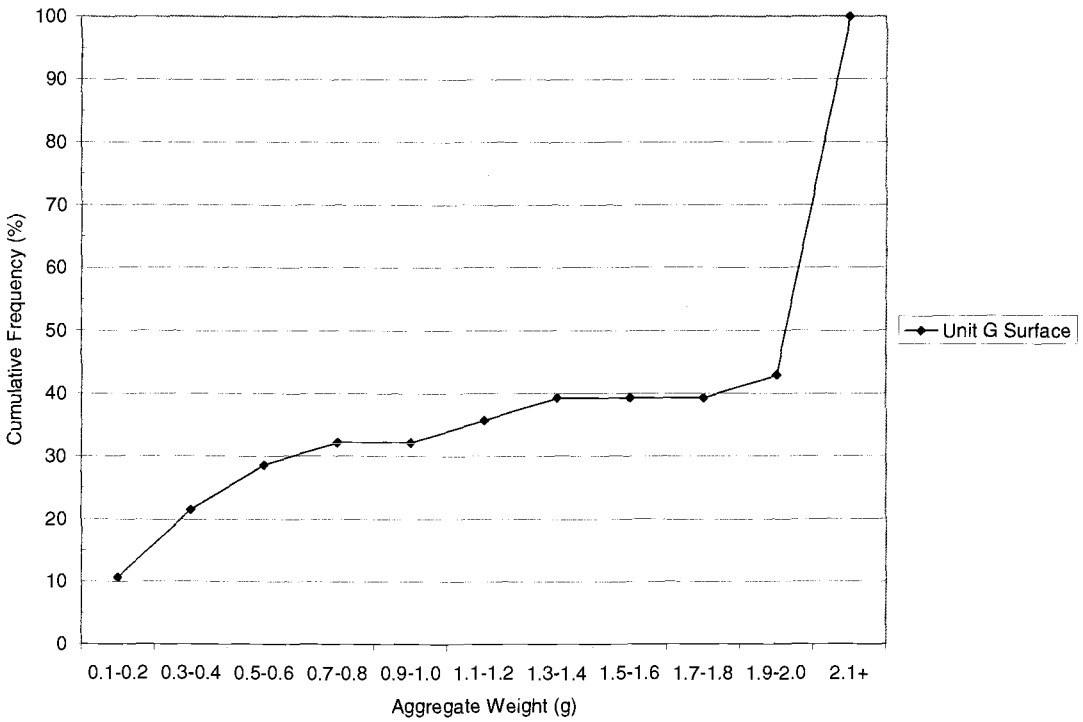

Figure 4.30: Cumulative frequency graph showing aggregate weight class results for the surface assemblage for Unit G.

Tool Analysis

Core (n=1)

Specimen 173, surface level (Figure B.48): The specimen is considered to be a unidirectional core based on the pattern of flake removal. There is no evidence of

platform preparation, and 50+% of the cortex remains on the specimen. The raw material is light rhyolite.

(mm/g) MxL	MxWDT	MxTHK	WGT	DIR	COR%
40	51.2	38	48.6	uni	50+

Non-formal modified flake (n=1)

Specimen 114, surface level: The specimen shows signs of modification on the left lateral area and is manufactured on a primary broken flake. Flake removal characteristics include a straight uni-marginal area with a continuous wear pattern. The edge angle is 60°, suggesting scraping activities. The raw material is dark rhyolite.

(mm/g) MxL	MxWDT	MxTHK	WGT	Edge°	TCT	FST	Edge#
66.6	42	24	53.5	60	primary	broken	1

RT Loc	TEC	RTA	RTD
left lateral	straight	uni-marginal	continuous

Unit H

Debitage Analysis

The surface level of unit H includes one formed lithic tool and 34 pieces of lithic debitage. Level 1 contains 10 formed lithic tools and 98 pieces of lithic debitage. Level 2 contains 10 formed lithic tools and 31 pieces of lithic debitage. Level 3 contains no formed lithic tools and 13 pieces of lithic debitage. The results of the triple cortex typology are seen in Figure 4.31 and Table A.1. The surface level is composed of 55.9% interior flakes, 29.4% secondary flakes, and 14.7% primary flakes. The level 1 assemblage is comparable with the surface level containing 61.7%

of the assemblage falling in the interior flakes category, 23.5% in the secondary flakes category, and 14.8% in the primary flake category. The level 2 assemblage contains 59.3% interior flakes, 25.9% primary flakes, and 14.8% secondary flakes. This level varies slightly from the norm in that there are more primary flakes then secondary flakes. The level 3 assemblage varies greatly from the rest of the levels. The majority of the flakes are secondary with 57.1% of the population. The primary flakes account for 28.6% of the assemblage and the remaining 14.3% falls in the interior flake category.

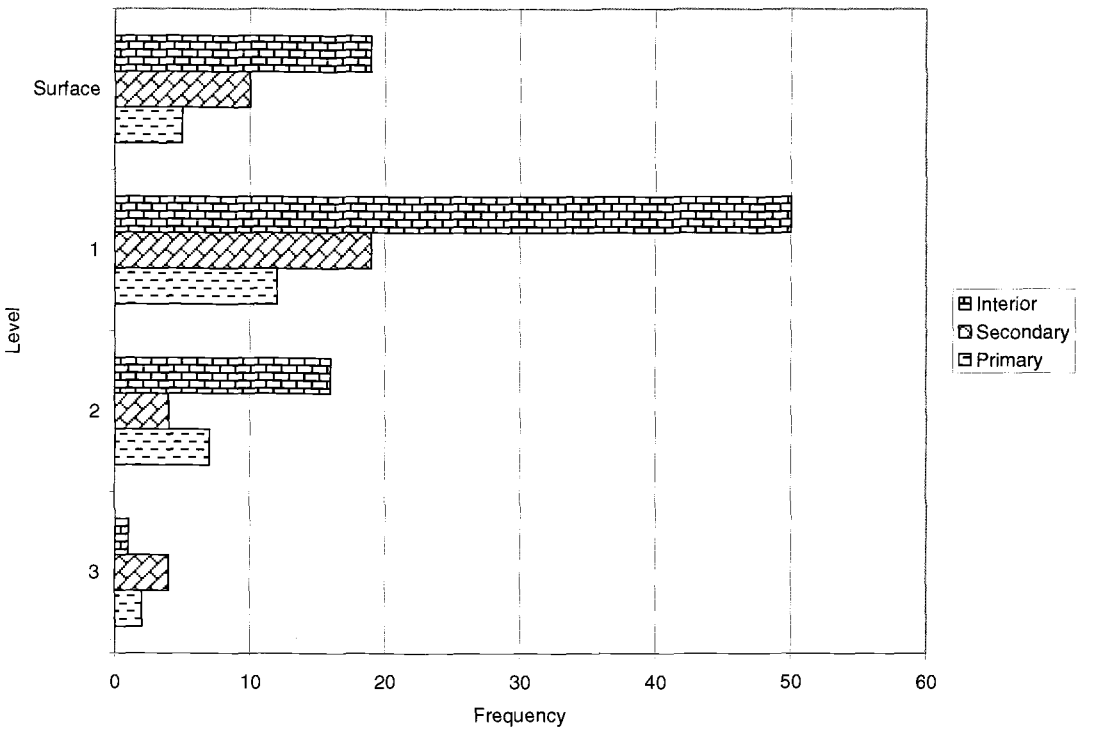

Figure 4.31: Barchart showing the triple cortex typology results for the surface and levels 1, 2, & 3 of Unit H.

The results of the free-standing typology can be seen in Figure 4.32 and Table A.2. The surface contains a fairly uniform spread of complete (35.3%), broken (38.2%), and fragment flakes (26.5%). Level 1 contained the same amount of

complete and fragment flakes (35.7%). The debris accounted for 18.4% and the broken flakes made up the remaining 16.3%. Level 2 yielded a higher percentage of fragment flakes (41.9%). The broken and complete flakes contained the same amount with 25.8% and the debris made up the remaining 6.5%. Level 3 had the highest percentage of fragmented flakes (53.8%). The broken flakes, complete flakes, and debris each contained 15.4% of the population.

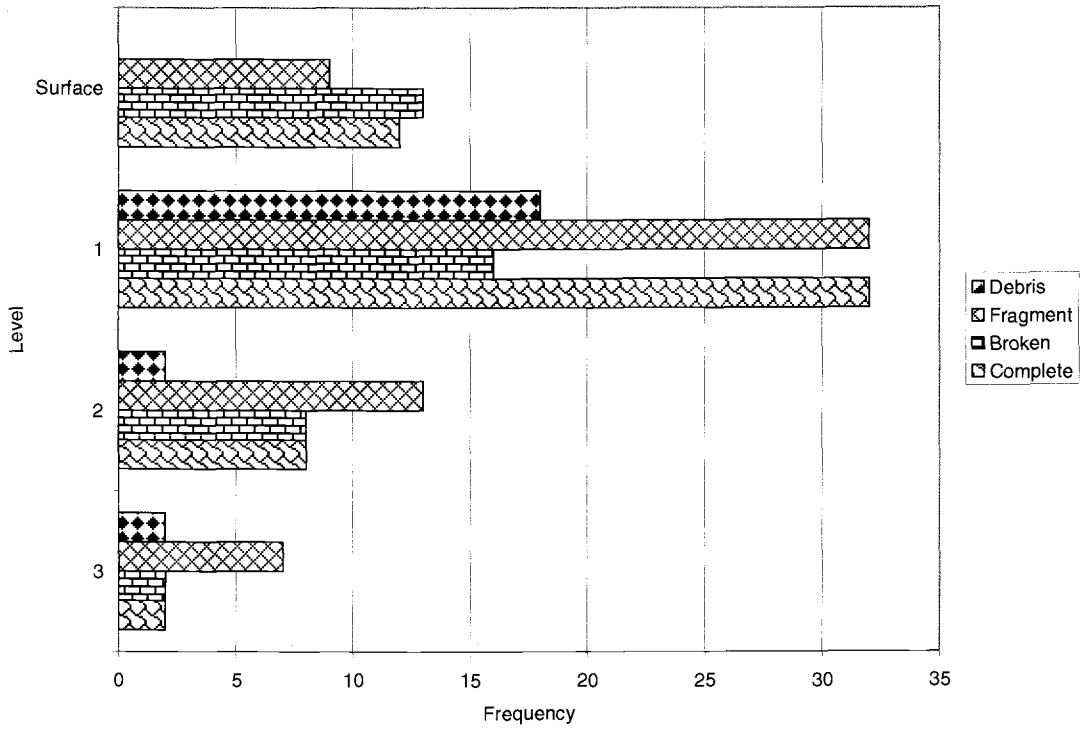

Figure 4.32: Barchart showing free-standing typology results for the surface and levels 1, 2, & 3 of Unit H.

The results of the size and weight aggregate analysis for unit H are shown in Figure 4.33 and 4.34 as well as Tables A.3 and A.4. All of the levels show a trend in early to middle stage reduction. The surface contains 76.4% of the assemblage in the 3-5 cm size classes. The remaining 23.6% is divided evenly between size class 2 cm and 6 cm. The weight analysis for the surface shows that 82.4% of the assemblage

falls in the highest weight class. The remainder of the assemblage is unevenly distributed within the middle weight classes. Level 1 contains 80.7% of the assemblage in size classes 2-4 cm. The smallest size class accounts for 4.5% of the assemblage. The remaining 14.8% of the assemblage is found in the size classes 5-6+ cm. The weight analysis for level 1 shows that 71.6% of the assemblage falls in the highest weight class; this follows the pattern seen for all of the weight analyses. The weight classes between 1.0 and 2.0 g contain 17.9% of the assemblage. The remaining 10.5% is unevenly distributed among the lower weight classes.

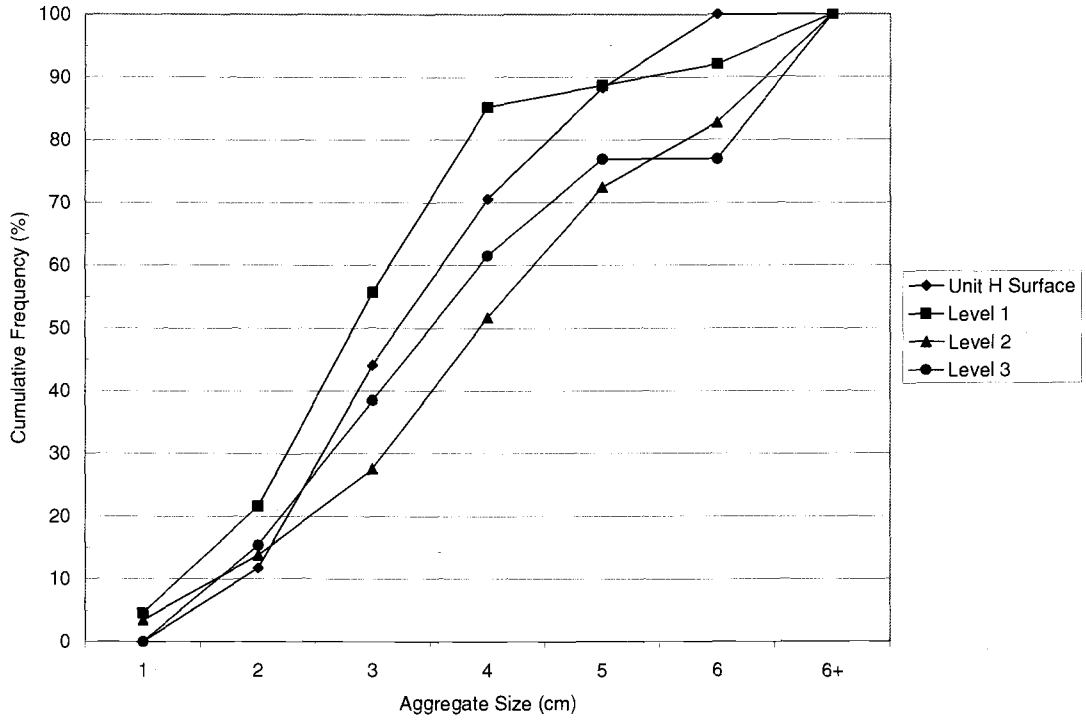

Figure 4.33: Cumulative frequency graph showing aggregate size class results for the surface and levels 1, 2, & 3 of Unit H.

Level 2 contains 58.6% of the assemblage in size classes 3-5 cm. The two smallest size classes' account for 13.8% of the assemblage and 27.6% of the population falls in the two highest size classes. The weight analysis for level 2 shows that 86.2% of the

assemblage falls in the highest weight class (2.1+ g). The weight classes of 0.6 and smaller account for 10.3% of the assemblage. The remaining 3.5% can be found in the 1.7-1.8 g category. Level 3 contains 76.9% of the assemblage in size classes 2-5 cm. The remainder of the assemblage falls in size class 6+ with 23.1%. The weight analysis for level 3 shows that 84.6% of the assemblage falls in the highest weight class. The remainder of the assemblage falls in the weight class of 0.5-0.6 grams with 15.4%.

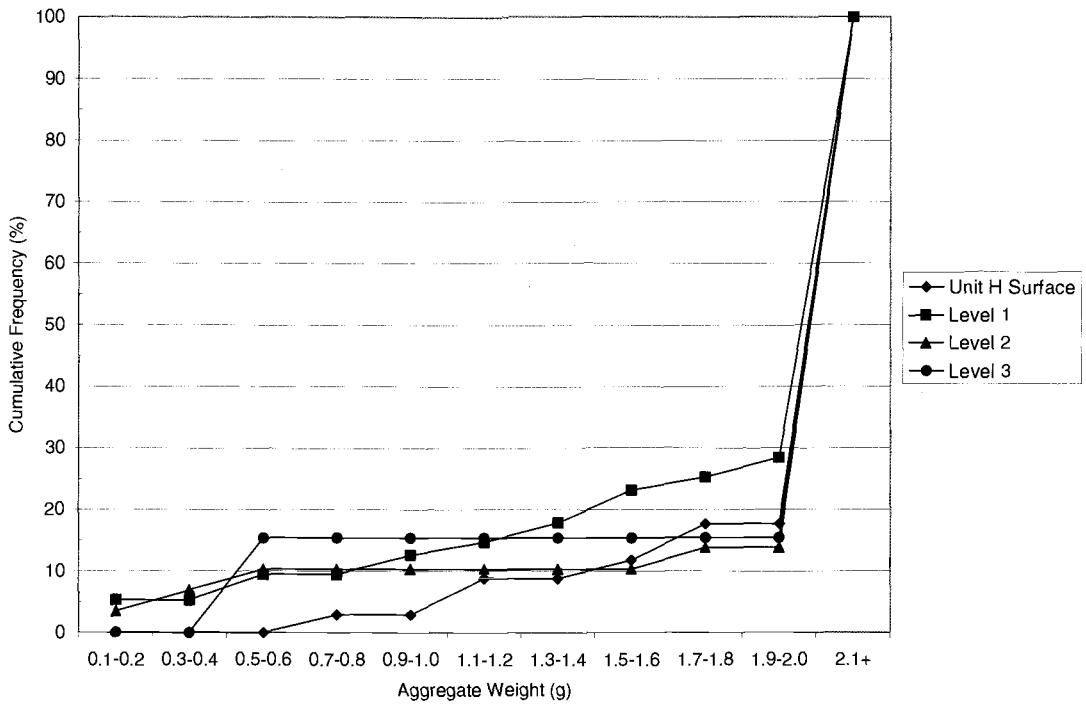

Figure 3.34: Cumulative frequency graph showing aggregate weight class results for the surface assemblage for Unit H.

Tool Analysis

Core (n=8)

Specimen 174, surface level (Figure B.32): The specimen is considered to be a unidirectional core based on the pattern of flake removal. There is no evidence of

platform preparation, and ~20% of the cortex remains on the specimen. The raw material is light rhyolite.

(mm/g)	MxL	MxWDT	MxTHK	WGT	DIR	COR%
	42	28.7	27.7	34.4	uni	20

Specimen 175, level 1(Figure B.17): The specimen is considered to be a unidirectional core based on the pattern of flake removal. There is evidence of platform preparation and grinding, and 10% of the cortex remains on the specimen. The raw material is light rhyolite.

(mm/g)	MxL	MxWDT	MxTHK	WGT	DIR	COR%
	39.9	33.5	22	26.3	uni	10

Specimen 176, level 1(Figure B.29): The specimen is considered to be a unidirectional core based on the pattern of flake removal. There is evidence of platform preparation and grinding, and 50+% of the cortex remains on the specimen. The raw material is light rhyolite.

(mm/g)	MxL	MxWDT	MxTHK	WGT	DIR	COR%
	60	50.8	41.2	99.4	uni	50+

Specimen 178, level 1 (Figure B.17): The specimen is considered to be a unidirectional core based on the pattern of flake removal. There is evidence of platform preparation and grinding, and 30% of the cortex remains on the specimen. The raw material is dark rhyolite.

(mm/g)	MxL	MxWDT	MxTHK	WGT	DIR	COR%
	78	60.2	45.6	199	uni	30

Specimen 179, level 1 (Figure B.30): The specimen is considered to be a multidirectional core based on the pattern of flake removal. There is no evidence of platform preparation, and 5% of the cortex remains on the specimen. The raw material is dark rhyolite.

(mm/g) MxL	MxWDT	MxTHK	WGT	DIR	COR%
49	52.7	45	125.2	multiple	5

Specimen 180, level 1 (Figure B.28): The specimen is considered to be a unidirectional core based on the pattern of flake removal. There is no evidence of platform preparation, and 20% of the cortex remains on the specimen. The raw material is light rhyolite.

(mm/g) MxL	MxWDT	MxTHK	WGT	DIR	COR%
57.4	48.4	39.3	82.7	uni	20

Specimen 181, level 2 (Figure B.25): The specimen is considered to be a unidirectional core based on the pattern of flake removal. There is evidence of platform preparation and grinding, and 5% of the cortex remains on the specimen. The raw material is light rhyolite.

(mm/g) MxL	MxWDT	MxTHK	WGT	DIR	COR%
60.9	38.4	37.8	69.7	uni	5

Specimen 183, level 2 (Figure B.26): The specimen is considered to be a unidirectional core based on the pattern of flake removal. There is evidence of platform preparation and grinding, and 50+% of the cortex remains on the specimen. The raw material is dark rhyolite.

(mm/g) MxL	MxWDT	MxTHK	WGT	DIR	COR%
54.5	50.7	25.6	91.3	uni	50+

Groundstone (n=4)

Specimen 219, level 1: This specimen is considered to be a grinding implement due to the smoothed appearance on one end of the stone. The smoothed end has also been flattened. The specimen is complete and made from light rhyolite.

(mm/g) MxL	MxWDT	MxTHK	WGT
51.8	62	32.9	104.1

Specimen 220, level 2: This specimen is considered to be a grinding implement due to the smoothed flattened appearance on one end of the stone. The specimen has been shaped for a specific use. The specimen is complete and made from light rhyolite.

(mm/g) MxL	MxWDT	MxTHK	WGT
106	58	32.6	200+

Specimen 221, level 2: This specimen is considered to be hammerstone due to the battered appearance on one corner of an end of the stone, most likely due to impact. In the area of the battered end there is discoloration. The specimen is complete and made from basalt.

(mm/g) MxL	MxWDT	MxTHK	WGT
72.9	59.8	40	199.8

Specimen 247, level 2 (Figure B.60): This specimen is considered to be a grinding implement due to the smoothed appearance on one end of the stone. The specimen is complete and made from basalt.

(mm/g) MxL	MxWDT	MxTHK	WGT
58.1	31.6	36.2	83.3

Non-formal modified flakes (n=9)

Specimen 115, level 1: The specimen shows signs of modification on the distal end and is manufactured on a complete interior flake. Flake removal characteristics include a concave uni-marginal area with a continuous wear pattern. The edge angle is 77°, suggesting scraping activities. The raw material is light rhyolite.

(mm/g) MxL	MxWDT	MxTHK	WGT	Edge°	TCT	FST	Edge#
30	36.8	12.6	11.6	77	interior	complete	1

RT Loc	TEC	RTA	RTD
distal	concave	uni-marginal	continuous

Specimen 116, level 1: The specimen shows signs of modification on the left lateral edge and is manufactured on a complete primary flake. Flake removal characteristics include a straight uni-marginal area with a clustered wear pattern. The edge angle is 38°, suggesting this specimen was used as a knife. The raw material is cryptocrystalline silica (CCS).

(mm/g) MxL	MxWDT	MxTHK	WGT	Edge°	TCT	FST	Edge#
46.8	32	11.6	15.7	38	primary	complete	1

RT Loc	TEC	RTA	RTD
left lateral	straight	uni-marginal	clustered

Specimen 142, level 1: The specimen shows signs of modification on the right lateral edge and is manufactured on a broken secondary flake. Flake removal characteristics include a straight uni-marginal area with a continuous wear pattern. The edge angle is 65°, suggesting scraping activities. The raw material is light rhyolite.

(mm/g)	MxL	MxWDT	MxTHK	WGT	Edge°	TCT	FST	Edge#
	41.2	37.5	20.3	32.1	65	secondary	broken	1

RT Loc	TEC	RTA	RTD
right lateral	straight	uni-marginal	continuous

Specimen 160, level 1: The specimen shows signs of modification on the right lateral edge and is manufactured on an interior broken flake. Flake removal characteristics include a concave uni-marginal area with a continuous wear pattern. The edge angle is 67°, suggesting scraping activities. This specimen has been bifacially utilized. The raw material is light rhyolite.

(mm/g)	MxL	MxWDT	MxTHK	WGT	Edge°	TCT	FST	Edge#
	65.8	31.2	13.6	22	67	interior	broken	1

RT Loc	TEC	RTA	RTD
right lateral	concave	uni-marginal	continuous

Specimen 117, level 2: The specimen shows signs of modification on the right lateral area and is manufactured on an interior flake fragment. Flake removal characteristics include a concave uni-marginal area with a continuous wear pattern. The edge angle is 69°, suggesting scraping activities. The raw material is dark rhyolite.

(mm/g)	MxL	MxWDT	MxTHK	WGT	Edge°	TCT	FST	Edge#
	36.1	23	7	5.5	69	interior	fragment	1

RT Loc	TEC	RTA	RTD
right lateral	concave	uni-marginal	continuous

Specimen 118, level 2: The specimen shows signs of modification on the right distal end and is manufactured on a secondary flake fragment. Flake removal characteristics include a straight uni-marginal area with a continuous wear pattern. The edge angle is 64°, suggesting scraping activities. The raw material is dark rhyolite.

(mm/g)	MxL	MxWDT	MxTHK	WGT	Edge°	TCT	FST	Edge#
	26.5	34.4	10	7.3	64	secondary	fragment	1

RT Loc	TEC	RTA	RTD
right distal	straight	uni-marginal	continuous

Specimen 141, level 2: The specimen shows signs of modification on the distal and right lateral edges and is manufactured on a complete interior flake. Flake removal characteristics include a concave surface on the distal end and a straight surface on the right lateral edge. The specimen is bi-marginal with a continuous wear pattern. The edge angle is 29° on the distal end and 71°on the right lateral edge. The raw material is light rhyolite.

(mm/g)	MxL	MxWDT	MxTHK	WGT	Edge°	TCT	FST	Edge#	
	39.1	17	9.3	5.4	29/71	interior	complete	2	distal/

RT Loc	TEC	RTA	RTD
right lateral	Concave/straight	bi-marginal	continuous

Specimen 143, level 2: The specimen shows signs of modification on the left lateral area and is manufactured on an interior flake fragment. Flake removal characteristics include a straight uni-marginal area with a continuous wear pattern. The edge angle is 55°, suggesting some type of saw. The raw material is dark rhyolite.

(mm/g)	MxL	MxWDT	MxTHK	WGT	Edge°	TCT	FST	Edge#
	39.7	32.2	10.7	10.5	55	interior	fragment	1

RT Loc	TEC	RTA	RTD
left lateral	straight	uni-marginal	continuous

Specimen 182, level 2: The specimen shows signs of modification on the left lateral area and is manufactured on an interior flake fragment. Flake removal characteristics

include a straight uni-marginal area with a continuous wear pattern. The edge angle is 82°, suggesting scraping activities. The raw material is dark rhyolite.

(mm/g) MxL	MxWDT	MxTHK	WGT	Edge°	TCT	FST	Edge#
37	34.2	22.4	17.4	82	interior	fragment	1

RT Loc	TEC	RTA	RTD
left lateral	straight	uni-marginal	continuous

Uniface (n=1)

Specimen 177, level 1 (Figure B.3): The specimen is considered a unifacial scraper due to its high edge angle. The uniface contains a grinding pattern usually seen with scrapers. The specimen has a thick cross section. The wear pattern is random. The edge angle is 65-75°. The unifacial scraper is made from light rhyolite.

(mm/g) MxL	MxWDT	MxTHK	WGT	Edge°
60.3	51.5	25.6	56.9	65-75

Unit I

Debitage Analysis

The surface level of unit I includes two formed lithic tools and 71 pieces of lithic debitage; level 1 contains four formed lithic tools and 94 pieces of lithic debitage; level 2 contains five formed lithic tools and 44 pieces of lithic debitage. The results of the triple cortex typology are seen in Figure 4.35 and Table A.1.

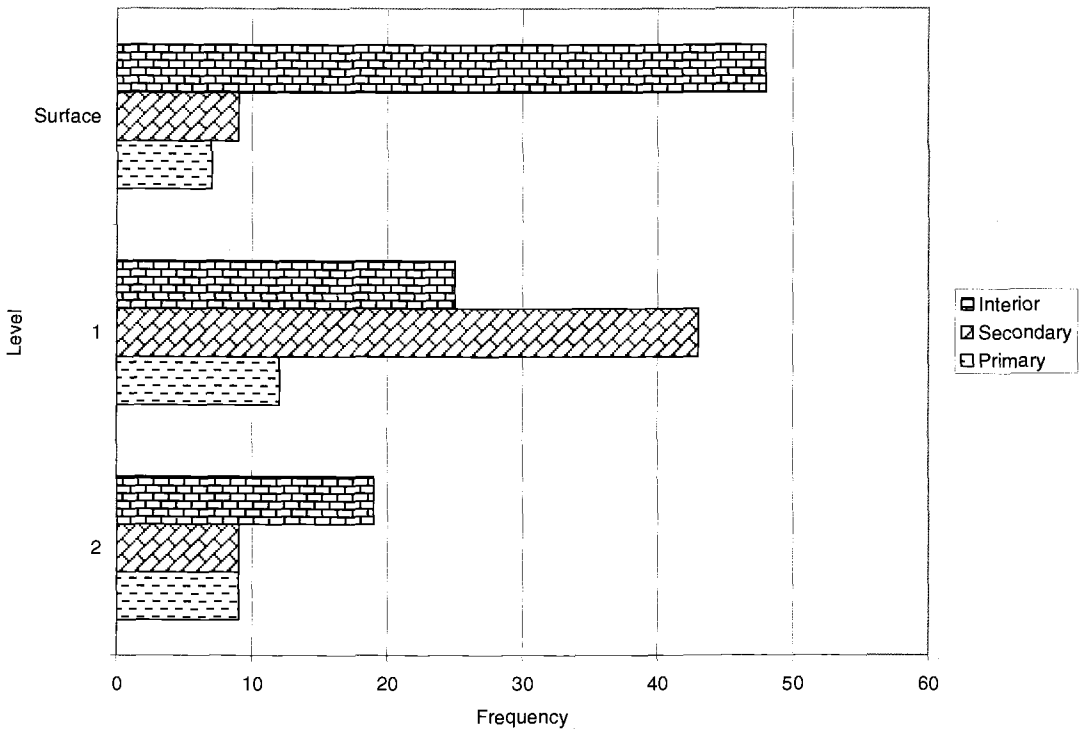

Figure 4.35: Barchart showing triple cortex typology results for the surface and levels 1 & 2 for Unit I.

The surface level is composed of 75% interior flakes, 14.1% secondary flakes, and 10.9% primary flakes. Level 1 contains 53.8% secondary flakes, 31.2% interior flakes, and 15% primary flakes. The level 2 assemblage contains 51.4% interior flakes and the remaining 48.6% is divided evenly among the primary flakes and the secondary flakes. Level 1 contains the variation within the unit.

The results of the free-standing typology can be seen in Figure 4.36 and Table A.2. The surface consisted of 35.2% broken flakes, 31% fragment flakes, 19.7% complete flakes, and 14.1% debris. Level 1 contains a fairly uniform spread of complete flakes (35.1%), broken flakes (27.7%), and fragment flakes (25.5%).

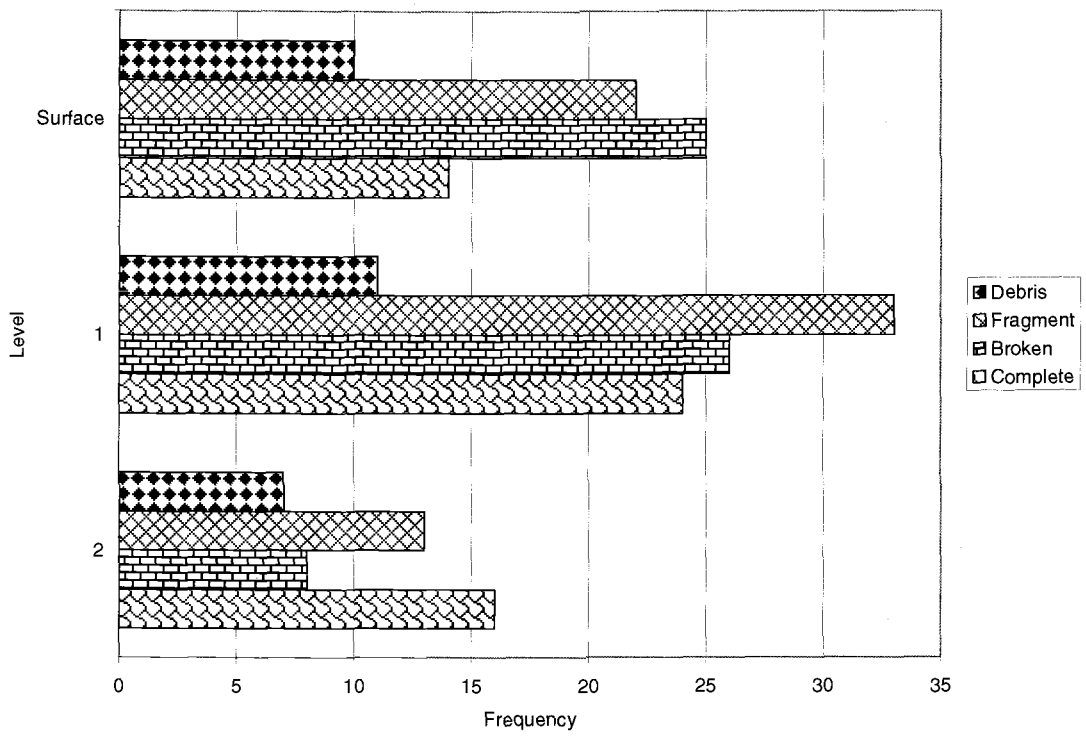

Figure 4.36: Barchart showing free-standing typology results for the surface and levels 1 & 2 of Unit I.

The debris accounted for the remainder of the 11.7% of the population. Level 2 produced a higher percentage of complete flakes (36.4%). The flake fragments accounted for 29.5% of the assemblage while the broken flakes made up 18.2%. The remaining 15.9% was debris.

The results of the size and weight aggregate analysis for unit I are shown in Figure 4.37 and 4.38 as well as Tables A.3 and A.4. All of the levels show a trend in middle stage reduction with a slight peak in the late stage reduction. The surface contains an astonishing 92.6% of the assemblage in the middle size classes (2-5 cm). The remaining 7.4% is divided evenly between size class 1cm and 6cm. The weight analysis for the surface shows that 77.1% of the assemblage falls in the highest weight class. The lower weight classes (0.1-1.0 g) contain 17.1% of the assemblage. The remainder of the assemblage is unevenly distributed within the middle weight classes.

Level 1 contains 64.5% of the assemblage in size classes 3-5cm. The two smallest size classes account for 16.1% of the assemblage. The remaining 19.4% of the assemblage is found in the size classes 6-6+ cm. The weight analysis for level 1 shows that 79.3% of the assemblage falls in the highest weight class; this follows the pattern seen for all of the weight analyses. The weight classes between 0.1 and 1.0 grams contain 17.4% of the assemblage. The remaining 3.3% is unevenly distributed among the middle weight classes.

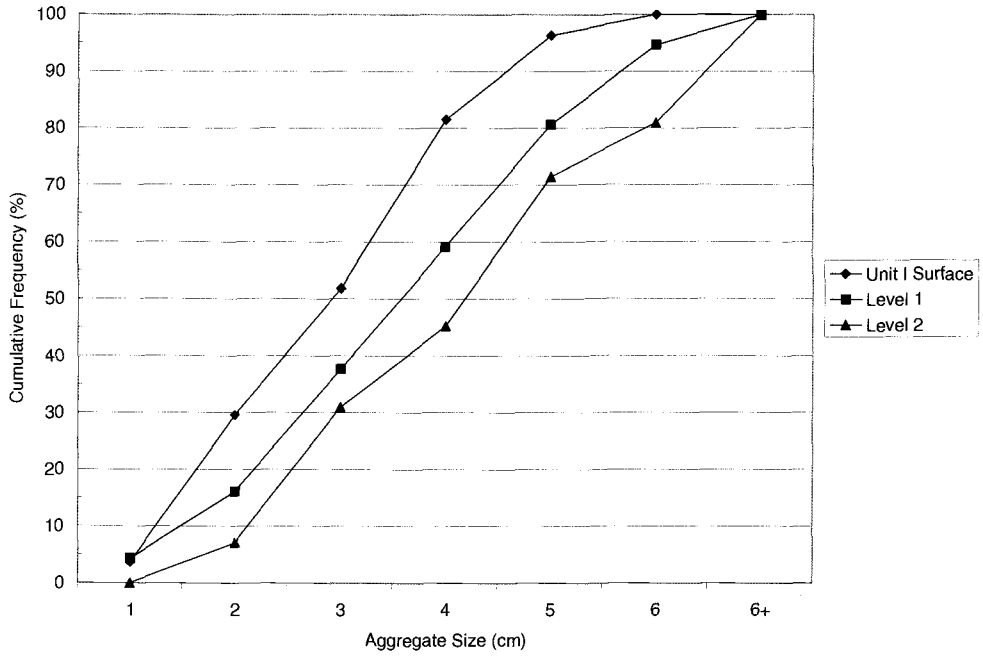

Figure 4.37: Cumulative frequency graph showing aggregate size class results for the surface and levels 1 & 2 of Unit I.

Level 2 shows 64.3% of the assemblage falls in the 3-5 cm size classes. The 2 cm size class contains 7.1% of the assemblage and the 6-6+ cm size class makes up the remaining 28.6%. The weight analysis for level 2 shows 85.4% of the assemblage falls in the 2+ g weight class. The remaining 14.6% is unevenly distributed among the other weight classes.

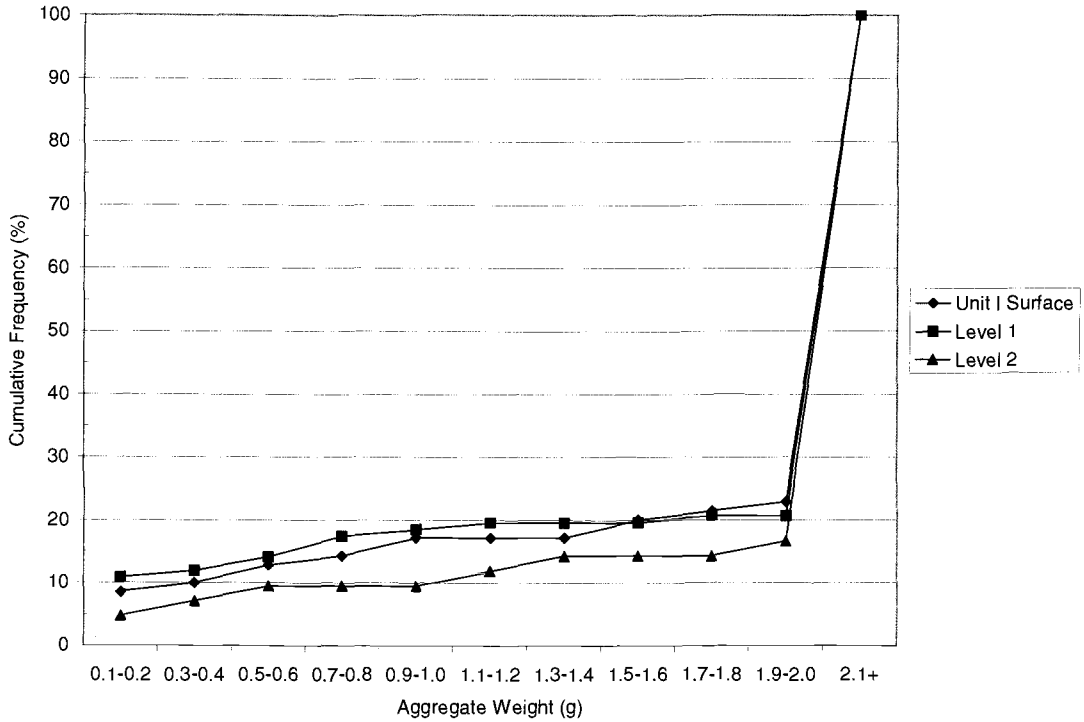

Figure 4.38: Cumulative frequency graph showing aggregate weight class results for the surface and levels 1 & 2 of Unit I.

Tool Analysis

Core (n=4)

Specimen 184, surface level (Figure B.45): The specimen is considered to be a multidirectional core based on the pattern of flake removal. There is no evidence of platform preparation, and less than 5% of the cortex remains on the specimen. The raw material is light rhyolite.

(mm/g)	MxL	MxWDT	MxTHK	WGT	DIR	COR%
	54.3	41	38	59.7	multiple	<5

Specimen 185, level 1 (Figure B.22): The specimen is considered to be a unidirectional core based on the pattern of flake removal. There is evidence of

platform preparation and grinding, and less than 5% of the cortex remains on the specimen. The raw material is light rhyolite.

(mm/g)	MxL	MxWDT	MxTHK	WGT	DIR	COR%
	43.3	38	33.4	54.5	multiple	<5

Specimen 186, level 1 (Figure B.20): The specimen is considered to be a unidirectional core based on the pattern of flake removal. There is no evidence of platform preparation, and 50% of the cortex remains on the specimen. The raw material is quartz.

(mm/g)	MxL	MxWDT	MxTHK	WGT	DIR	COR%
	65.9	64.4	37.5	142.3	uni	50+

Specimen 187, level 2 (Figure B.24): The specimen is considered to be a unidirectional core based on the pattern of flake removal. There is no evidence of platform preparation, and 15% of the cortex remains on the specimen. The raw material is dark rhyolite.

(mm/g)	MxL	MxWDT	MxTHK	WGT	DIR	COR%
	55	38	37.5	65.2	uni	15

Groundstone (n=1)

Specimen 248, level 2 (Figure B.59): This specimen is considered to be a hammerstone due to the crushing on the corner of the stone. The specimen is complete and made of light rhyolite.

(mm/g)	MxL	MxWDT	MxTHK	WGT
	87.8	59.8	36.7	200

Non-formal modified flake (n=5)

Specimen 119, surface level: The specimen shows signs of modification on the left lateral edge and is manufactured on an interior flake fragment. Flake removal characteristics include a straight uni-marginal edge with a continuous wear pattern. The edge angle is 67°, suggesting scraping activities. The raw material is light rhyolite.

(mm/g) MxL	MxWDT	MxTHK	WGT	Edge°	TCT	FST	Edge#
36	49	19.9	25.4	67	interior	fragment	1

RT Loc	TEC	RTA	RTD
left lateral	straight	uni-marginal	continuous

Specimen 156, level 1: The specimen shows signs of modification on the proximal end and is manufactured on an interior broken flake. Flake removal characteristics include a concave uni-marginal area with a continuous wear pattern. The edge angle is 79°, suggesting scraping activities. The raw material is light rhyolite.

(mm/g) MxL	MxWDT	MxTHK	WGT	Edge°	TCT	FST	Edge#
44	34.7	12.5	18.5	79	interior	broken	1

RT Loc	TEC	RTA	RTD
proximal	concave	uni-marginal	continuous

Specimen 157, level 1: The specimen shows signs of modification on the distal end and is manufactured on a secondary broken flake. Flake removal characteristics include a concave uni-marginal surface with a continuous wear pattern. The edge angle is 48°, suggesting some type of saw. The raw material is light rhyolite.

(mm/g)	MxL	MxWDT	MxTHK	WGT	Edge°	TCT	FST	Edge#
	55.6	37.9	11.3	23.9	48	secondary	broken	1

RT Loc	TEC	RTA	RTD
distal	concave	uni-marginal	continuous

Specimen 120, level 2: The specimen shows signs of modification on the right lateral edge and is manufactured on a complete interior flake. Flake removal characteristics include a straight uni-marginal surface with a continuous wear pattern. The edge angle is 79°, suggesting scraping activities. The raw material is dark rhyolite.

(mm/g)	MxL	MxWDT	MxTHK	WGT	Edge°	TCT	FST	Edge#
	50	28.6	16.6	13.8	79	interior	complete	1

RT Loc	TEC	RTA	RTD
right lateral	straight	uni-marginal	continuous

Specimen 188, level 2: The specimen shows signs of modification on the right lateral area and is manufactured on a primary broken flake. Flake removal characteristics include a straight uni-marginal surface with a continuous wear pattern. The edge angle is 65°, suggesting scraping activities. The raw material is dark rhyolite.

(mm/g)	MxL	MxWDT	MxTHK	WGT	Edge°	TCT	FST	Edge#
	53.2	59	21.8	69.8	65	primary	broken	1

RT Loc	TEC	RTA	RTD
right lateral	straight	uni-marginal	continuous

Biface (n=1)

Specimen 159, level 2 (Figure B.5): The specimen is considered a biface blank due to the lack of formal flake removal. It contains a thick cross section. There are multiple small flakes removed from one side of the specimen. There is no grinding present on

the biface. The range of the edge angle is 60-70°, suggesting that the tool was used for scraping activities. The raw material is light rhyolite.

(mm/g) MxL	MxWDT	MxTHK	WGT	Edge°
52	42.4	20.5	35.7	60-70

Unit J

Debitage Analysis

The surface level of unit J includes one formed lithic tool and 35 pieces of lithic debitage; level 1 contains five formed lithic tools and 103 pieces of lithic debitage; level 2 contains three formed lithic tools and 50 pieces of lithic debitage. The results of the triple cortex typology are seen in Figure 4.39 and Table A.1. The surface level comprises 62.9% interior flakes, 25.7% secondary flakes, and 11.4% primary flakes. Level 1 contains similar results to the surface with 63.9% being interior flakes, 24.7% secondary flakes, and 11.3% primary flakes. The level 2 assemblage contains a majority of interior flakes, with 89.6% of the population. The secondary flakes account for 8.3% of the assemblage and the remaining 2.1% is primary flakes.

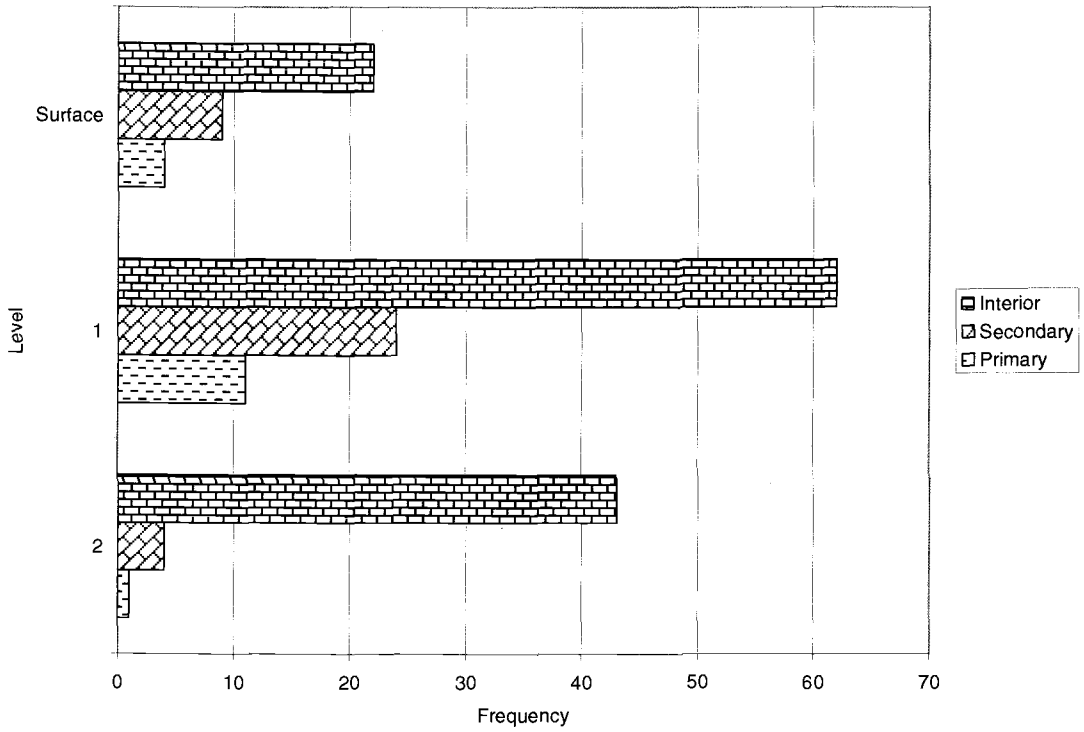

Figure 4.39: Barchart showing triple cortex typology results for the surface and levels 1 & 2 of Unit J.

The results of the free-standing typology can be seen in Figure 4.40 and Table A.2. The surface consists of 42.6% fragment flakes, 37.1% broken flakes, and 20% complete flakes. Level 1 contains a uniform spread of complete flakes (32%), broken flakes (29.1%), and fragment flakes (35%). The debris accounted for the remainder of the 3.9% of the population. Level 2 produced a higher percentage of broken flakes, with 50% of the population. The complete flakes account for 24% of the assemblage while the fragment flakes make up 20%. The remaining 6% is debris.

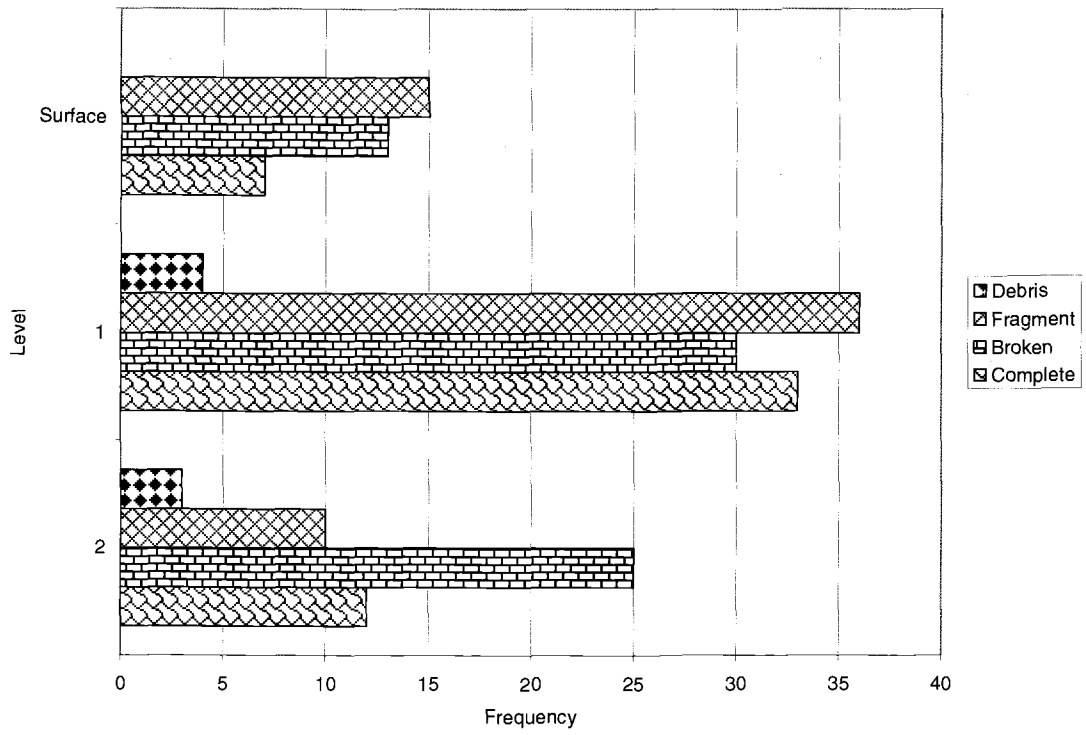

Figure 4.40: Barchart showing free-standing typology results for the surface and levels 1 & 2 of Unit J.

The results of the size and weight aggregate analysis for unit J are shown in Figure 4.41 and 4.42 as well as Tables A.3 and A.4. All the levels of unit J show a trend in middle stage reduction when looking at the size analysis and an early stage reduction when looking at the weight analysis. The surface contains an anticipated 88.2% of the assemblage in the middle size classes (3-5 cm). The remaining 11.8% falls in the 6-6+ cm size class. The weight analysis for the surface shows that 76.5% of the assemblage falls in the highest weight class. The remaining 23.5% of the assemblage falls in the middle weight classes. Level 1 contains 75.5% of the assemblage in size classes 3-5 cm. The two smallest size classes account for 6.7% of the assemblage. The remaining 17.8% of the assemblage is found in the size classes 6-6+ cm. The weight analysis for level 1 shows that 85.3% of the assemblage falls in

the highest weight class. The weight classes between 1.0 and 2.0 g contain 12.7% of the assemblage. The remaining 2% is unevenly distributed among the lowest weight classes.

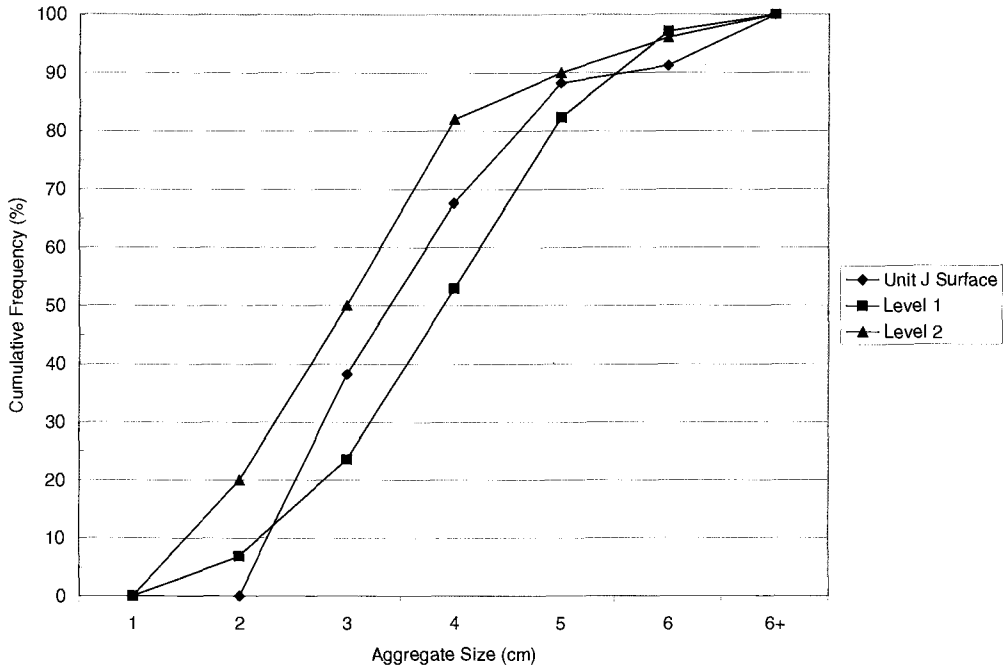

Figure 4.41: Cumulative frequency graph showing aggregate size class results of the surface and levels 1 & 2 of Unit J.

Level 2 shows 82% of the assemblage falls in the 2-4 cm size classes. The 5-6+ cm size classes make up the remaining 18%. The weight analysis for level 2 shows 63.3% of the assemblage falls in the 2+ g weight class. The weight classes between 0.1 and 1.0 contain 24.5% of the assemblage. The remaining 10.2% of the assemblage falls within 1.2 and 2.0 g.

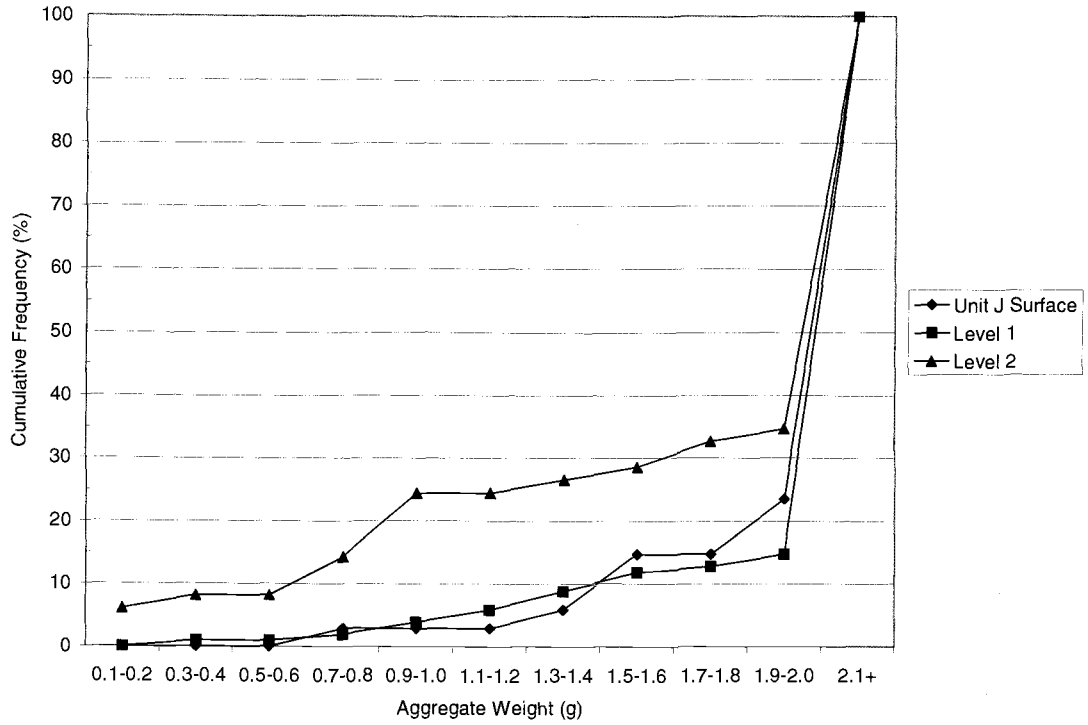

Figure 4.42: Cumulative frequency graph showing aggregate weight class results for the surface and levels 1 & 2 of Unit J.

Tool Analysis

Core (n=5)

Specimen 189, level 1(Figure B.21): The specimen is considered to be a unidirectional core based on the pattern of flake removal. There is evidence of platform preparation and grinding, and greater than 50% of the cortex remains on the specimen. The raw material is dark rhyolite.

(mm/g) MxL	MxWDT	MxTHK	WGT	DIR	COR%
42.2	36.8	22.4	57.4	uni	50+

Specimen 190, level 1 (Figure B.23): The specimen is considered to be a multidirectional core based on the pattern of flake removal. There is evidence of

platform preparation and grinding, and less than 5% of the cortex remains on the specimen. The raw material is dark rhyolite.

(mm/g) MxL	MxWDT	MxTHK	WGT	DIR	COR%
53.2	37.7	24	52	multiple	<5

Specimen 191, level 1 (Figure B.18): The specimen is considered to be a unidirectional core based on the pattern of flake removal. There is evidence of platform preparation and grinding, and greater than 50% of the cortex remains on the specimen. The raw material is light rhyolite.

(mm/g) MxL	MxWDT	MxTHK	WGT	DIR	COR%
67	52.6	43	121.8	uni	50+

Specimen 192, level 2 (Figure B.41): The specimen is considered to be a unidirectional core based on the pattern of flake removal. There is evidence of platform preparation and grinding, and 30% of the cortex remains on the specimen. The raw material is light rhyolite.

(mm/g) MxL	MxWDT	MxTHK	WGT	DIR	COR%
52.1	29.1	28.7	43.6	uni	30

Specimen 193, level 2 (Figure B.42): The specimen is considered to be a unidirectional core based on the pattern of flake removal. There is evidence of platform preparation and grinding, and 30% of the cortex remains on the specimen. The raw material is dark rhyolite.

(mm/g) MxL	MxWDT	MxTHK	WGT	DIR	COR%
50.2	34	35	57.2	uni	30

Non-formal modified flake (n=3)

Specimen 121, surface level: The specimen shows signs of modification on the left lateral edge and is manufactured on an interior broken flake. Flake removal characteristics include a concave uni-marginal surface with a continuous wear pattern. The edge angle is 70°, suggesting scraping activities. The raw material is light rhyolite.

(mm/g)	MxL	MxWDT	MxTHK	WGT	Edge°	TCT	FST	Edge#
	58	37.1	22.2	36.4	70	interior	broken	1

RT Loc	TEC	RTA	RTD
left lateral	concave	uni-marginal	continuous

Specimen 122, level 1: The specimen shows signs of modification on the left lateral edge and is manufactured on a secondary broken flake. Flake removal characteristics include a concave uni-marginal surface with a continuous wear pattern. The edge angle is 56°, suggesting some type of saw. The raw material is cryptocrystalline silica (CCS).

(mm/g)	MxL	MxWDT	MxTHK	WGT	Edge°	TCT	FST	Edge#
	35.6	31.2	10	10.4	56	secondary	broken	1

RT Loc	TEC	RTA	RTD
left lateral	concave	uni-marginal	continuous

Specimen 123, level 1: The specimen shows signs of modification on the left lateral edge and is manufactured on a primary broken flake. Flake removal characteristics

include a concave uni-marginal surface with a continuous wear pattern. The edge angle is 64°, suggesting scraping activities. The raw material is light rhyolite.

(mm/g) MxL	MxWDT	MxTHK	WGT	Edge°	TCT	FST	Edge#
42.2	61	14.2	26.5	64	primary	broken	1

RT Loc	TEC	RTA	RTD
left lateral	concave	uni-marginal	continuous

Uniface (n=1)

Specimen 154, level 2 (Figure B.1): The specimen is considered a unifacial scraper due to the degree of the edge angle. The specimen is broken. Where the broken surface meets the lateral edge there is evidence of grinding. The flake removal characteristics show random wear patterning. The range of the edge angle is 62-75°, suggesting that the tool was used for scraping activities. The raw material is dark rhyolite.

(mm/g) MxL	MxWDT	MxTHK	WGT	Edge°
53	41.9	16.4	39.6	62-75

Unit K

Debitage Analysis

One formed lithic tool and 27 pieces of lithic debitage were recovered from Unit K. Figure 4.43 and Table A.1 show the results of analysis using the triple cortex typology.

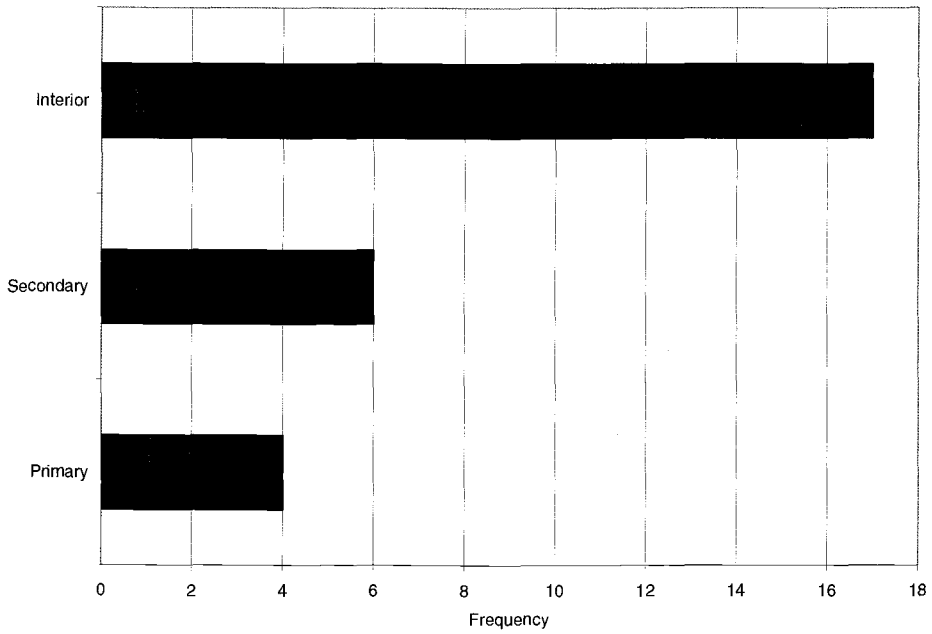

Figure 4.43: Barchart showing the triple cortex typology results for the surface of Unit K.

The surface assemblage of unit A contained a majority of interior flakes (63%). The secondary flakes accounted for 22.2% and the primary flakes made up the remaining 14.8% of the population.

The results of the free-standing typology are shown in Figure 4.44 and Table A.2. The fragment flakes account for 36.7% of the assemblage, followed by broken flakes with 33.3%. The complete flakes account for 20% and the debris made up the remaining 10%.

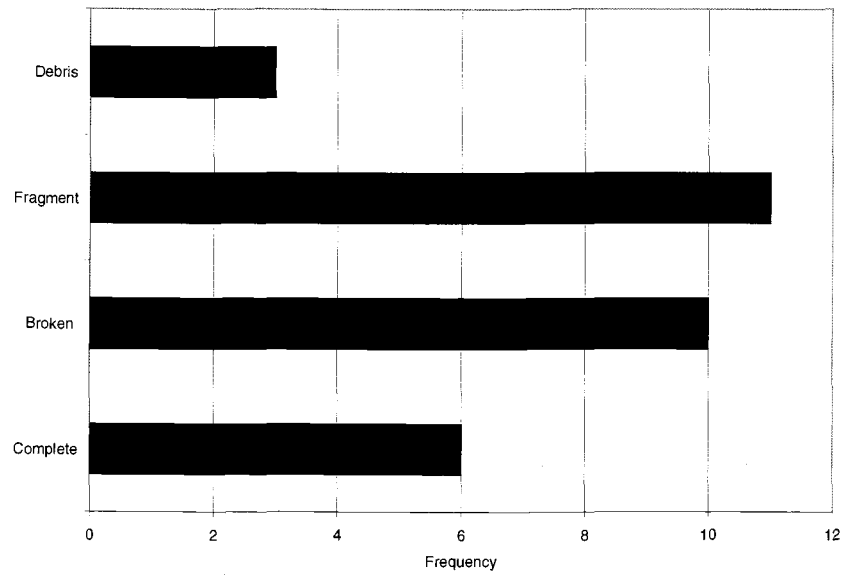

Figure 4.44: Barchart showing free-standing typology results for the surface of Unit K.

Size and weight aggregate analyses for unit K are illustrated in Table A.3 and A.4. A cumulative frequency chart (Figure 4.45) shows 86.2% of the flakes fall within the three middle size classes (3-5 cm).

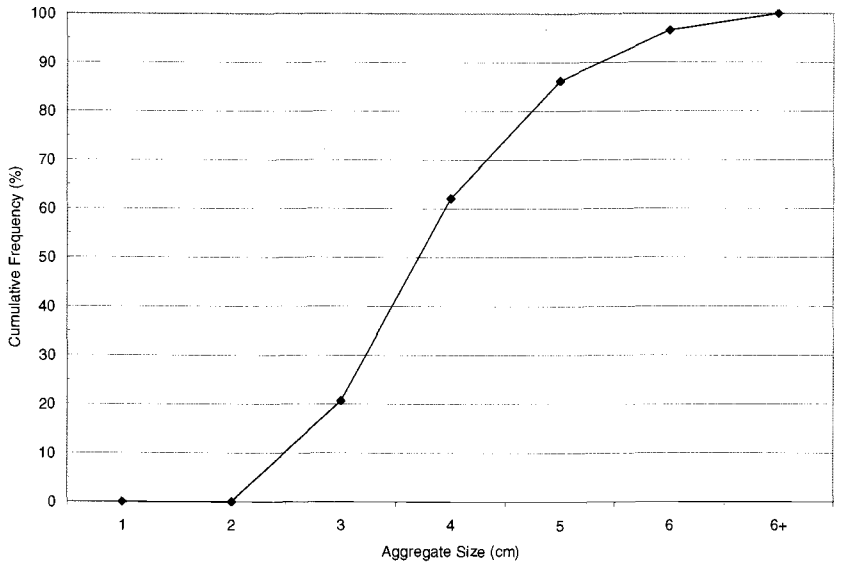

Figure 4.45: Cumulative frequency graph showing aggregate size class results for the surface assemblage of Unit K.

The remaining 13.8% of the assemblage falls in the two largest size classes. Weight analysis (Figure 4.46) for the surface shows 93.1% of the assemblage falls in the highest weight class. The remaining 6.9% is unevenly distributed among the other weight classes.

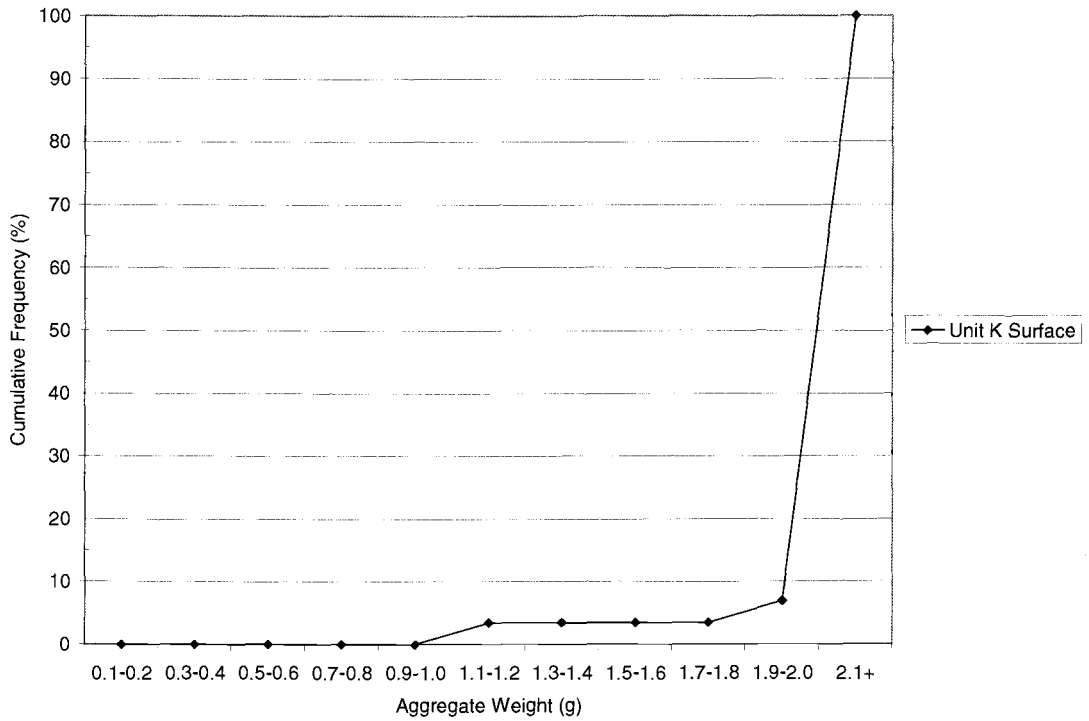

Figure 4.46: Cumulative frequency graph showing aggregate weight class results for the surface assemblage of Unit K.

Tool Analysis

Non-formal modified flake (n=1)

Specimen 161, surface level: The specimen shows signs of modification on the right lateral edge and is manufactured on an interior broken flake. Flake removal characteristics include a concave uni-marginal surface with a continuous wear pattern.

The edge angle is 61°, suggesting scraping activities. The specimen is bifacially utilized. The raw material is dark rhyolite.

(mm/g) MxL	MxWDT	MxTHK	WGT	Edge°	TCT	FST	Edge#
67.6	20.1	15	12.4	61	interior	broken	1

RT Loc	TEC	RTA	RTD
right lateral	concave	uni-marginal	continuous

Unit L

Debitage Analysis

The surface level of unit L generated no tools and 17 pieces of lithic debitage. Figure 4.47 and Table A.1 show the results of the triple cortex typology. The majority of the flakes were interior flakes (58.8%). Secondary flakes accounted for 23.5 % of the assemblage with primary flakes making up the remaining 17.7%.

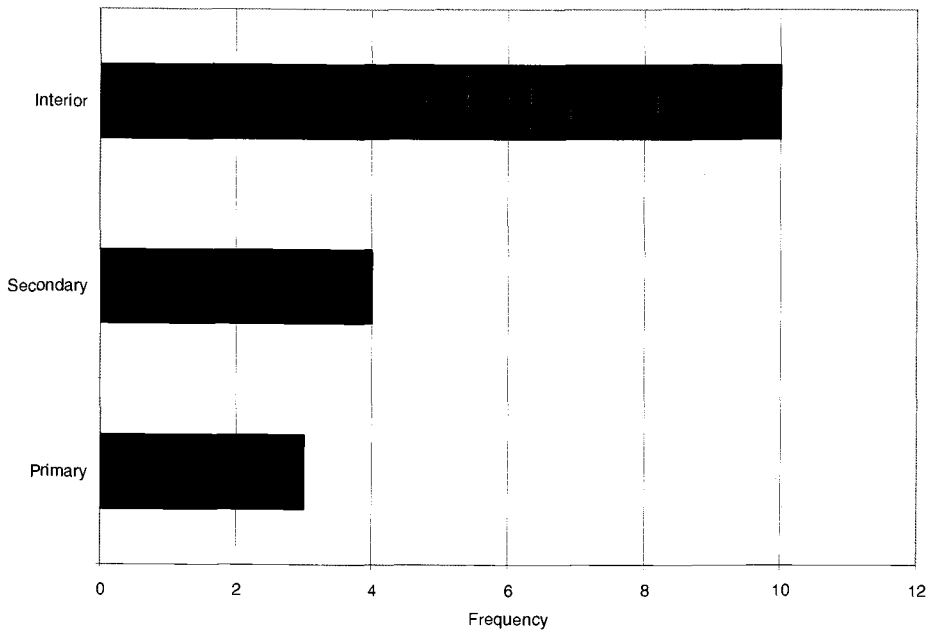

Figure 4.47: Barchart showing triple cortex typology results for the surface assemblage of Unit L.

The results of the free-standing typology are shown in Figure 4.48 and Table A.2. The complete flakes account for 38.9% of the assemblage, followed by fragment flakes with 33.3%. The broken flakes account for 22.2% and the debris made up the remaining 5.6%.

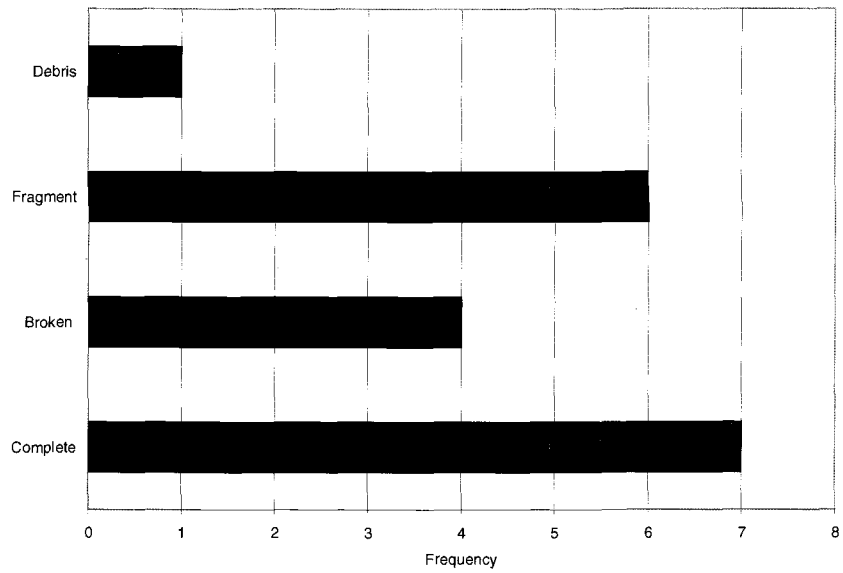

Figure 4.48: Barchart showing results for the free-standing typology of the surface assemblage of Unit L.

Size and weight aggregate analyses for unit L are illustrated in Table A.3 and A.4. The size analysis (Figure 4.49) shows that 83.3% of the flakes fall within the three middle size classes (3-5 cm). The 2 cm size class contains 5.5% of the assemblage while the 6cm size class contains the remaining 11.2% of the assemblage. The weight analysis (Figure 4.50) for the surface shows 77.8% of the assemblage falls in the highest weight class. The remaining 22.2% is unevenly distributed among the other weight classes.

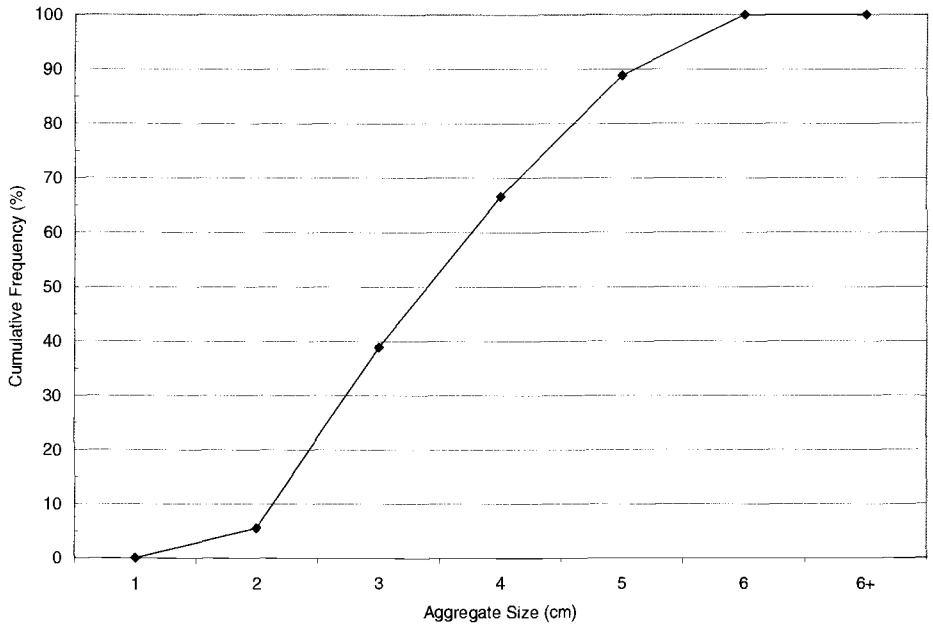

Figure 4.49: Cumulative frequency graph showing aggregate size analysis results for the surface assemblage of Unit L.

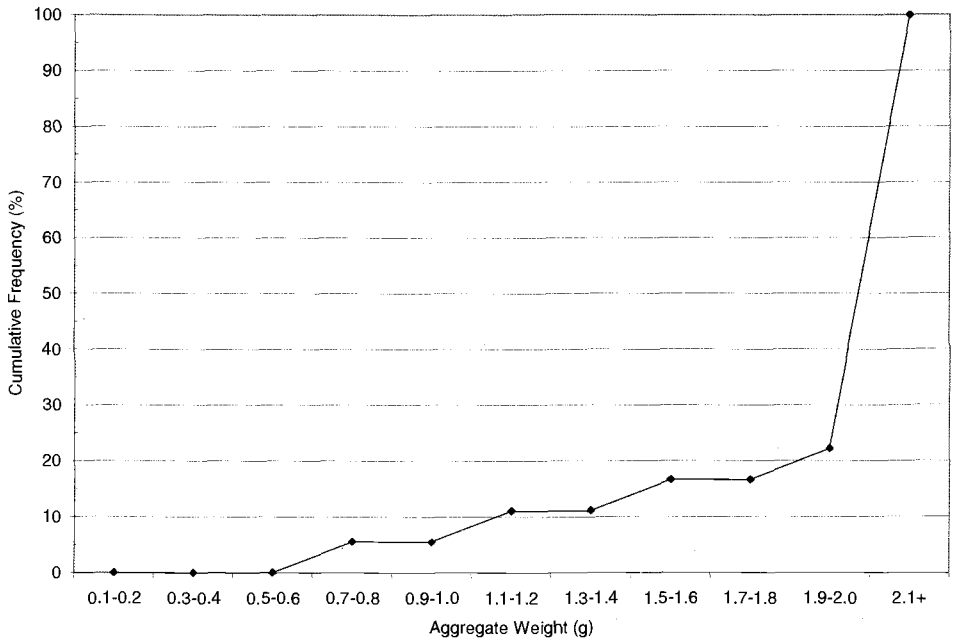

Figure 4.50: Cumulative frequency graph showing aggregate weight class results for the surface assemblage of Unit L.

Unit M

Debitage Analysis

The surface level of unit M includes two formed lithic tools and 23 pieces of lithic debitage. Level 1 contains six formed lithic tools and 189 pieces of lithic debitage. Level 2 contains seven formed lithic tools and 27 pieces of lithic debitage. Level 3 contains one formed lithic tool and 5 pieces of lithic debitage. The results of the triple cortex typology are seen in Figure 4.51 and Table A.1. The surface level is composed of 80% interior flakes and 20% secondary flakes. Level 1 contains 85.9% interior flakes, 9.8% secondary flakes, and 4.4% primary flakes. The level 2 assemblage contains 68.2% interior flakes, 22.7% secondary flakes, and 9.1% primary flakes. The majority of the flakes in level 3 are interior, with 80% of the population. Surprisingly, the primary flakes account for the remaining 20% of the assemblage.

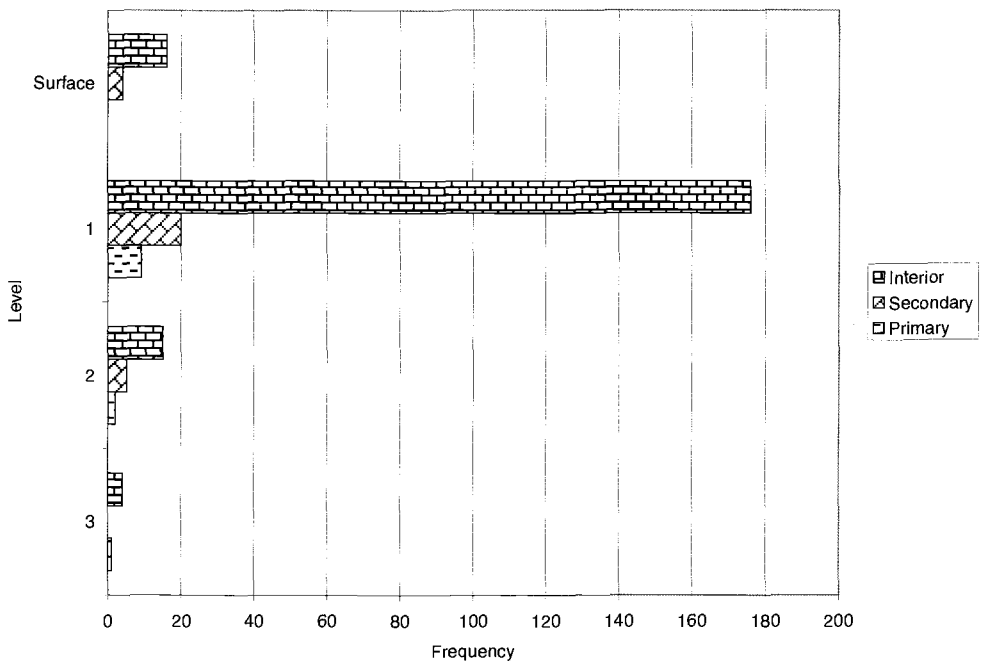

Figure 4.51: Barchart showing the triple cortex typology results for the surface and levels 1, 2, & 3 of Unit M.

The results of the free-standing typology can be seen in Figure 4.52 and Table A.2. The majority of the surface flakes fall in the category of broken flakes, with 56.5% of the assemblage. The fragment flakes account for 17.4% of the population and the complete flakes account for 13%. The remaining 13% is debris. Level 1 contained 35.5% fragment flakes, 32.3% broken flakes, 25.9% complete flakes, and 6.3% is debris. The assemblage for level 2 shows 37% going for the complete flakes, 29.6% for the fragment flakes, 14.8% for the broken flakes, and 18.5% for the debris. Level 3 splits 80% of the assemblage evenly between fragmented flakes and broken flakes. The complete flakes make up the remaining 20% of the population.

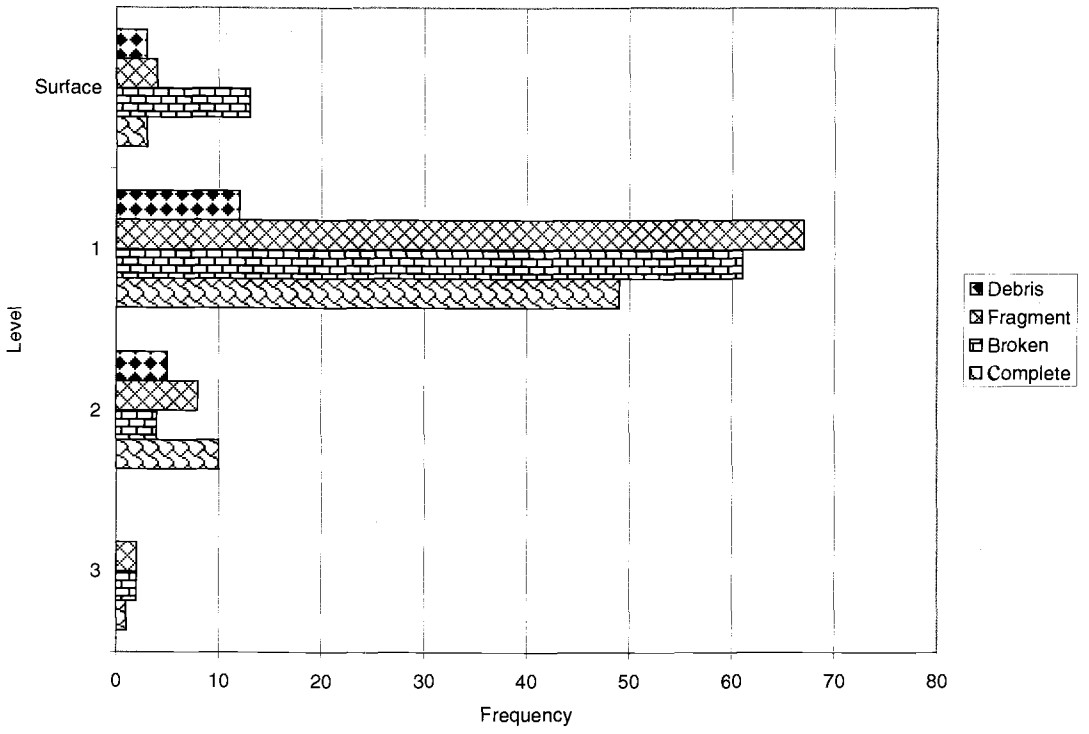

Figure 4.52: Barchart showing free-standing typology results for the surface and levels 1, 2, & 3 of Unit M

The results of the size and weight aggregate analysis for unit M are shown in Figure 4.53 and 4.54 as well as Tables A.3 and A.4. All of the levels show a trend in

middle stage reduction, with the exception of level 1 which has an unusually high percentage of flakes in the late stage reduction classes. The surface contains 95.7% of the assemblage in the 3-5 cm size classes. The remaining 4.3% is in the 6+ cm class. The weight analysis for the surface shows that 91.3% of the assemblage falls in the highest weight class. The remainder of the assemblage is unevenly distributed within the middle weight classes. Level 1 contains 37.6% of the assemblage in size classes 3-5 cm. The smallest size class accounts for an astonishing 54.5% of the assemblage. The remaining 7.9% of the assemblage is found in the size classes 6-6+ cm. The weight analysis for level 1 shows that 36.4% of the assemblage falls in the highest weight class. The weight classes between 0.1 and 1.0 g contain 54% of the assemblage. The remaining 9.6% is unevenly distributed among the middle weight classes.

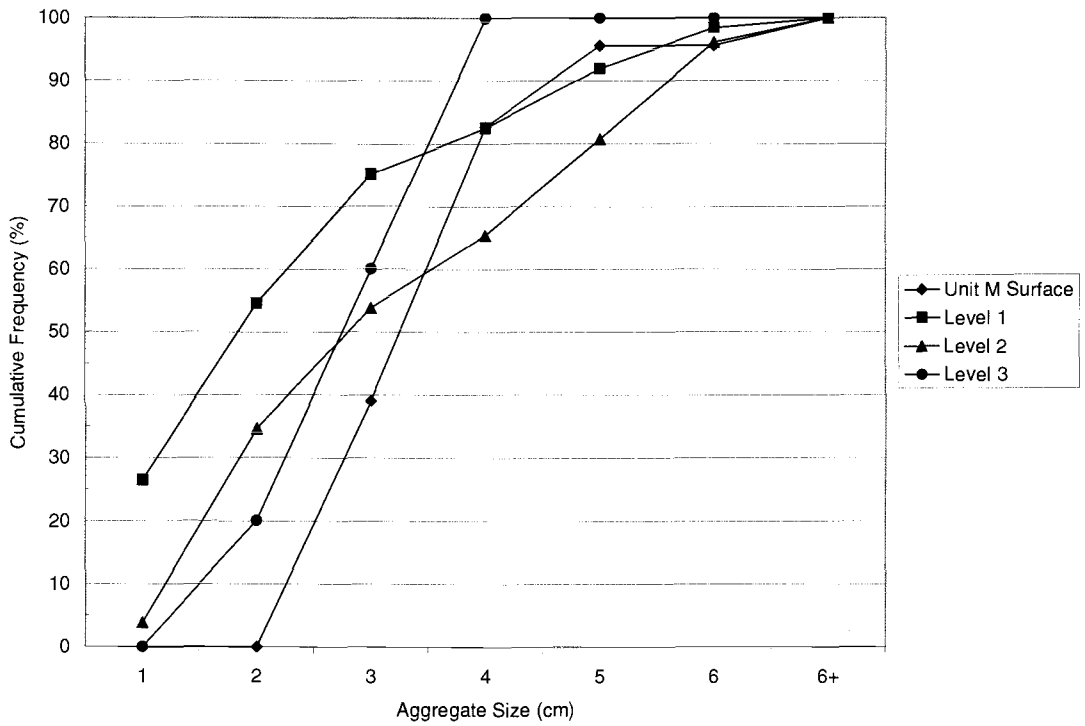

Figure 4.53: Cumulative frequency graph showing the results from the size aggregate analysis for the surface and levels 1, 2, & 3 of Unit M.

Level 2 contains 50% of the assemblage in size classes 2-3 cm and 42.4% of the assemblage in size classes 4-6 cm. The smallest size classes accounts for 3.8% of the assemblage and the remaining 3.8% of the population falls in the highest size class. The weight analysis for level 2 shows that 51.9% of the assemblage falls in the highest weight class (2.1+ g). The weight classes of 0.6 and smaller account for 29.6% of the assemblage. The remaining 18.5% is unevenly distributed among the middle weight classes. Level 3 contains 100% of the assemblage in size classes 2-4 cm. The weight analysis for level 3 shows that 83.3% of the assemblage falls in the highest weight class. The remainder of the assemblage falls in the lowest weight class, with 16.7%.

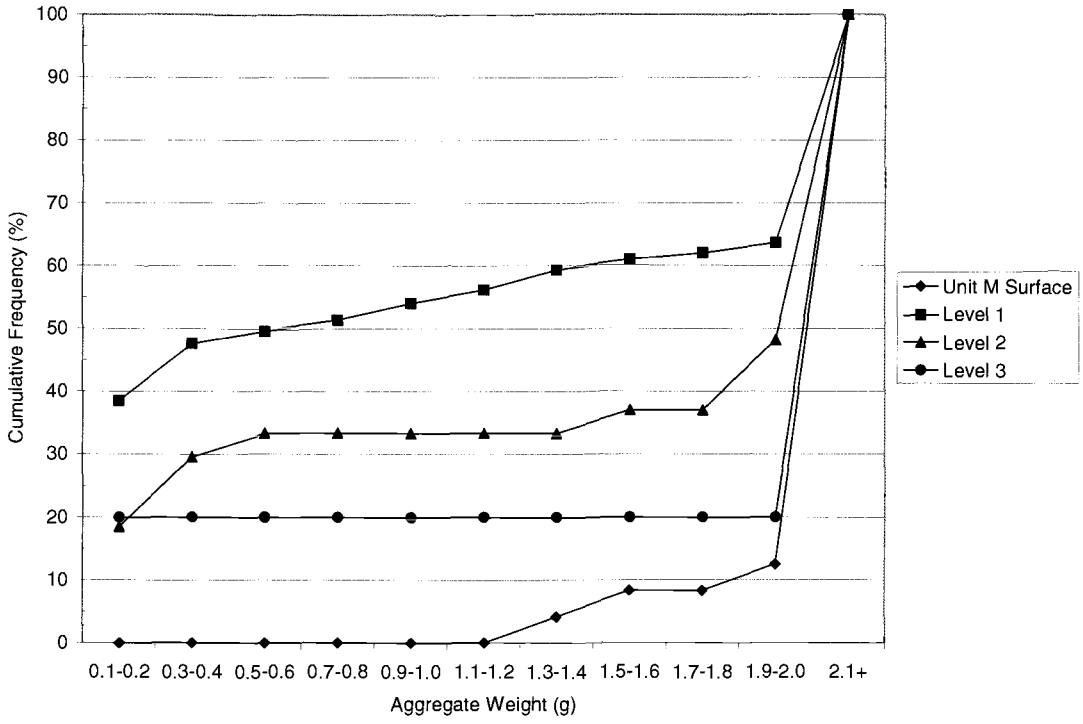

Figure 4.54: Cumulative frequency graph showing aggregate weight class results for the surface and levels 1, 2, & 3 of Unit M.

Tool Analysis

Core (n=4)

Specimen 194, level 1 (Figure B.19): The specimen is considered to be a multidirectional core based on the pattern of flake removal. There is evidence of platform preparation and grinding, and 30% of the cortex remains on the specimen. The raw material is dark rhyolite.

(mm/g)	MxL	MxWDT	MxTHK	WGT	DIR	COR%
	50.8	42.4	46	106	multiple	30

Specimen 195, level 2 (Figure B.43): The specimen is considered to be a unidirectional core based on the pattern of flake removal. There is evidence of platform preparation and grinding, and 10% of the cortex remains on the specimen. The raw material is dark rhyolite.

(mm/g)	MxL	MxWDT	MxTHK	WGT	DIR	COR%
	49.8	52	30.6	97.6	uni	10

Specimen 196, level 2 (Figure B.47): The specimen is considered to be a unidirectional core based on the pattern of flake removal. There is no evidence of platform preparation, and greater than 50% of the cortex remains on the specimen. The raw material is light rhyolite.

(mm/g)	MxL	MxWDT	MxTHK	WGT	DIR	COR%
	54.6	45.2	36	82.9	uni	50+

Specimen 197, level 2 (Figure B.49): The specimen is considered to be a unidirectional core based on the pattern of flake removal. There is evidence of

platform preparation and grinding, and less than 5% of the cortex remains on the specimen. The raw material is light rhyolite.

(mm/g)	MxL	MxWDT	MxTHK	WGT	DIR	COR%
	128.8	85.1	43.3	200+	uni	<5

Groundstone (n=3)

Specimen 226, level 1 (Figure B.64): This specimen is considered to be a grinding implementation due to the smoothed surface on the face of the stone. The specimen has been shaped and there is discoloration around the utilized surface. The specimen is complete and made from basalt.

(mm/g)	MxL	MxWDT	MxTHK	WGT
	125.5	85	104	200+

Specimen 222, level 2: This specimen is considered to be a grinding stone due to the smoothed surface on one of the ends. It has been utilized to the point that it is flattened. The specimen is complete and made from light rhyolite.

(mm/g)	MxL	MxWDT	MxTHK	WGT
	61.9	48.8	33.6	138.1

Specimen 249, level 2 (Figure B.58): This specimen is considered to be a grinding stone due to the smooth surface on one end of the stone. It has been evidence of being shaped. The other end of the tool displays discolorations. The specimen is complete and made from light rhyolite.

(mm/g)	MxL	MxWDT	MxTHK	WGT
	74.8	38.7	31.8	115.1

Non-formal modified flake (n=7)

Specimen 124, surface level: The specimen exhibits modification on the right lateral edge and is manufactured on an interior flake fragment. Flake removal characteristics include a concave uni-marginal surface with a continuous wear pattern. The edge angle is 45°, possibly a saw. The raw material is dark rhyolite.

(mm/g)	MxL	MxWDT	MxTHK	WGT	Edge°	TCT	FST	Edge#
	53.4	44.3	11.7	25	45	interior	fragment	1

RT Loc	TEC	RTA	RTD
right lateral	concave	uni-marginal	continuous

Specimen 125, surface level: The specimen shows signs of modification on the distal end and is manufactured on an interior flake fragment. Flake removal characteristics include a concave uni-marginal surface with a continuous wear pattern. The edge angle is 55°, suggesting use as a saw. The raw material is light rhyolite.

(mm/g)	MxL	MxWDT	MxTHK	WGT	Edge°	TCT	FST	Edge#
	53	36	24	39.8	55	interior	fragment	1

RT Loc	TEC	RTA	RTD
distal	concave	uni-marginal	continuous

Specimen 126, level 1: The specimen shows signs of modification on the distal end and is manufactured on an interior flake fragment. Flake removal characteristics include a concave uni-marginal surface with a continuous wear pattern. The edge angle is 64°, suggesting scraping activities. There is evidence for a polish on the micro fractures. The raw material is light rhyolite.

(mm/g)	MxL	MxWDT	MxTHK	WGT	Edge°	TCT	FST	Edge#
	28	18	6.4	2.9	64	interior	fragment	1

RT Loc	TEC	RTA	RTD
distal	concave	uni-marginal	continuous

Specimen 127, level 1: The specimen shows signs of modification on the right lateral edge and is manufactured on a secondary flake fragment. Flake removal characteristics include a concave uni-marginal surface with a continuous wear pattern. The edge angle is 60°, suggesting scraping activities. The raw material is light rhyolite.

(mm/g)	MxL	MxWDT	MxTHK	WGT	Edge°	TCT	FST	Edge#
	42.5	30.5	17	20.9	60	secondary	fragment	1

RT Loc	TEC	RTA	RTD
right lateral	concave	uni-marginal	continuous

Specimen 128, level 1: The specimen shows signs of modification on the proximal end and is manufactured on a broken interior flake. Flake removal characteristics include a concave uni-marginal surface with a continuous wear pattern. The edge angle is 62°, suggesting scraping activities. The raw material is light rhyolite.

(mm/g)	MxL	MxWDT	MxTHK	WGT	Edge°	TCT	FST	Edge#
	45	36	13	17.8	62	interior	broken	1

RT Loc	TEC	RTA	RTD
proximal	concave	uni-marginal	continuous

Specimen 129, level 2: The specimen shows signs of modification on the left lateral edge and is manufactured on a secondary flake fragment. Flake removal characteristics include a convex uni-marginal surface with a continuous wear pattern. The edge angle is 72°, suggesting scraping activities. The raw material is light rhyolite.

(mm/g)	MxL	MxWDT	MxTHK	WGT	Edge°	TCT	FST	Edge#
	43	75	20.5	62.6	72	secondary	fragment	1

RT Loc	TEC	RTA	RTD
left lateral	convex	uni-marginal	continuous

Specimen 144, level 3: The specimen shows signs of modification on the proximal end and is manufactured on a primary flake fragment. Flake removal characteristics include a straight uni-marginal edge with a continuous micro-wear pattern. The edge angle is 25°, suggesting use as a knife. The raw material is red conglomerate rhyolite.

(mm/g)	MxL	MxWDT	MxTHK	WGT	Edge°	TCT	FST	Edge#
	42.5	39.5	25.9	53	25	primary	fragment	1

RT Loc	TEC	RTA	RTD
proximal	straight	uni-marginal	continuous

Biface (n=3)

Specimen 162, level 1 (Figure B.6): The specimen is considered a biface blank due to the lack of formal thinning flake removal. There are multiple step fractures apparent on one side of the specimen. There is some cortex still noticeable on the surface of the stone. Flake removal characteristics include a collateral wear pattern. There is no

grinding present on the biface. The range of the edge angle is 60-70°, suggesting that the tool was used for scraping activities. The raw material is light rhyolite.

(mm/g) MxL	MxWDT	MxTHK	WGT	Edge°
54.7	30.7	14.2	22	60-70

Specimen 163, level 1 (Figure B.7): The specimen is considered a biface blank due to the lack of formal thinning flake removal. Flake removal characteristics include a collateral wear pattern. There is no grinding present on the biface. The range of the edge angle is 75-85°, suggesting that the tool was used for scraping activities. The raw material is light rhyolite.

(mm/g) MxL	MxWDT	MxTHK	WGT	Edge°
58.6	47.2	21.5	62.7	75-85

Specimen 164, level 3 (Figure B.8): The specimen is considered a biface blank due to the lack of formal thinning flake removal. There is grinding present on the biface. Flake removal characteristics include a collateral wear pattern. The range of the edge angle is 45-55°, suggesting that the tool was used as a saw. The raw material is red conglomerate rhyolite.

(mm/g) MxL	MxWDT	MxTHK	WGT	Edge°
47.5	31.8	19.9	20	45-55

Unit N

Debitage Analysis

The surface assemblage for unit N comprises six formed lithic tools and 70 pieces of lithic debitage. Level 1 contains six formed lithic tools and 77 pieces of lithic

debitage. Level 2 resulted in two formed lithic tools and 60 pieces of lithic debitage. Figure 4.55 and Table A.1 give the results of the triple cortex typology analysis. The interior flakes account for 75.7% of the population and secondary flakes make up 12.9% of the surface assemblage. The primary flakes account for the remainder of the 11.4%. Level 1 follows a similar pattern where 64.9% of the assemblage is interior flakes, 26% is secondary flakes, and 9.1% is primary flakes. Level 2 shows that 76.7% of the assemblage is interior flakes, 20% are secondary flakes, and 3.3% is primary flakes.

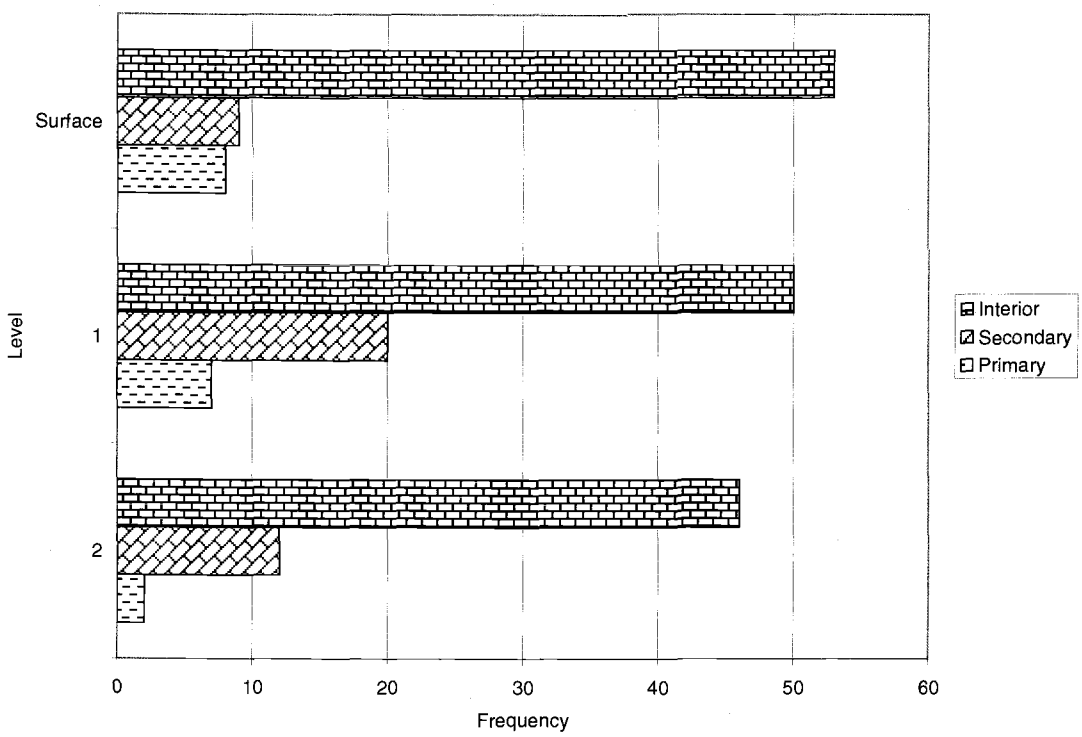

Figure 4.55: Barchart showing triple cortex typology results for the surface and levels 1 & 2 of Unit N.

The results of the free-standing typology are illustrated in Figure 4.56 and Table A.2. The debitage on the surface of unit N is distributed so that 28.9% of the population is in the fragment flake category as well as in the complete flake category.

The broken flakes account for 21.7% of the assemblage and the remaining 20.5% is considered debris.

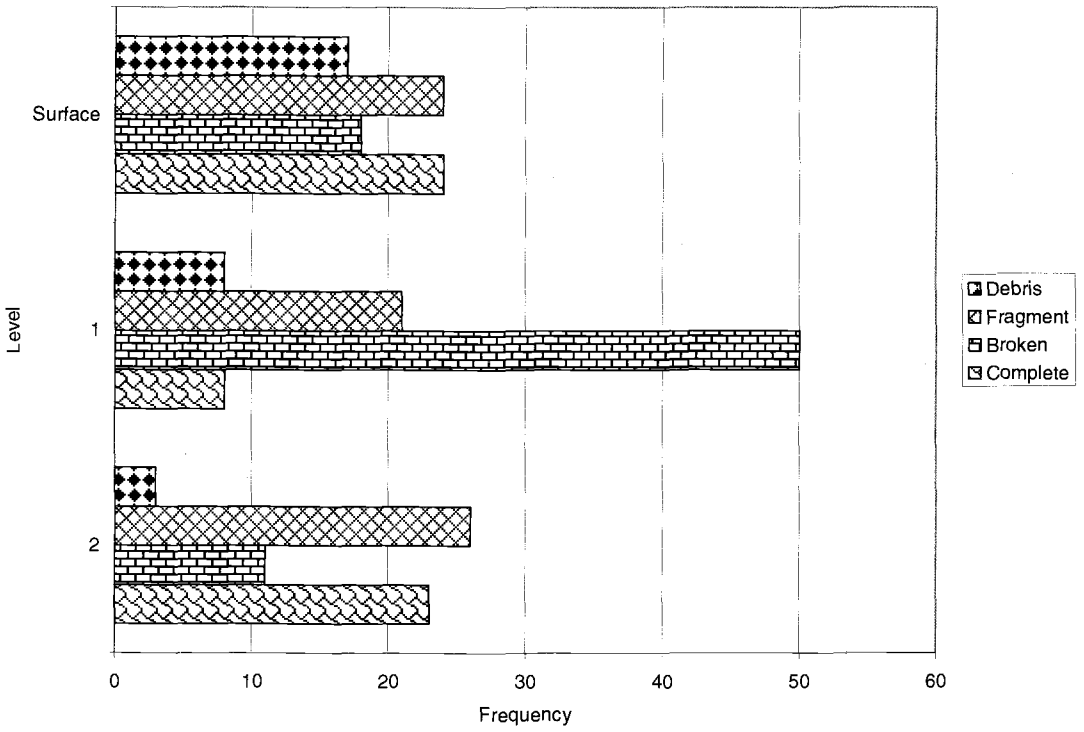

Figure 4.56: Barchart showing free-standing typology results for the surface levels 1 & 2 of Unit N.

Level 1 consists of 57.5% broken flakes, 24.1% fragment flakes, 9.2% complete flakes, and 9.2% debris. Level 2 resulted in 41.3% fragment flakes, 36.5% complete flakes, 17.5% broken flakes, and 4.8% debris.

The results of the size and weight aggregate analysis for unit N are shown in Figure 4.57 and 4.58 as well as Tables A.3 and A.4. Each of the levels expresses a different trend. The surface contains 54.1% of the assemblage in the 3-5 cm size classes. The two smallest size classes contain 38.8% of the assemblage. The remaining 7.1% falls in the two highest size classes. The weight analysis for the surface shows that 48.8% of the assemblage falls in the highest weight class. The

weight classes less than 1.0 g contain 39% of the assemblage and the remaining 12.2% of the assemblage falls within the middle weight classes. The surface shows a trend towards late-middle stage reduction. Level 1 contains 72.4% of the assemblage in size classes 3-5 cm. The smallest size class account for 7.4% of the assemblage. The remaining 20.2% of the assemblage is found in the size classes 6-6+ cm. The weight analysis for level 1 shows that 86.2% of the assemblage falls in the highest weight class. The weight classes between 0.1 and 0.6 grams contain 5% of the assemblage. The remaining 8.8% is unevenly distributed among the middle weight classes. Level 1 expresses a trend towards middle stage reduction.

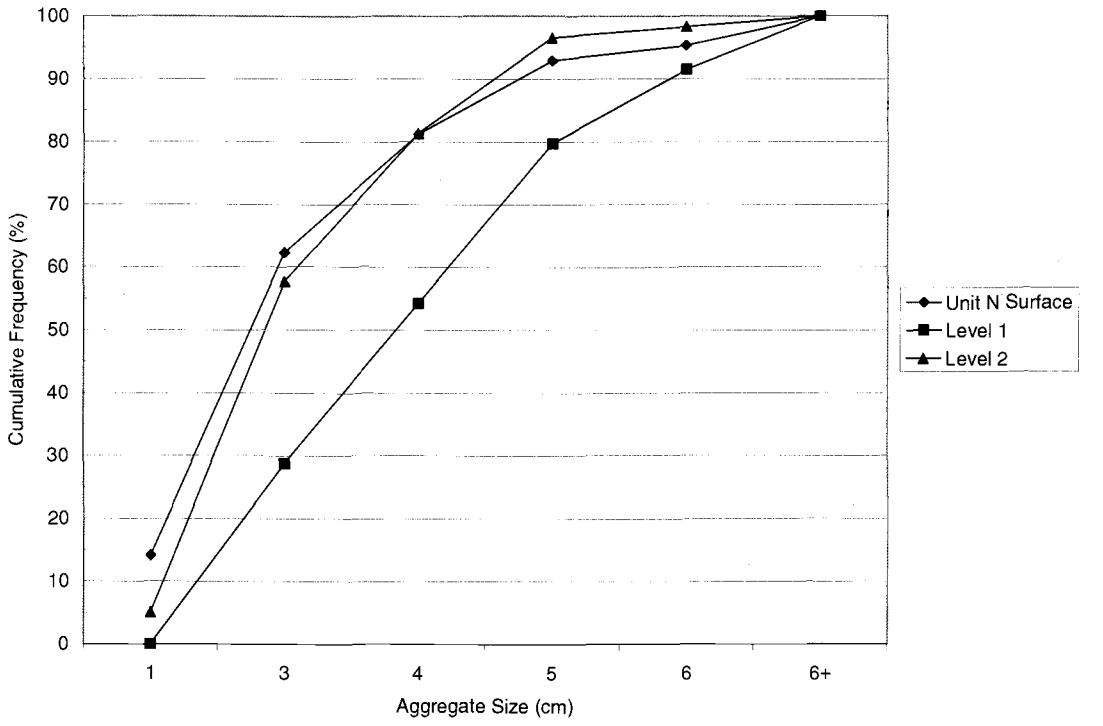

Figure 4.57: Cumulative frequency graph showing the results from the size aggregate analysis for the surface and levels 1 & 2 of Unit N.

Level 2 contains 69.5% of the assemblage in size classes 3-5 cm and 27.1% of the assemblage in size classes 1-2 cm. The largest size classes account for the

remaining 3.4% of the assemblage. The weight analysis for level 2 shows that 54.7% of the assemblage falls in the highest weight class (2.1+ g). The weight classes of 1.0 and smaller account for 35.9% of the assemblage. The remaining 9.4% is distributed between 1.3 and 2.0 g. Level 2 shows a trend in middle stage reduction.

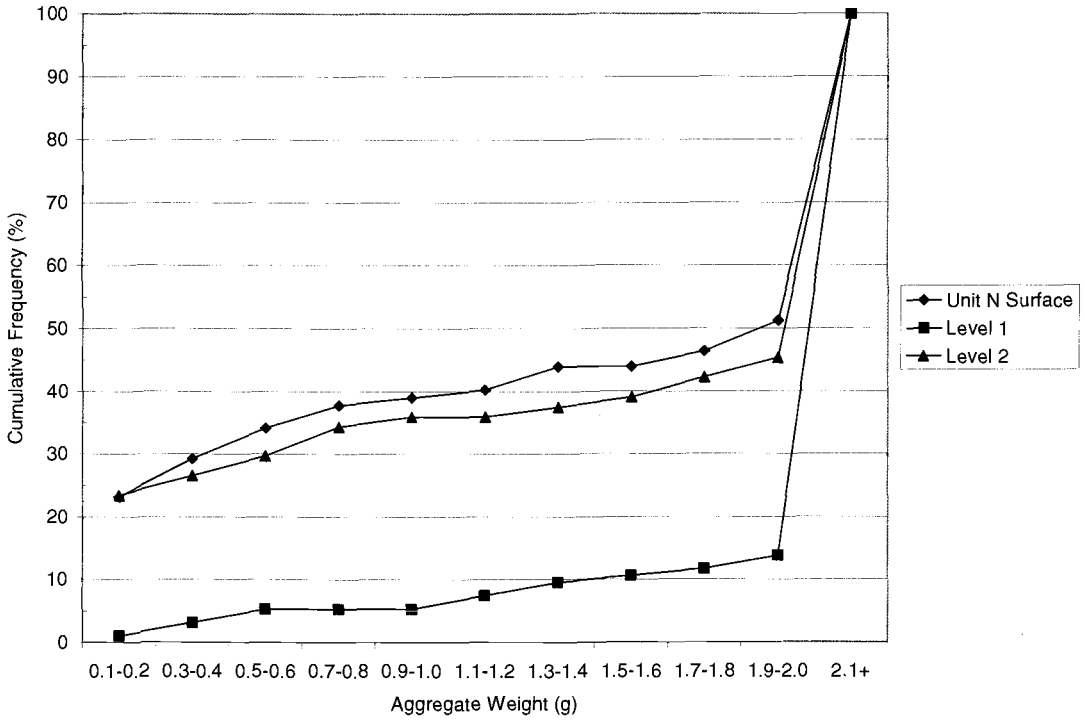

Figure 4.58: Cumulative frequency graph showing aggregate weight class results for the surface and levels 1 & 2 of Unit N.

Tool Analysis

Core (n=5)

Specimen 198, surface level (Figure B.15): The specimen is considered to be a unidirectional core based on the pattern of flake removal. There is evidence of platform preparation and grinding, and greater than 50% of the cortex remains on the specimen. The raw material is light rhyolite.

(mm/g)	MxL	MxWDT	MxTHK	WGT	DIR	COR%
	44.6	47.4	21.6	32.9	uni	50+

Specimen 199, surface level (Figure B.46): The specimen is considered to be a unidirectional core based on the pattern of flake removal. There is no evidence of platform preparation, and greater than 50% of the cortex remains on the specimen. The raw material is dark rhyolite.

(mm/g)	MxL	MxWDT	MxTHK	WGT	DIR	COR%
	57.7	41.2	28.4	92.1	uni	50+

Specimen 200, surface level (Figure B.15): The specimen is considered to be a unidirectional core based on the pattern of flake removal. There is no evidence of platform preparation, and less than 5% of the cortex remains on the specimen. The raw material is light rhyolite.

(mm/g)	MxL	MxWDT	MxTHK	WGT	DIR	COR%
	50.9	37.6	25.7	46.7	uni	<5

Specimen 201, level 1 (Figure B.44): The specimen is considered to be a multidirectional core based on the pattern of flake removal. There is evidence of platform preparation and grinding, and less than 5% of the cortex remains on the specimen. The raw material is light rhyolite.

(mm/g)	MxL	MxWDT	MxTHK	WGT	DIR	COR%
	54.5	53.4	47	84.8	multiple	<5

Specimen 202, level 2 (Figure B.39): The specimen is considered to be a unidirectional core based on the pattern of flake removal. There is no evidence of

platform preparation, and less than 5% of the cortex remains on the specimen. The raw material is light rhyolite.

(mm/g)	MxL	MxWDT	MxTHK	WGT	DIR	COR%
	35.9	40	41.8	51.4	uni	<5

Groundstone (n=3)

Specimen 223, level 1 (Figure B.66): This specimen is considered to be a hammerstone due to the battering on the end of the stone. The specimen is complete and made from glassy rhyolite.

(mm/g)	MxL	MxWDT	MxTHK	WGT
	66.1	39.8	32.5	106.6

Specimen 246, level 1 (Figure B.62): This specimen is considered to be a hammerstone due to the crushed surface on the end of the stone. The specimen has discoloration around the utilized surface. The specimen is complete and made from light rhyolite.

(mm/g)	MxL	MxWDT	MxTHK	WGT
	78.7	39.2	29.9	118

Specimen 274, level 1 (Figure B.55): This specimen is considered to be a hammerstone due to the crushed surface on one end of the stone. The specimen is complete and made from light rhyolite.

(mm/g)	MxL	MxWDT	MxTHK	WGT
	74.6	55.5	30	159.9

Non-formal modified flake (n=6)

Specimen 130, surface level: The specimen shows signs of modification on the left lateral edge and is manufactured on a secondary flake fragment. Flake removal characteristics include a convex uni-marginal surface with a continuous wear pattern. The edge angle is 72°, suggesting scraping activities. The raw material is light rhyolite.

(mm/g)	MxL	MxWDT	MxTHK	WGT	Edge°	TCT	FST	Edge#
	43	75	20.5	62.6	72	secondary	fragment	1

RT Loc	TEC	RTA	RTD
left lateral	convex	uni-marginal	continuous

Unit O

Debitage Analysis

The surface level of unit O includes two formed lithic tools and 16 pieces of lithic debitage; level 1 contains two formed lithic tools and 166 pieces of lithic debitage; level 2 contains 24 pieces of lithic debitage. The results of the triple cortex typology are seen in Figure 4.59 and Table A.1. The surface level is composed of 87.5% interior flakes and 12.5% secondary flakes. Level 1 contains 78.3% interior flakes, 15.1% secondary flakes, and 6.6% primary flakes. The level 2 assemblage contains 70.8% interior flakes, 20.8% secondary flakes, and 8.4% primary flakes.

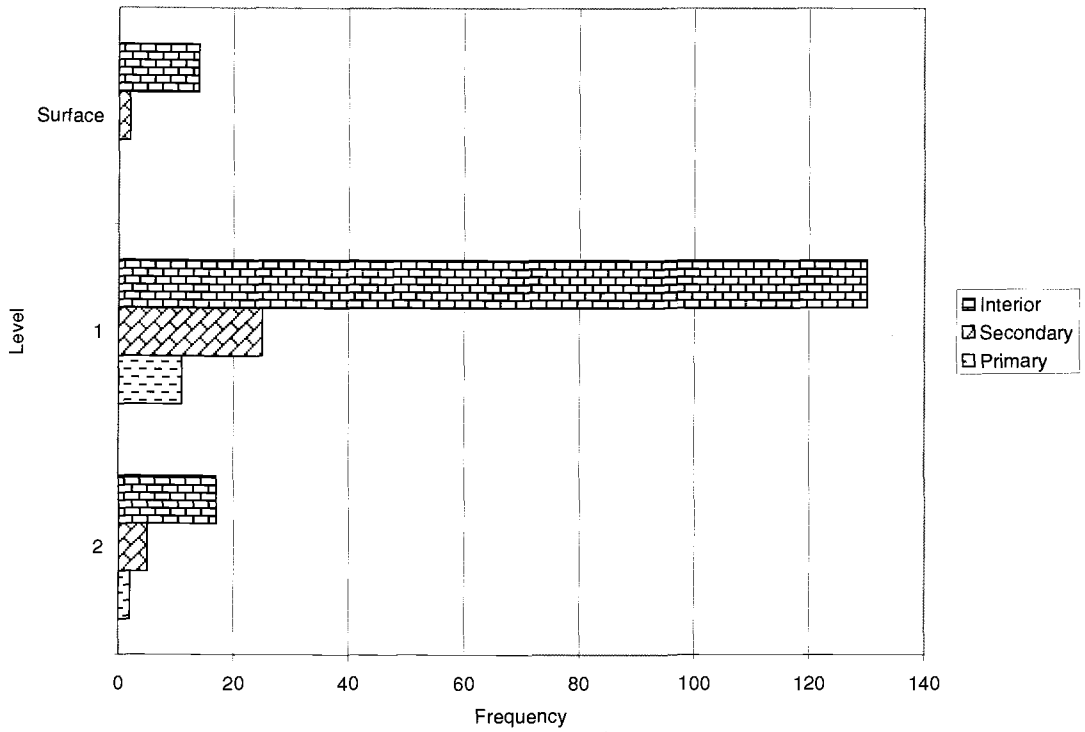

Figure 4.59: Barchart showing triple cortex typology results for the surface and levels 1 & 2 for Unit O.

The results of the free-standing typology can be seen in Figure 4.60 and Table A.2. The surface consisted of 58.8% fragment flakes, 23.5% broken flakes, 5.9% complete flakes, and 11.8% debris. Level 1 contains 61.1% broken flakes. The complete flakes (14.7%), fragment flakes (12.1%), and debris (12.1%) are uniformly distributed among the assemblage. Level 2 produced 44.4% broken flakes, 29.6% fragment flakes, and 22.2% complete flakes. The remaining 3.7% was debris.

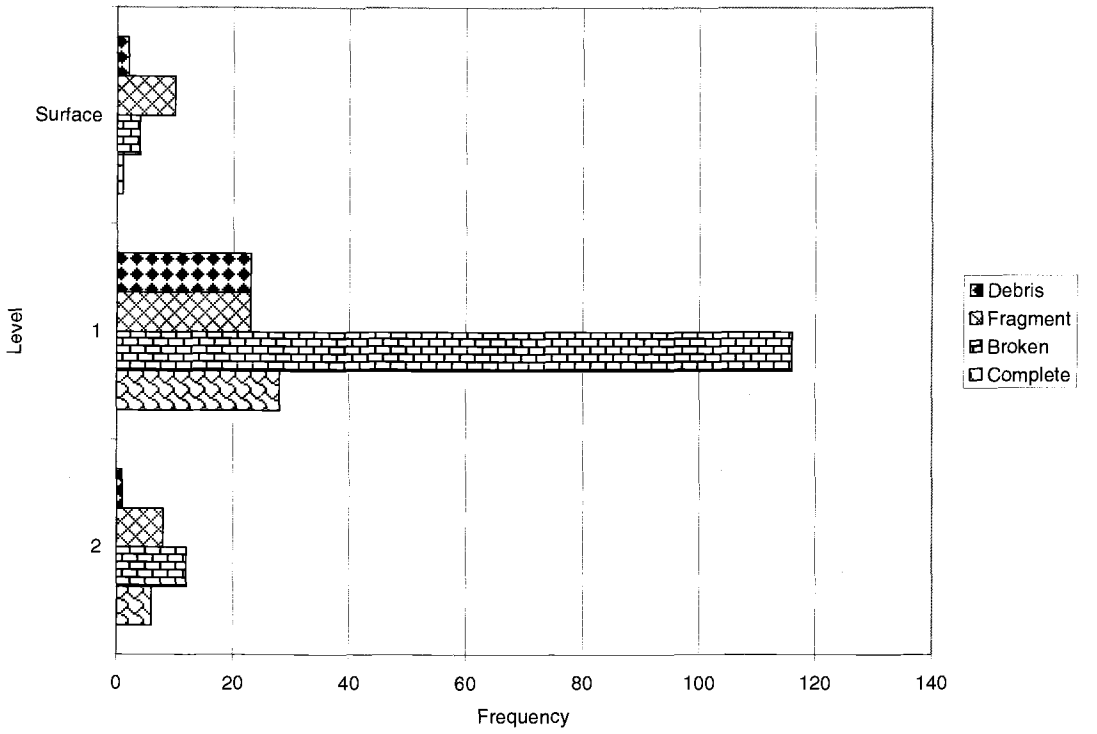

Figure 4.60: Barchart showing free-standing typology results for the surface and levels 1 & 2 of Unit O.

The results of the size and weight aggregate analysis for unit O are shown in Figure 4.61 and 4.62 as well as Tables A.3 and A.4. All of the levels show a trend in middle stage reduction with a slight trend in the late stage reduction. The surface contains 87.5% of the assemblage in the middle size classes (3-5 cm). The remaining 12.5% is in the size classes 6-6+ cm. The weight analysis for the surface shows that 100% of the assemblage falls in the two highest weight classes. Level 1 contains 71.3% of the assemblage in size classes 3-5 cm. The two smallest size classes account for 17% of the assemblage. The remaining 11.7% of the assemblage is found in the size classes 6-6+ cm. The weight analysis for level 1 shows that 72.9% of the assemblage falls in the highest weight class; this follows the pattern seen for all of the

units. The weight classes between 0.1 and 1.0 g contain 18.6% of the assemblage. The remaining 8.5% is distributed among the middle weight classes (1.1-2.0 g).

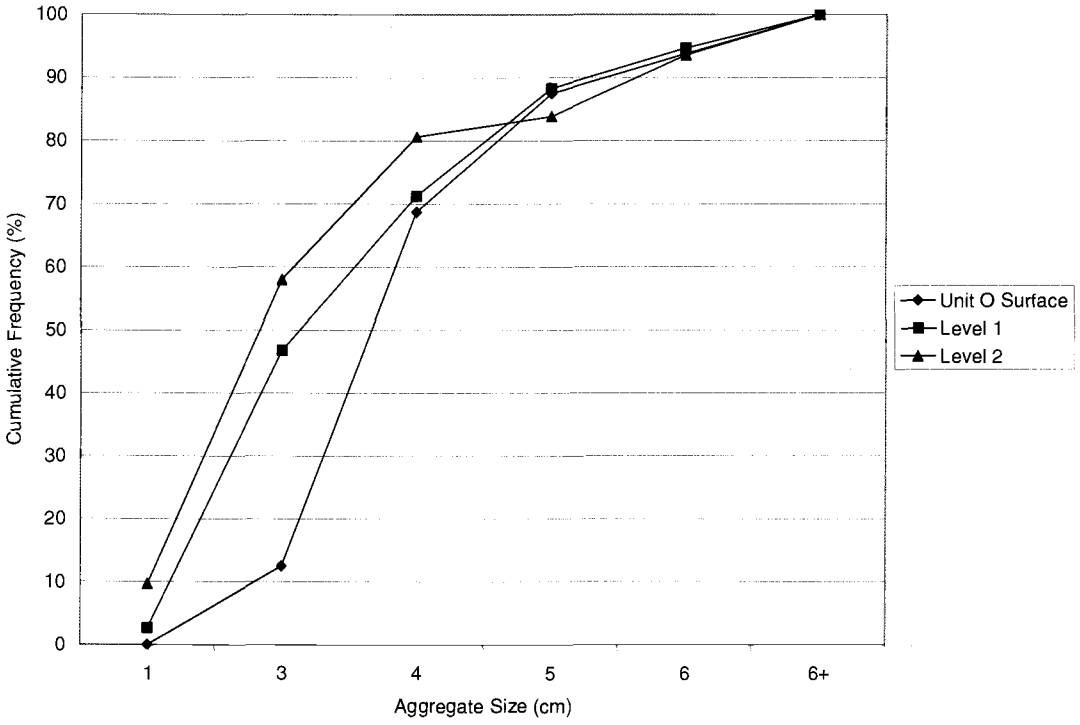

Figure 4.61: Cumulative frequency graph showing the results of the aggregate size analysis for the surface and levels 1 & 2 of Unit O.

Level 2 shows 42% of the assemblage falls in the 3-5 cm size classes. The two smallest size classes contain 41.9% of the assemblage and the 6-6+ cm size class makes up the remaining 16.1%. The weight analysis for level 2 shows 48.4% of the assemblage falls in the 2+ g weight class. The weight classes 0.1 to 1.0 g contain 35.5% of the assemblage. The remaining 16.4% falls in the weight classes 1.1-2.0 g.

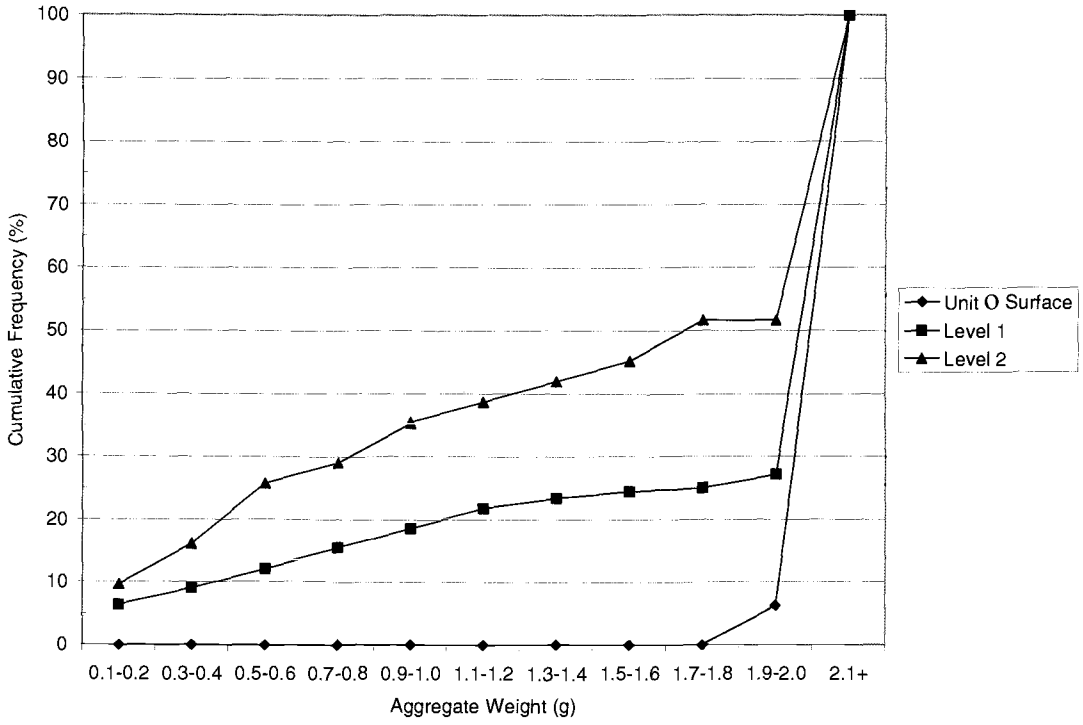

Figure 4.62: Cumulative frequency graph showing aggregate weight class results for the surface and levels 1 & 2 for Unit O.

Tool Analysis

Core (n=1)

Specimen 203, level 1 (Figure B.36): The specimen is considered to be a unidirectional core based on the pattern of flake removal. There is no evidence of platform preparation, and greater than 50% of the cortex remains on the specimen. The raw material is dark rhyolite.

(mm/g)	MxL	MxWDT	MxTHK	WGT	DIR	COR%
	69.2	54.9	48.8	134	uni	50+

Non-formal modified flake (n=3)

Specimen 145, surface level: The specimen shows signs of modification on the left lateral edge and is manufactured on an interior flake fragment. Flake removal characteristics include a straight uni-marginal surface with a continuous wear pattern. The edge angle is 84°, suggesting scraping activities. The raw material is light rhyolite.

(mm/g)	MxL	MxWDT	MxTHK	WGT	Edge°	TCT	FST	Edge#
	37	39.2	10.2	15.8	84	interior	fragment	1

RT Loc	TEC	RTA	RTD
left lateral	concave	uni-marginal	continuous

Specimen 146, surface level: The specimen shows signs of modification on the distal end and is manufactured on a secondary flake fragment. Flake removal characteristics include a concave uni-marginal surface with a continuous wear pattern. The edge angle is 67°, suggesting scraping activities. The raw material is light rhyolite.

(mm/g)	MxL	MxWDT	MxTHK	WGT	Edge°	TCT	FST	Edge#
	42.3	21.6	14.2	15.5	67	secondary	fragment	1

RT Loc	TEC	RTA	RTD
distal	concave	uni-marginal	continuous

Specimen 168, level 1: The specimen shows signs of modification on the right distal end and is manufactured on a primary flake fragment. Flake removal characteristics include a concave uni-marginal surface with a continuous wear pattern. The edge angle is 74°, suggesting scraping activities. The specimen has been bifacially utilized. The raw material is light rhyolite.

(mm/g) MxL	MxWDT	MxTHK	WGT	Edge°	TCT	FST	Edge#
37.6	49.1	35.4	55.1	74	primary	fragment	1

RT Loc	TEC	RTA	RTD
right distal	concave	uni-marginal	continuous

Unit R

Debitage Analysis

The surface level of unit R includes six formed lithic tools and 82 pieces of lithic debitage. Level 1 contains nine formed lithic tools and 118 pieces of lithic debitage. Level 2 contains nine formed lithic tools and 62 pieces of lithic debitage. Level 3 contains two formed lithic tools and one piece of lithic debitage. The results of the triple cortex t typology are seen in Figure 4.63 and Table A.1. The surface level is composed of 73.2% interior flakes, 17.1% secondary flakes, and 9.8% primary flakes. Level 1 contains 57.6% interior flakes, 32.2% secondary flakes, and 10.2% primary flakes. The level 2 assemblage contains 59.7% interior flakes, 30.6% secondary flakes, and 9.7% primary flakes. The flake in level 3 is secondary. With the exception of level 3, the levels follow the same trend as the other units, with a high percentage of interior flakes.

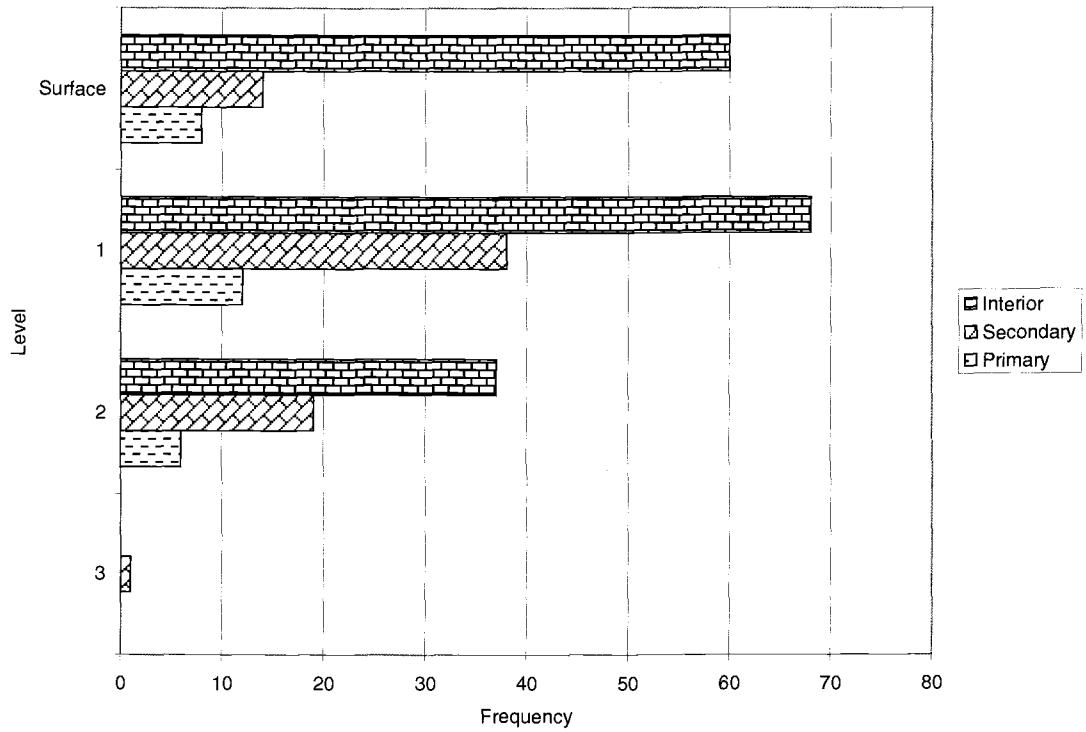

Figure 4.63: Barchart showing the triple cortex typology results for the surface and levels 1, 2, & 3 of Unit R.

The results of the free-standing typology can be seen in Figure 4.64 and Table A.2. The surface assemblage is divided into 35.2% fragment flakes, 31.8% broken flakes, 26.1% complete flakes, and 6.8% debris. Level 1 contains 40.5% fragment flakes, 32.1% complete flakes, 23.7% broken flakes, and 3.8% is debris. The assemblage for level 2 shows 41.7% broken flakes, 23.6% fragment flakes, 20.8% complete flakes, and 13.9% is debris. The flake in level 3 is a broken flake.

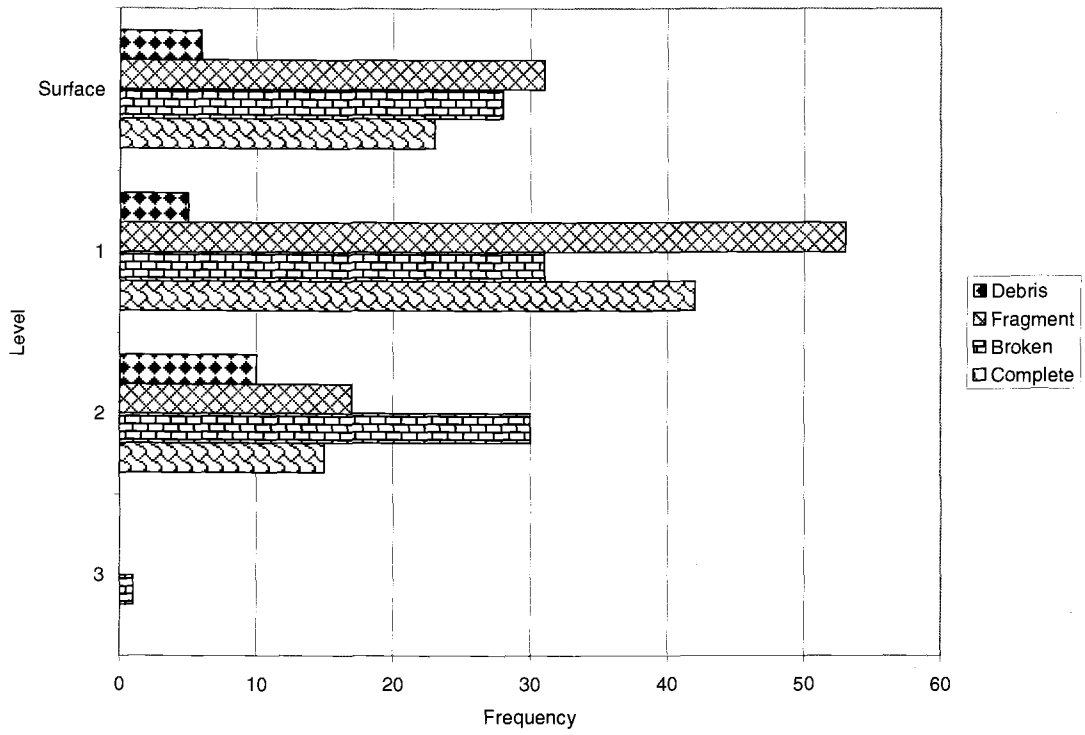

Figure 4.64: Barchart showing free-standing typology results for the surface and levels 1, 2, & 3 of Unit R.

The results of the size and weight aggregate analysis for unit R are shown in Figure 4.65 and 4.66 as well as Tables A.3 and A.4. All of the levels show a trend in middle stage reduction. The surface contains 53.2% of the assemblage in the 3-5 cm size classes, 35.4% of the assemblage is in size classes 1-2 cm, and the remaining 11.4% is in the 6-6+ cm classes. The weight analysis for the surface shows that 58.9% of the assemblage falls in the highest weight class. The weight classes of 0.1-1.0 g contain 34.4% of the assemblage. The remainder of the assemblage is distributed within the middle weight classes (1.1-2.0 g). Level 1 contains 59% of the assemblage in size classes 3-5 cm. The smallest size class accounts for 32.3% of the assemblage. The remaining 8.7% of the assemblage is found in the size classes 6-6+ cm. The weight analysis for level 1 shows 58.1% of the assemblage falls in the highest weight

class. The weight classes between 0.1 and 1.0 g contain 24.8% of the assemblage. The remaining 17.8% is distributed among the middle weight classes (1.1-2.0 g).

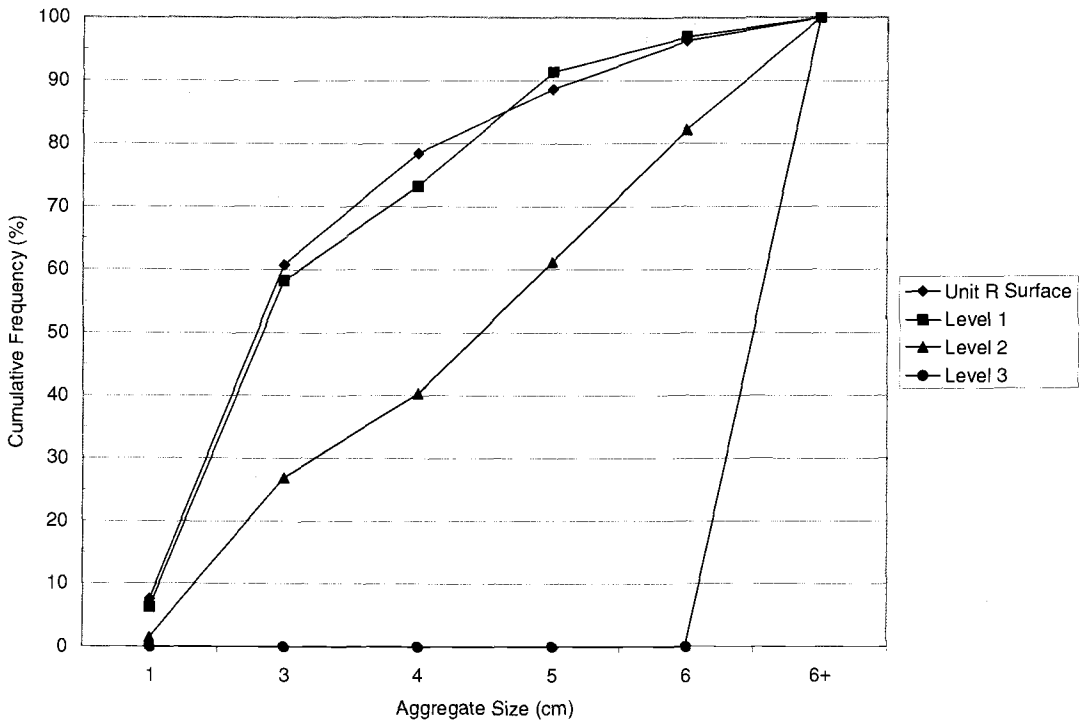

Figure 4.65: Cumulative frequency graph showing the results from the size aggregate analysis for the surface and levels 1 & 2 of Unit R.

Level 2 contains 47.8% of the assemblage in size classes 3-5 cm and 13.4% of the assemblage in size classes 1-2 cm. The largest size classes account for 38.9% of the assemblage. This level contains the highest percentage of flakes in the largest size classes seen in the entire site assemblage. The weight analysis for level 2 shows that 83.8% of the assemblage falls in the highest weight class (2.1+ g). The weight classes of 0.8 and smaller account for 13% of the assemblage. The remaining 3.2% is unevenly distributed among the middle weight classes. The flake from level 3 was not included in this analysis.

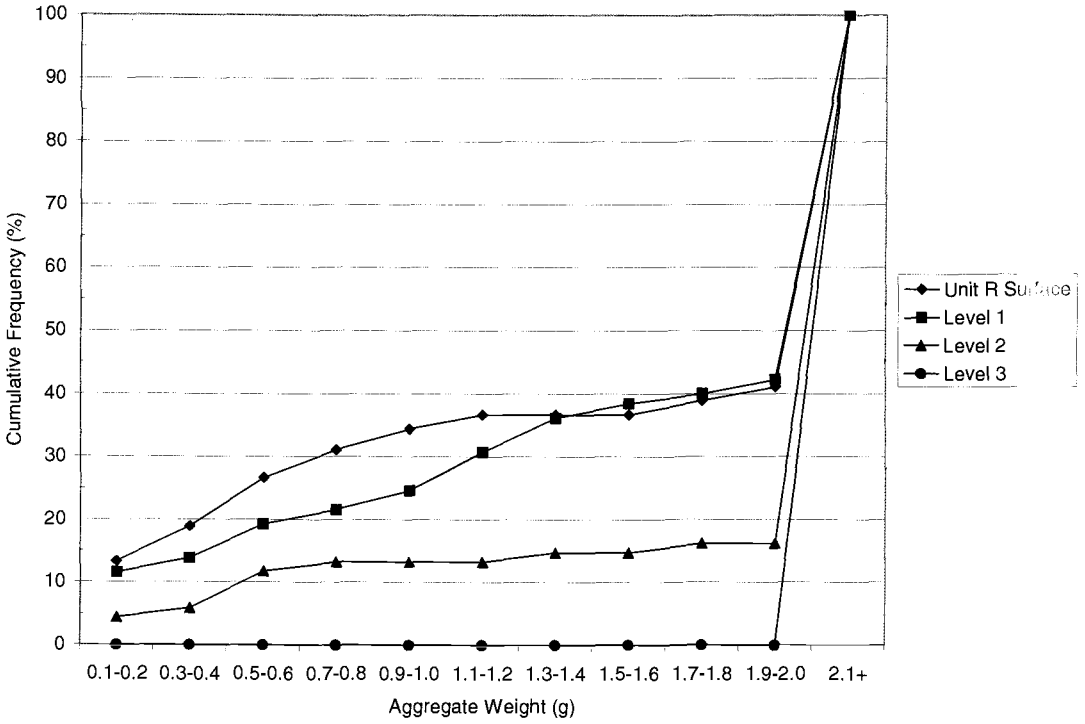

Figure 4.66: Cumulative frequency graph showing aggregate weight class results for the surface and levels 1, 2, & 3 of Unit R.

Tool Analysis

Core (n=3)

Specimen 205, level 1 (Figure B.37): The specimen is considered to be a unidirectional core based on the pattern of flake removal. There is no evidence of platform preparation, and less than 5% of the cortex remains on the specimen. The raw material is basalt.

(mm/g)	MxL	MxWDT	MxTHK	WGT	DIR	COR%
	86	66.6	46	200+	uni	<5

Specimen 207, level 2 (Figure B.40): The specimen is considered to be a unidirectional core based on the pattern of flake removal. There is no evidence of

platform preparation, and 10% of the cortex remains on the specimen. The raw material is glassy rhyolite.

(mm/g)	MxL	MxWDT	MxTHK	WGT	DIR	COR%
	43.1	36.4	31.6	39.6	uni	10

Specimen 208, level 3 (Figure B.38): The specimen is considered to be a unidirectional core based on the pattern of flake removal. There is evidence of platform preparation and grinding, and less than 5% of the cortex remains on the specimen. The raw material is glassy rhyolite.

(mm/g)	MxL	MxWDT	MxTHK	WGT	DIR	COR%
	64.5	47.8	42	85.3	uni	<5

Groundstone (n=3)

Specimen 244, level 2 (Figure B.63): This specimen is considered to be a hammerstone due to the crushed surface on opposite ends of the stone. The specimen is complete and made from dark rhyolite.

(mm/g)	MxL	MxWDT	MxTHK	WGT
	106.3	39.7	32	169.3

Specimen 245, level 2 (Figure B.61): This specimen is considered to be a hammerstone due to the crushed surface on one of the ends. The specimen is complete and made from basalt.

(mm/g)	MxL	MxWDT	MxTHK	WGT
	64	32.5	34.2	103.7

Specimen 251, level 2 (Figure B.56): This specimen is considered to be a grinding stone due to the edge modification on one end of the stone. The specimen is complete and made from light rhyolite.

(mm/g)	MxL	MxWDT	MxTHK	WGT
	76.2	43.7	32.8	134.4

Non-formal modified flake (n=17)

Specimen 134, surface level: The specimen exhibits modification on the proximal end and is manufactured on an interior flake fragment. Flake removal characteristics include a concave uni-marginal surface with a continuous wear pattern. The edge angle is 30°, possibly a knife. The raw material is dark rhyolite.

(mm/g)	MxL	MxWDT	MxTHK	WGT	Edge°	TCT	FST	Edge#
	36	33.8	7.4	10.8	30	interior	fragment	1

RT Loc	TEC	RTA	RTD
proximal	concave	uni-marginal	continuous

Specimen 135, surface level: The specimen exhibits modification on the right lateral edge and is manufactured on an interior flake fragment. Flake removal characteristics include a concave uni-marginal surface with a continuous wear pattern. The edge angle is 60°, suggesting scraping activities. The raw material is light rhyolite.

(mm/g)	MxL	MxWDT	MxTHK	WGT	Edge°	TCT	FST	Edge#
	33	32.8	12	7.9	60	interior	fragment	1

RT Loc	TEC	RTA	RTD
Right lateral	concave	uni-marginal	continuous

Specimen 136, surface level: The specimen exhibits modification on the proximal end and right lateral edge. The specimen has been manufactured on a broken interior flake. Flake removal characteristics include a straight bi-marginal surface with a clustered wear pattern. The edge angles are 57° and 30°. The raw material is light rhyolite.

(mm/g)	MxL	MxWDT	MxTHK	WGT	Edge°	TCT	FST	Edge#
	32.3	55	9.6	18.6	57/30	interior	broken	2

RT Loc	TEC	RTA	RTD
Proximal/right lateral	straight	bi-marginal	clustered

Specimen 147, surface level: The specimen shows signs of modification on the right lateral edge and is manufactured on an broken interior flake. Flake removal characteristics include a concave uni-marginal surface with a continuous wear pattern. The edge angle is 35°, possibly a knife. The raw material is dark rhyolite.

(mm/g)	MxL	MxWDT	MxTHK	WGT	Edge°	TCT	FST	Edge#
	54.4	41.4	22	45.4	35	interior	broken	1

RT Loc	TEC	RTA	RTD
Right lateral	concave	uni-marginal	continuous

Specimen 148, surface level: The specimen exhibits modification on the right lateral edge and is manufactured on a complete secondary flake. Flake removal characteristics include a straight uni-marginal surface with a continuous wear pattern. The edge angle is 72°, suggesting scraping activities. The raw material is light rhyolite.

(mm/g)	MxL	MxWDT	MxTHK	WGT	Edge°	TCT	FST	Edge#
	56.8	38	16.7	24.8	72	secondary	complete	1

RT Loc	TEC	RTA	RTD
Right lateral	concave	uni-marginal	continuous

Specimen 204, surface level: The specimen exhibits modification on the left lateral edge and is manufactured on a broken secondary flake. Flake removal characteristics include a convex uni-marginal surface with a continuous wear pattern. The edge angle is 79°, suggesting scraping activities. The raw material is dark rhyolite.

(mm/g)	MxL	MxWDT	MxTHK	WGT	Edge°	TCT	FST	Edge#
	45	38	25.2	39.6	79	secondary	broken	1

RT Loc	TEC	RTA	RTD
Left lateral	convex	uni-marginal	continuous

Specimen 137, level 1: The specimen shows signs of modification on the right lateral edge and is manufactured on an interior flake fragment. Flake removal characteristics include a convex uni-marginal surface with a continuous wear pattern. The edge angle is 71°, suggesting scraping activities. The raw material is light rhyolite.

(mm/g)	MxL	MxWDT	MxTHK	WGT	Edge°	TCT	FST	Edge#
	32.2	22	14	11.2	71	interior	fragment	1

RT Loc	TEC	RTA	RTD
Right lateral	convex	uni-marginal	continuous

Specimen 149, level 1: The specimen exhibits modification on the left lateral edge and is manufactured on a broken interior flake. Flake removal characteristics include

a straight uni-marginal surface with a continuous wear pattern. The edge angle is 54°, suggesting possible use as a saw. The raw material is light rhyolite.

(mm/g)	MxL	MxWDT	MxTHK	WGT	Edge°	TCT	FST	Edge#
	22.2	49	13.6	9.6	54	interior	broken	1

RT Loc	TEC	RTA	RTD
Left lateral	straight	uni-marginal	continuous

Specimen 150, level 1: The specimen exhibits modification on the proximal end and is manufactured on an interior flake fragment. Flake removal characteristics include a straight uni-marginal surface with a continuous wear pattern. The edge angle is 40°, suggesting possible use as a saw. The raw material is light rhyolite.

(mm/g)	MxL	MxWDT	MxTHK	WGT	Edge°	TCT	FST	Edge#
	33.6	21.5	7.8	4.2	40	interior	fragment	1

RT Loc	TEC	RTA	RTD
proximal	straight	uni-marginal	continuous

Specimen 151, level 1: The specimen exhibits modification on the left lateral edge and is manufactured on a broken secondary flake. Flake removal characteristics include a straight uni-marginal surface with a continuous wear pattern. The edge angle is 64°, suggesting scraping activities. The raw material is light rhyolite.

(mm/g)	MxL	MxWDT	MxTHK	WGT	Edge°	TCT	FST	Edge#
	29	18.3	9	3.6	64	secondary	broken	1

RT Loc	TEC	RTA	RTD
Left lateral	straight	uni-marginal	continuous

Specimen 152, level 1: The specimen exhibits modification on the proximal and distal ends and is manufactured on an interior flake fragment. Flake removal characteristics include a concave surface on the proximal end and a convex surface on the distal end. It is bi-marginal with a continuous wear pattern. The edge angle is 61°, suggesting scraping activities. The raw material is light rhyolite.

(mm/g)	MxL	MxWDT	MxTHK	WGT	Edge°	TCT	FST	Edge#
	30.9	58.8	12.2	17	61	interior	fragment	2

RT Loc	TEC	RTA	RTD
Proximal/distal	concave/convex	bi-marginal	continuous

Specimen 153, level 1: The specimen exhibits modification on the right lateral edge and proximal end. It is manufactured on a broken interior flake. Flake removal characteristics include a straight bi-marginal surface with a continuous wear pattern. The edge angle is 56° and 52°, suggesting possible use as a saw. The raw material is light rhyolite.

(mm/g)	MxL	MxWDT	MxTHK	WGT	Edge°	TCT	FST	Edge#
	55	30.7	10.5	16.1	56/52	interior	broken	2

RT Loc	TEC	RTA	RTD
Right lateral/proximal	straight	bi-marginal	continuous

Specimen 138, level 2: The specimen exhibits modification on the right lateral edge and is manufactured on a broken secondary flake. Flake removal characteristics include a straight uni-marginal surface with a continuous wear pattern. The edge angle is 52°, suggesting possible use as a saw. The raw material is dark rhyolite.

(mm/g)	MxL	MxWDT	MxTHK	WGT	Edge°	TCT	FST	Edge#
	46.1	67	17	47.9	52	secondary	broken	1

RT Loc	TEC	RTA	RTD
Right lateral	straight	uni-marginal	continuous

Specimen 139, level 2: The specimen exhibits modification on the left lateral edge and is manufactured on a complete interior flake. Flake removal characteristics include a straight uni-marginal surface with a continuous wear pattern. The edge angle is 57°, suggesting possible use as a saw. The raw material is dark rhyolite.

(mm/g)	MxL	MxWDT	MxTHK	WGT	Edge°	TCT	FST	Edge#
	27.7	10.1	5.7	1.5	57	interior	complete	1

RT Loc	TEC	RTA	RTD
Left lateral	straight	uni-marginal	continuous

Specimen 169, level 2: The specimen exhibits modification on the distal end and is manufactured on a broken interior flake. Flake removal characteristics include a concave uni-marginal surface with a continuous wear pattern. The edge angle is 40°, suggesting possible use as a saw. The raw material is dark rhyolite.

(mm/g)	MxL	MxWDT	MxTHK	WGT	Edge°	TCT	FST	Edge#
	53.4	44.3	11.7	25	40	interior	broken	1

RT Loc	TEC	RTA	RTD
Right lateral	concave	uni-marginal	continuous

Specimen 170, level 2: The specimen exhibits modification on the right distal edge and is manufactured on an interior flake fragment. Flake removal characteristics include a concave uni-marginal surface with a continuous wear pattern. The edge

angle is 55°, suggesting possible use as a saw. The specimen has been bifacially utilized. The raw material is dark rhyolite.

(mm/g)	MxL	MxWDT	MxTHK	WGT	Edge°	TCT	FST	Edge#
	69.1	40.8	15.9	53.9	55	interior	fragment	1

RT Loc	TEC	RTA	RTD
Right distal	concave	uni-marginal	continuous

Specimen 140, level 3: The specimen exhibits modification on the distal end and is manufactured on a primary flake fragment. Flake removal characteristics include a convex uni-marginal surface with a continuous wear pattern. The edge angle is 53°, suggesting possible use as a saw. The raw material is glassy rhyolite.

(mm/g)	MxL	MxWDT	MxTHK	WGT	Edge°	TCT	FST	Edge#
	48	47	23.4	43.3	53	primary	fragment	1

RT Loc	TEC	RTA	RTD
Distal	convex	uni-marginal	continuous

Uniface (n=2)

Specimen 155, level 1 (Figure B.2): The specimen is considered a Uniface due to the wear pattern exhibited on one side of the stone. Flake removal characteristics include a collateral wear pattern. There is slight grinding present on the Uniface. The specimen is complete. The range of the edge angle is 75-85°, suggesting that the tool was used for scraping activities. The raw material is cryptocrystalline silica.

(mm/g)	MxL	MxWDT	MxTHK	WGT	Edge°
	64.3	17.3	11.1	13.6	75-85

Specimen 206, level 2: The specimen is considered a Uniface due to the wear pattern on one side of the stone. Flake remocal characteristics include a collateral wear pattern. There is grinding present on the Uniface. The specimen exhibits a thick cross section. The range of the edge angle is 45-60°, suggesting that the tool was used as a saw. The raw material is light rhyolite.

(mm/g)	MxL	MxWDT	MxTHK	WGT	Edge°
	47.4	37.6	20	29.9	45-60

Biface (n=1)

Specimen 165, level 1 (Figure b.9): The specimen is considered a notch Perform II due to the thin cross section and evidence of grinding for hafting. There is a notch present in the center of the tool. Flake removal characteristics include a collateral wear pattern. The range of the edge angle is 45-55°, suggesting that the tool was used as a saw. The raw material is light rhyolite.

(mm/g)	MxL	MxWDT	MxTHK	WGT	Edge°
	60.2	31.5	8.6	12.6	45-55

Feature 1

Debitage Analysis

There was a unique feature found in unit N comprised of a cluster of four overturned metates (Figures B.11-B.14). The matrix beneath and around this feature also contained lithic materials; including six formed lithic tools and four pieces of lithic debitage. The materials found with this feature do not represent the entire assemblage for the level. The debitage analyses were preformed on the four pieces of lithic debitage but were not conclusive and therefore will not be shown.

Tool Analysis

Core (n=3)

Specimen 209, Feature 1 (Figure B.33): The specimen is considered to be a unidirectional core based on the pattern of flake removal. There is no evidence of platform preparation, and greater than 50% of the cortex remains on the specimen. The raw material is light rhyolite.

(mm/g)	MxL	MxWDT	MxTHK	WGT	DIR	COR%
	50.2	47.6	35	60.1	uni	50+

Specimen 210, Feature 1 (Figure B.35): The specimen is considered to be a unidirectional core based on the pattern of flake removal. There is evidence of platform preparation and grinding, and less than 5% of the cortex remains on the specimen. The raw material is red conglomerate rhyolite.

(mm/g)	MxL	MxWDT	MxTHK	WGT	DIR	COR%
	69.4	51.7	37.4	116	uni	<5

Specimen 211, Feature 1 (Figure B.34): The specimen is considered to be a unidirectional core based on the pattern of flake removal. There is no evidence of platform preparation, and less than 5% of the cortex remains on the specimen. The raw material is quartzite.

(mm/g)	MxL	MxWDT	MxTHK	WGT	DIR	COR%
	25.9	25.9	19.5	18.8	uni	<5

Groundstone (n=3)

Specimen 224, Feature 1: This specimen is considered to be a hammerstone due to the battered surface on the end of the stone. The specimen displays discoloration around the utilized surface. The specimen is complete and made from light rhyolite.

(mm/g)	MxL	MxWDT	MxTHK	WGT
	61.7	26	16.6	46.2

Specimen 225, Feature 1(Figure B.65): This specimen is considered to be a hammerstone due to the battered surface on the side and on one end of the stone. The specimen has been bifacially utilized. The specimen is complete and made from dark rhyolite.

(mm/g)	MxL	MxWDT	MxTHK	WGT
	89.3	47	16.2	125.6

Specimen 250, Feature 1 (Figure B.57): This specimen is considered to be a grinding implement due to the smoothed surface on one end of the stone. The specimen is complete and made from light rhyolite.

(mm/g)	MxL	MxWDT	MxTHK	WGT
	64.5	52.4	38.2	173.5

A Summary of the Lithic Assemblage for J69E

The debitage analysis shows that the majority of the lithic materials are associated with middle stage reduction technologies. The triple cortex typology shows that 62.3% of all of the lithic debitage were interior flakes. The secondary flakes account for 24.8% and primary flakes make up the remaining 12.9%. The free-standing typology shows that 36% of the total assemblage is made of broken flakes,

30.5% are fragment flakes, 24.8% are complete flakes, and 8.6% are debris. The aggregate analyses show that the majority of the assemblage falls within the size class 3-5 cm and in the weight class of 2.1+ g. All of the analyses express a trend in expedient tool technologies.

The non-formal and formal tool frequencies are expressed in Table 4.3 by level and unit.

Table 4.3: Frequency of lithic tools by unit and level of site J69E.

Level	Unit	Core	Groundstone	Modified Flake	Uniface	Biface
A	Surface	1	0	0	0	0
B	Surface	0	1	1	0	1
C	Surface	0	1	0	0	0
D	Surface	0	0	0	0	0
E	Surface	0	0	2	0	0
F	Surface	0	0	0	0	1
G	Surface	1	0	1	0	0
H	Surface	1	0	0	0	0
I	Surface	1	0	1	0	0
J	Surface	0	0	1	0	0
K	Surface	0	0	1	0	0
L	Surface	0	0	0	0	0
M	Surface	0	0	2	0	0
N	Surface	3	3	3	0	0
O	Surface	0	0	2	0	0
R	Surface	0	0	6	0	0
Subtotal	Surface	7	5	20	0	2
H	1	5	1	4	1	0
I	1	2	0	2	0	0
J	1	3	0	2	0	0
M	1	1	1	3	0	2
N	1	1	0	2	0	0
O	1	1	0	1	0	0
R	1	1	0	6	1	1
Subtotal	1	14	2	20	2	3
H	2	2	3	5	0	0
I	2	1	1	2	0	1
J	2	2	0	0	1	0
M	2	3	2	1	0	1
N	2	1	0	1	0	0

Table 4.3 (Continued): Frequency of lithic tools by unit and level of site J69E

O	2	0	0	0	0	0
R	2	1	3	4	1	0
Subtotal	2	10	9	13	2	2
H	3	0	0	0	0	0
M	3	0	0	1	0	0
R	3	1	0	1	0	0
Subtotal	3	1	0	2	0	0
Feature 1		3	3	0	0	0

The tool analyses for the surface show that there was one formal lithic tool (bifaces and unifaces), 20 non-formal lithic tools (modified flakes), seven cores, and two groundstone pieces. The distribution of the surface tools can be seen in Figure 4.67.

Unit A ♦=1	Unit B ■=1 ♥=1 ♣=1	Unit C ■=1	Unit D	Unit E ♥=2
Unit F ♣=1	Unit G ♦=1 ♥=1	Unit H ♦=1	Unit I ♦=1 ♥=1	Unit J ♥=1
Unit K ♥=1	Unit L	Unit M ♥=2	Unit N ♦=3 ♥=3	Unit O ♥=2
		Unit R ♥=6		

Figure 4.67: Distribution chart of the tools from the surface levels at site J69E. (♥Modified Flake, ●Uniface, ♣Biface, ■Groundstone, ♦Core)

Level 1 exhibited five formal lithic tools, 20 non-formal tools, five groundstone pieces, and 14 cores. Figure 4.68 shows the distribution of the formal tools, non-formal tools, groundstone, and cores for level 1.

Unit H ♦= 5 ■= 1 ♥= 4 ●=1	Unit I ♦= 2 ♥= 2	Unit J ♦=3 ♥=2
Unit M ♦=1 ■=1 ♥=3 ♣=2	Unit N ♦=1 ■=3 ♥=2	Unit O ♦=1 ♥=1
Unit R ♦=1 ♥=6 ●=1 ♣=1		

Figure 4.68: Distribution chart of the tools from level 1 at site J69E.
(♥Modified Flake, ●Uniface, ♣Biface, ■Groundstone, ♦Core)

Level 2 reveals four formal lithic tools, 13 non-formal tools, nine groundstone pieces, and 10 cores. Figure 4.69 shows the distribution of the tools as seen in each of the units.

Unit H ♦=2 ■=3 ♥=5	Unit I ♦=1 ■=1 ♥=2 ♣=1	Unit J ♦=2 ●=1
Unit M ♦=3 ■=2 ♥=1 ♣=1	Unit N ♦=1 ♥=1	Unit O
Unit R ♦=1 ■=3 ♥= 4 ●=1		

Figure 4.69: Distribution chart of the tools from level 2 at site J69E.
(♥Modified Flake, ●Uniface, ♣Biface, ■Groundstone, ♦Core)

Level 3 shows two non-formal lithic tools, three groundstone pieces, and four cores. Figure 4.70 shows the distribution of the tools for level 3.

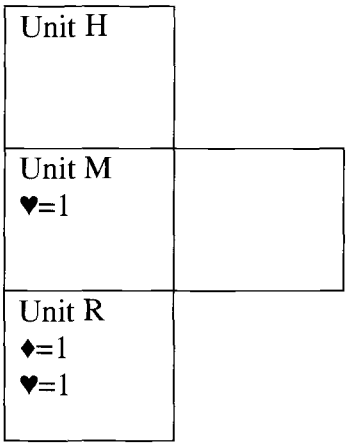

Figure 4.70: Distribution chart of the tools from level 3 at site J69E.
(♥Modified Flake, ■Groundstone, ♦Core)

There is a change in the frequency of formal and non-formal lithic tools seen in each level. A chi-squared test was preformed on the data in order to evaluate whether these differences were significant. However there are other factors that need to be included in the evaluation of the test. The amount of soil that was excavated in each level varies significantly along with the amount of units excavated in each level. Approximate volumes have been calculated for each level. The surface has 0.16 m^3 (10%), level 1 has 0.70 m^3 (44%), level 2 has 0.59 m^3 (37%), and level 3 has 0.15 m^3 (9%). This information was used to normalize the quantities of tools from each level.

Table 4.5: Frequency of formal and non-formal tools by level. (formal tools= biface, uniface, groundstone; non-formal tools= cores & modified flakes)

Levels	Formal Tools	Non-formal Tool	Total
Surface	7	27	34
Level 1	7	34	41
Level 2	13	23	36
Level 3	0	3	3
Total	27	87	114

The null hypothesis being tested using the chi-squared test is as follows: there is a significant relationship in the quantity of formal to non-formal tools between the four levels. For there to be significance at the 0.05 level, the chi-squared value needs to exceed 7.82. The chi-squared value for this data is 5.18. Therefore, the null hypothesis has been rejected, meaning there is no significant relationship in the frequency of formal to non-formal tools between levels.

Chapter 5: Discussion and Conclusion

Behavioral aspects of the early native inhabitants of Espiritu Santo Island can be determined through a study of the lithic assemblage of J69E's archaeological record. The goals of this thesis revolve around producing insights into technological and economic behaviors associated with the coastal adaptations of J69E's prehistoric inhabitants. To address these issues I will discuss the five research questions stated at the beginning of this thesis.

The first research question was: what does a lithic assemblage of late Pleistocene to early Holocene age look like in a Baja California Sur coastal setting? And what can the assemblage tell us about technological behaviors? The first part of this question can be addressed using the results from the analyses of lithic debitage and tools. The lithic technologies that were present at the site mainly consisted of core reduction and tool manufacturing debris, food preparation technologies, and formed tools. These three categories will be examined separately but keep in mind that they all work together to form a technological system.

The lithic production artifacts that remain in the archaeological record of J69E consist of the cores and debitage. The lithology of the lithic artifacts tell us that the people living at this site were bringing in pieces of raw material from other locations for the purpose of making stone tools. The sources of the raw materials can be determined using remote sensing techniques that will be discussed later. From the analysis of the artifacts we can see that the people at this site favored tool manufacture of the light rhyolite. The majority of the cores are made of light rhyolite and a great portion of the debitage is comprised of light rhyolite.

Cores make up 29% of all of the tools analyzed, indicating an emphasis on the production of flakes for both formal and non-formal tool. From the debitage analysis we can see that there is a significant difference in the number of primary flakes compared to the number of interior flakes. Primary flakes have lower quantities while the interior flakes have greater quantities. There could be two reasons for this: 1) the cores that were being used were partially prepared prior to transport to J69E, or 2) the initial flake removal process removed larger pieces of debitage containing the cortex in smaller quantities; and, the interior flakes being removed were smaller in size and greater in quantity, causing there to be a greater quantity of interior flakes than exterior flakes. Whatever the case may be, the flakes that were being driven off of the center of the core were in greater numbers than the pieces that were being taken off the outer core, suggesting an emphasis towards tool manufacture and maintenance, not quarrying activities at J69E.

Using the freestanding typology analysis we can see that the people were focusing on tool manufacture. According to Sullivan and Rozen (1985) an assemblage containing high percentages of broken and fragmented flakes concludes an emphasis on shaped stone tool manufacture. Assemblages containing high percentages of complete flakes and debris show an emphasis on core reduction. 66.5% of the flakes at site J69E were either broken or fragmented showing a trend in late stage reduction patterns. Modified flakes also show a trend towards shaped stone tool manufacture.

Aggregate analysis shows that the majority of the flakes measured within the 3-5 cm size range and 2.1+ g weight category. Quantities in the first two weight categories (0.1-0.3 g) and the first size category (1 cm) show evidence of pressure

flaking. The rest of the weights indicate a fairly uneven distribution up to but not including the 2.1+ g class. There are a greater number of flakes found in the middle sizes and fewer flakes found in the lower and higher sizes.

The relatively high percentage of groundstone (16%) recovered during excavations indicates that food processing occurred at the site. Nineteen groundstone were recovered from the site, of which seven were grinding stones that had a smoothed surface and 12 were hammerstones with battered surfaces. Grinding stones are indicative of food production behaviors and the hammerstones could be used for tool manufacture and food processing.

The use and relative importance of expedient tool technologies at J69E are evident in the recovery of modified flakes. Modified flakes constitute 46% of the tool assemblage. There is a wide range of activities associated with modified flakes including scraping, sawing, and use as a knife. These modified flakes would have been used to manufacture organic tools, prepare hides, and process foods.

Organic tools were not seen in abundance at J69E; however, from the presence of the modified flakes we can infer that organic tools were being manufactured. The process of manufacturing organic tools involves various shaping techniques. This can be achieved by fracture (including splitting), flaking, cutting (including grooving), scraping, chopping, grinding, perforating, or frequently by a combination of these methods. The basic functions of the modified flakes found at site J69E can be associated with the shaping techniques used to create organic tools. We cannot say for certain what organic tools were being manufactured, only that we believe they were being manufactured.

Formed lithic tools were limited to unifaces and bifaces and are indicative of greater preparation and planning than for modified flake tools. There were only 11 of these tools found at the site which constitutes 9% of the total tool assemblage. This is a very small percent.

As previously discussed, Binford categorizes hunter-gatherer organization as foragers and collectors. The expedient nature of the lithic assemblage indicates that the people inhabiting site J69E were foragers. They used this site as a residential camp bringing food and lithic resources from other locations there for processing. The forager lifestyle occupies environments that have low interseasonal mobility in subsistence resources, as mentioned in chapter 2. The known environment of the area in the late Pleistocene to early Holocene age indicates a wetter climate than seen today. Under these conditions, the people inhabiting the island would have had more resources available to them year round allowing for the use of one residential camp and a few location camps. The residential camps were placed on top of the terraces while the location sites were closer to the sea (i.e. the main food source). These people spent their time hunting and gathering resources for daily use. There is no evidence for food storage at this site. The camp supported a small band of people using the resources readily available to them.

The second research question was: do the lithic materials from site J69E reflect changes in technology through time? There were two different dates that were recovered from the site. The original date of 11,284 BP was determined from a shell colleceted on the surface (Fujita & Poyatos De Paz 1998). The lithic material from the surface and the first ten centimeters potentially coincides with the 11,284 BP date.

The second set of dates, 7,820 to 8,540 BP, potentially coincides with the second and third levels (10-30 cm) that directly rest on the bedrock. Because of post-depositional effects on organic materials at J69E, the accuracy of these dates has been questioned by Davis (2006), who is currently working to clarify the site's geochronology. Regardless, the site appears to generally date within the late Pleistocene to early Holocene. A chi-squared test determined that there was no significant difference in the frequency of formal and non-formal lithic tools, and thus the structure of the lithic technology, through time. From the perspective of lithic tool production, technological and economic patterns seem consistent during the entire span of site occupation.

The third research question was: how are raw lithic resources of Espiritu Santo Island distributed in relation to J69E? This question was answered through the analysis of remote sensing data, which revealed the distribution of the various lithic resources available on the island. Various maps were created to determine locations of possible quarry sites and distances to the materials.

The raw lithic material sources found on the island are reflected in the materials found at the site. Varieties of rhyolites were used most frequently by the inhabitants of J69E and was also one of the closest raw lithic material sources used in the past, occurring within 420 meters of the site. Basalt was used for almost all of the groundstone and is found within 400 meters of the site in nearby talus slopes. The availability of the lithic resources made it easy for the people living in that area to retrieve the material necessary for tool manufacture.

It is necessary to note that andesite was not found in the vicinity of La Ballena Bay but was present in the site's lithic assemblage. The nearest source of the andesite

is 1500 meters from site J69E. This material was recovered in very small quantities and only as debitage. The occupants of J69E did not travel long distances for their raw materials nor were they trading for better quality materials. The remaining raw lithic materials, cryptocrystalline silicate, quartz, and quartzite, were seen near site J69E in veins among the bedrock. These materials could not be identified in the satellite imagery and therefore could not be interpreted in the same manner as the other materials.

The fourth research question was: what can the lithic assemblage of site J69E tell us about the economy of the native inhabitants? The inhabitants would have been attracted to the coastal environment for its richness in food varieties, quantities of plants growing near water sources, lithic resources, and climatic conditions. The coast would possibly have been extremely rocky with little vegetation coverage, except where water sources were present, consisting of mangroves, cacti, and thorny shrubs. The position of the sea would have been at least a kilometer out from the current position. Terrestrial animals would have consisted of small and large game, such as birds, rabbit, and deer. Marine animals would have been sea mammals, fish, and shellfish. Fresh water was collected in natural rock tinajas. This coastal setting would have been self sufficient for the people inhabiting the area. All of the resources needed to sustain life were readily available to the inhabitants.

Based on the distribution of the lithic materials and the tool technologies that were determined to be present at the site, the economic patterning is consistent with food processing and tool manufacture for short periods of time when the resources would have been available in the area. All of the lithic material found was present at

some location on the island. It seems as if the people were following the marine resources around the island. They harvested the available resources and then moved to a different residential camp to continue the cycle. The tool technologies are expedient and the material is from nearby sources. This site was visited over a span of thousands of years and yet the technologies remained unchanged. The forager lifestyle was maintainable for the people using this residential camp.

The economy of the native inhabitants of site J69E is similar to that of the Las Palmas culture described in chapter 1. Technological organization is consistent with a marine environment where the lithic tools being found are used in processing marine resources. One would expect to see knives, manos and metates, groundstone, and crude flake tools for processing shellfish, fish, sea mammals, plants, and some terrestrial animals (Massey 1961; Massey 1947). The link between the Las Palmas culture and the island inhabitants allows for further conclusion to be drawn about the possible economic patterns associated with marine adaptations. Site J69E is believed to be associated with late Pleistocene and early Holocene ages whereas the Las Palmas culture is more recent. The links in the technology between these two time periods show that the marine adaptations were very successful through time. People were creating tools that would be useful in varying environmental conditions, so as the environment changes the tool technologies remain constant. This is seen in the cultural continuity between the inhabitants of J69E and the neighboring Las Palmas and Comundo cultures.

The fifth and final research question was: is there any indication of mobility within the island and/or the mainland that can be seen in the lithic assemblage? There

is no clear evidence from the lithic materials of transportation from the mainland to the island. There are not any specific material types that are found on the mainland and not on the island that are present at the site. Before 10,000 BP, the lower sea level would have allowed people to walk back and forth from the mainland to the island. Today, the island is separated from the peninsula by a short distance of open water, easily crossed with watercraft. It is believed that because suitable raw lithic materials were locally available, hunter-gatherers had little need to acquire other lithic resources from the peninsula or to move local materials from one location to another. Although the people probably traveled to the peninsula, this is not reflected in the lithic assemblage of J69E.

There is some evidence of mobility within the island. There are lithic resources found at the site that are not found around La Ballena Bay. The native people would have needed to travel to other locations to acquire this material; however, based on the lithic resources and technological patterns it would seem like the native people remained sedentary. Looking at the bigger picture, we know that the people would not have been able to sustain themselves year round at this site alone.

Conclusion

This thesis has presented and considered the results of analyses conducted on lithic artifacts found at site J69E in order to draw conclusions about the cultural behaviors associated with marine coastal settings in Baja California Sur. The abundance of expedient tools at site J69E leads me to conclude that the inhabitants were focusing on food preparation and organic tool manufacture. Although the

chronology of site occupation is tentative at this time, the archaeological record at J69E probably reflects multiple reoccupations by coastal foragers, spanning thousands of years. During their stays at site J69E, the foragers used the abundant material resources, geologic and marine, that were within close proximity to local water sources.

Although much older, the assemblage at J69E is very similar to the Las Palmas culture in that it shows a reliance on non-formal tool technologies and forager strategies. The lithic material types do not indicate mobility between the mainland and the island but the organization of the assemblage reflects patterns seen among peninsular cultural groups. The people inhabiting the island organized their technologies with a focus on expedient tools rather than specialized technologies.

This research has shown that the early inhabitants of site J69E were logistically organized as foragers successfully oriented towards their coastal environment. The people adapted to this New World coastal environment much earlier than previously thought. The fact that the people of this site remained relatively unchanged in their technologies throughout thousands of years allows us to conclude that the changing environment did not affect the successful adaptation to the coastal setting.

Future research at J69E will help to answer some of the underlying questions that were brought up in this research. Why might the people have stopped occupying this site? Did the environment change? What affect did the sea level increases have on the local people who continued to live on the island? These are only some of the many questions that need to be answered to understand fully the behaviors of the native peoples during this time.

REFERENCES

ASTER image, Jet Propulsion Laboratory
2003 California Institute of Technology. http://asterweb.jpl.nasa.gov

Adams, Jenny L.
2002 *Ground Stone Analysis: A Technological Approach.* The University of Utah Press, Utah.

Andrefsky Jr, William
2001 *Lithic Debitage: Context, Form, Meaning*. The University of Utah Press, Salt Lake City.

2004 Emerging Directions in Debitage Analysis. In *Aggregate Analysis in Chipped Stone,* Christopher T. Hall and Mary Lou Larson (eds). The University of Utah Press, Utah.

2004 Partitioning the Aggregate: Mass Analysis and Debitage Assemblages. In *Aggregate Analysis in Chipped Stone,* Edited by Christopher T. Hall and Mary Lou Larson. The University of Utah Press, Utah.

Baegert, Jacob
1982 The Letter of Jacob Baegert 1749-1761 Jesuit Missionary in Baja California. Doyce B. Nunis Jr. (ed). Dawson's book shop, Los Angeles.

Bamforth, Douglas B.
1986 Technological Efficiency and Tool Curation. *American Antiquity* 51(1):38-50

Bettinger, Robert L.
1991 *Hunter-Gatherers: Archaeology and Evolutionary Theory.* Plenum Press, New York.

Binford, Lewis R.
1967 Smudge Pits and Hide Smoking: The Use of Analogy in Archaeological Reasoning. *American Antiquity* 32(1):1-12

1980 Willow Smoke and Dogs' Tails: Hunter-Gatherer Settlement Systems and Archaeological Site Formation. *American Antiquity* 45(1):4-20

Bouey, Paul D.
1987 The Intensification of Hunter-Gatherer Economies in the Southern North Coast Ranges of California. *Research In Economic Anthropology*, Barry L. Isaac (ed). JAI Press, Connecticut.

Carew, McFall C.

1967 Reconnaissance Geology of the Conceptcion Bay Area, Baja California, Mexico. *Sciences* 10:5

Carmean, Kelli
1994 A Metric Study of Baja California Sur Projectile Points. *Pacific Coast Archaeological Society Quarterly* 30(1):52-74

Carmean, Kelli and J. Eldon Molto,
1991 The Las Palmas Burial Tradition of the Cape Region, Baja California Sur: Some New Research Questions. *Pacific Coast Archaeological Society Quarterly* 27(4):23-38

Carr, Phillip J. and Andrew P. Bradbury
2004 Flake Debris Analysis, Levels of Production, and the Organization of Technology. *Aggregate Analysis in Chipped Stone,* Christopher T. Hall and Mary Lou Larson (eds). The University of Utah Press, Utah.

2004 Exploring Mass Analysis, Screens, and Attributes. *Aggregate Analysis in Chipped Stone,* Christopher T. Hall and Mary Lou Larson (eds). The University of Utah Press, Utah.

Davis, Loren G.
2005 Preliminary Report of the 2004 Archaeological Investigations as Site J69E, Espiritu Santo Island, Baja California Sur, Mexico. Oregon State University.

2006 Baja California's Paleoenvironmental Context. *The Prehistory of Baja California: Advances in the Archaeology of the Forgotten Peninsula,* Don Laylander and Jerry D. Moore (eds). The University Press of Florida, Florida.

2006 Evaluating claims for early cultural occupation in the Laguna Seca Chapala basin, Baja California. In review by the 2006 INAH Binational Balances and Perspectives publication committee, Mexicali, Mexico.

2006 Proposal for Continuation of Archaeological Excavations at Site J69E, Espiritu Santo Island, B.C.S. Oregon State University.

Douglas, Robert, Oscar Gonzalez-Yajimovich, Donn Gorsline, Francisca Staines-Urias, and J. Fernando Arreola-Hernandez
2003 Holocene Ocean-Climate Variations in the Gulf of California, Mexico. *PAGES news,* 11(2-3):26-28.

Fujita, Harumi
2002 Isla Espiritu Santo, Baja California Sur: Evidencia de una Larga Tradicion Cultural. Paper presented at the third Balancen y Perspectivas symposio, Mexicali, Baja California, December 2002.

Fujita, Harumi and Gema Poyatos de Paz
1995 Prehistoric Coastal Adaptations in the Cape Region, Baja California Sur. *Pacific Coast Archaeological Society Quarterly* 31 (1 & 2): 4-19.

1998 Settlement Patterns on Espiritu Santo Island, Baja California Sur. *Pacific Coast Archaeological Society Quarterly* 34:67-105.

Gabel, Creighton
1968 *Analysis of Prehistoric Economic Patterns.* Holt, Rinehart and Winston, New York.

Hammond, Edwin H.
1954 A Geomorphic Study of the Cape Region of Baja California. *Geography* 10(2):45-112

Hall, Christopher T.
2004 Evaluating Prehistoric Hunter-Gatherer Mobility, Land Use, and Technological Organization Strategies Using Minimum Analytical Nodule Analysis. *Aggregate Analysis in Chipped Stone,* Christopher T. Hall and Mary Lou Larson (eds). The University of Utah Press, Utah.

Hovens, Pieter
1991 The Origins of Anthropology in Baja California: The Fieldwork and Excavations of Herman Ten Kate in 1883. *Pacific Coast Archaeological Society Quarterly* 27(4)15-22

Instituto Nacional de Estadistica, Geografia e Informatica (INEGI)
2004 www.inegi.gob.mx/inegi/default.asp

Jensen, John R.
2005 *Introductory Digital Image Processing: A Remote Sensing Perspective* 3rd edition. Prentice Hall, New Jersey.

Johnson, Markes E. & Maximino E. Simian
1997 Development & Founding of the Pliocene Santa Ines Archipelago in the Gulf of Baja California Sur, Mexico. *Pliocene Carbonates & Related Facies Flanking the Gulf of California, Baja California, Mexico.* Geological Society of America Special Paper 318:25-38

Johnson, Matthew
1999 *Archaeological Theory: An Introduction.* Blackwell Publishers, Massachusetts.

Kooyman, Brian P.
2004 *Understanding Stone Tools and Archaeological Sites.* University of Calgary Press, Alberta and University of New Mexico Press, New Mexico.

Larson, Mary Lou
2004 Chipped Stone Aggregate Analysis in Archaeology. *Aggregate Analysis in Chipped Stone,* Christopher T. Hall and Mary Lou Larson (eds). The University of Utah Press, Utah.

Lee, Grismer L.
2000 Amphibians and Reptiles of Baja California. University of California Press, Berkley.

Massey, William C.
1947 Brief Report on Archaeological Investigations in Baja California. *Southwest Journal of Anthropology* 3:344-359

1949 Tribes and Languages of Baja California. *Ethnology of the Baja California Indians* 362-397. University of California, Berkeley

1955 Culture History in the Cape Region of Baja California

1961 Archaeology and Ethnohistory of Lower California. *Ethnology of the Baja California Indians* 334-361 University of California, Berkeley

Mitchell, Donald and Leland Donald
1988 Archaeology and the Study of Northwest Coast Economies. *Research In Economic Anthropology: Supplement 3, Prehistoric Economies of the Pacific Northwest Coast,* Barry L. Isaac (ed). JAI Press, Connecticut.

Molto, J.E. and Harumi Fujita
1995 La Matancita: A Las Palmas Mortuary Site from the West Cape Region of Baja California Sur, Mexico. *Pacific Coast Archaeological Society Quarterly* 31(1&2):20-55

Ortlieb, Luc
1979 Quaternary Shorelines Around Baja California Peninsula, Mexico: Neotectonic Implications. *Abstracts with Programs, Geological Society of America* 11(7):490.

Rabb, L. Mark & Albert C. Goodyear
1984 Middle Range Theory in Archaeology: A Critical Review of Origins and Applications. *American Antiquity* 49(2)255-268

Rhode, David
2002 Early Holocene Juniper Woodland and Chaparral Taxa in the Central Baja California Peninsula, Mexico. *Quaternary Research* 57:102-108.

Ritter, Eric W., John W. Foster, Robert I. Orlins, Louis A. Payen, and Paul D. Bouey

1994 Archaeological Insights within a Marine Cornucopia: Baja California's Bahia De Las Animas. *Pacific Coast Archaeological Society Quarterly* 30(1):1-23

Sen, Gautam
2001 *Earth's Materials: Minerals and Rocks.* Prentice Hall: New Jersey.

Sullivan III, Alan P. and Kenneth C. Rozen
1985 Debitage Analysis and Archaeological Interpretation. *American Antiquity* 50 (4): 755-779.

Torrence, Robin
1989 *Time, Energy, and Stone Tools.* Cambridge University Press, London

Van Devender, Thomas R., Tony L. Burgess, R.S. Felger, and Raymond M. Turner
1990 Holocene Vegetation of the Hornaday Mountains. *Proceedings of the San Diego Society of Natural History* 2:1-19.

Appendices

Appendix A:

Results of Debitage Analyses

Note on abbreviations:
Material: DR=dark rhyolite, LR= light rhyolite, GR=glassy rhyolite, BS=basalt, CCS=cryptocrystalline silica, QZ=quartzite, RED= red conglomerate rhyolite/andesite, AND=andesite, QT=quartz, GRN=green rhyolite
Aggregate analysis: Size; 1=1cm, 2=2cm, 3=3cm, 4=4cm, 5=5cm, 6=6cm, 6+= more than 6cm. Weight: classes are in grams.

Table A.1: Results of Triple Cortex Typology Analysis

Unit	Level	Material	Primary	Secondary	Interior	Total
A	Surface	DR	0	2	6	8
A	Surface	LR	1	3	16	20
A	Surface	GR	0	1	0	1
A	Surface	QZ	0	0	1	1
A	Surface	RED	1	0	0	1
B	Surface	DR	6	7	7	20
B	Surface	LR	8	9	9	26
B	Surface	GR	0	0	2	2
B	Surface	QZ	0	0	0	0
C	Surface	DR	1	8	18	27
C	Surface	LR	2	1	17	20
C	Surface	GR	0	0	3	3
C	Surface	CCS	0	0	2	2
C	Surface	QZ	1	0	1	2
C	Surface	RED	0	1	0	1
C	Surface	QT	2	1	0	3

Table A.1 (Continued): Results of Triple Cortex Typology Analysis

Unit	Level	Material	Primary	Secondary	Interior	Total
D	Surface	DR	1	5	7	13
D	Surface	LR	5	8	19	32
D	Surface	CCS	0	0	1	1
D	Surface	QZ	0	0	0	0
E	Surface	DR	2	2	3	7
E	Surface	LR	4	6	12	22
E	Surface	GR	1	0	0	1
E	Surface	CCS	0	1	0	1
F	Surface	DR	0	0	1	1
F	Surface	LR	2	1	9	12
F	Surface	BS	0	2	1	3
F	Surface	QZ	1	0	0	1
G	Surface	DR	1	1	6	8
G	Surface	LR	5	2	9	16
G	Surface	BS	0	0	3	3
H	Surface	DR	0	4	7	11
H	Surface	LR	5	5	6	16
H	Surface	GR	0	0	2	2
H	Surface	CCS	0	1	0	1
H	Surface	QZ	0	0	3	3
H	Surface	GNR	0	0	1	1
H	1	DR	4	3	14	21
H	1	LR	7	14	31	52
H	1	BS	0	0	0	0
H	1	CCS	0	1	1	2
H	1	RED	0	1		1
H	1	QZ	1	0	4	5
H	2	DR	0	3	8	11

Table A.1 (Continued): Results of Triple Cortex Typology Analysis

Unit	Level	Material	Primary	Secondary	Interior	Total
H	2	LR	3	0	4	7
H	2	GR	1	0	0	1
H	2	BS	3	0	2	5
H	2	QZ	0	0	1	1
H	2	RED	0	0	1	1
H	2	AND	0	1	0	1
H	3	DR	1	1	0	2
H	3	LR	1	2	1	4
H	3	QZ	0	1	0	1
I	Surface	DR	2	1	13	16
I	Surface	LR	5	6	28	39
I	Surface	GR	0	0	1	1
I	Surface	CCS	0	1	0	1
I	Surface	QZ	0	1	5	6
I	Surface	RED	0	0	1	1
I	1	DR	5	10	3	18
I	1	LR	7	26	20	53
I	1	BS	0	3	1	4
I	1	CCS	0	1	0	1
I	1	QZ	0	3		3
I	1	QT	0	0	1	1
I	2	DR	3	3	3	9
I	2	LR	4	6	11	21
I	2	BS	1	0	2	3
I	2	CCS	1	0	2	3
I	2	QZ	0	0	0	0
I	2	RED	0	0	1	1
J	Surface	DR	2	3	9	14

Table A.1 (Continued): Results of Triple Cortex Typology Analysis

Unit	Level	Material	Primary	Secondary	Interior	Total
J	Surface	LR	1	5	10	16
J	Surface	GR	1	0	1	2
J	Surface	BS	0	0	1	1
J	Surface	CCS	0	0	1	1
J	Surface	QZ	0	1	0	1
J	1	DR	5	10	14	29
J	1	LR	6	13	45	64
J	1	BS	0	0	2	2
J	1	CCS	0	1	0	1
J	1	AND	0	0	1	1
J	1	QT	0	0	0	0
J	2	DR	0	2	18	20
J	2	LR	1	2	22	25
J	2	AND	0	0	1	1
J	2	CCS	0	0	1	1
J	2	QZ	0	0	1	1
K	Surface	DR	0	1	1	2
K	Surface	LR	4	4	14	22
K	Surface	QZ	0	0	1	1
K	Surface	QT	0	1	1	2
L	Surface	DR	0	2	3	5
L	Surface	LR	1	1	6	8
L	Surface	CCS	0	1	1	2
L	Surface	QZ	2	0	0	2
M	Surface	DR	0	1	4	5
M	Surface	LR	0	2	10	12
M	Surface	GR	0	0	1	1
M	Surface	BS	0	0	1	1

Table A.1 (Continued): Results of Triple Cortex Typology Analysis

Unit	Level	Material	Primary	Secondary	Interior	Total
M	Surface	QZ	0	1	0	1
M	1	DR	3	5	89	97
M	1	LR	5	7	69	81
M	1	GR	0	0	5	5
M	1	BS	0	2	2	4
M	1	CCS	0	1	3	4
M	1	QZ	0	5	2	7
M	1	RED	1	0	6	7
M	2	DR	0	0	5	5
M	2	LR	1	4	9	14
M	2	GR	0	0	0	0
M	2	BS	1	1	0	2
M	2	CCS	0	0	0	0
M	2	QZ	0	0	1	1
M	3	DR	0	0	3	3
M	3	LR	1	0	1	2
N	Surface	DR	1	2	10	13
N	Surface	LR	4	3	35	42
N	Surface	GR	0	0	0	0
N	Surface	BS	1	0	0	1
N	Surface	CCS	1	1	4	6
N	Surface	QZ	1	3	2	6
N	Surface	QT	0	0	2	2
N	1	DR	2	4	12	18
N	1	LR	3	12	32	47
N	1	GR	0	1	0	1
N	1	BS	2	3	2	7
N	1	CCS	0	0	2	2

Table A.1 (Continued): Results of Triple Cortex Typology Analysis

Unit	Level	Material	Primary	Secondary	Interior	Total
N	1	QZ	0	0	2	2
N	2	DR	1	1	13	15
N	2	LR	1	9	26	36
N	2	GR	0	0	4	4
N	2	CCS	0	0	1	1
N	2	QZ	0	2	2	4
O	Surface	DR	0	0	3	3
O	Surface	LR	0	1	10	11
O	Surface	QT	0	1	1	2
O	1	DR	3	6	43	52
O	1	LR	6	12	78	96
O	1	GR	0	1	1	2
O	1	BS	0	3	4	7
O	1	CCS	1	0	1	2
O	1	QZ	1	2	3	6
O	1	RED	0	1	0	1
O	2	DR	2	1	1	4
O	2	LR	0	3	13	16
O	2	CCS	0	0	1	1
O	2	QZ	0	1	1	2
O	2	RED	0	0	1	1
R	Surface	DR	4	3	10	17
R	Surface	LR	2	10	39	51
R	Surface	GR	0	0	1	1
R	Surface	BS	0	0	4	4
R	Surface	CCS	0	1	4	5
R	Surface	QZ	1	0	2	3
R	Surface	QT	1	0	0	1

Table A.1 (Continued): Results of Triple Cortex Typology Analysis

Unit	Level	Material	Primary	Secondary	Interior	Total
R	1	DR	1	11	29	41
R	1	LR	11	21	32	64
R	1	CCS	0	3	5	8
R	1	QZ	0	3	1	4
R	1	QT	0	0	1	1
R	2	DR	3	7	13	23
R	2	LR	3	12	22	37
R	2	BS	0	0	1	1
R	2	AND	0	0	1	1
R	2	RED	0	0	0	0
R	3	BS	0	1	0	1
Feature	1	DR	0	0	1	1
Feature	1	LR	0	1	1	2
Feature	1	BS	1	0	0	1

Table A.2: Results of Free-Standing Typology Analysis

Unit	Level	Material	Complete	Broken	Flake	Debris	Total Debitage	Heat Treated
A	Surface	DR	1	6	1	2	10	
A	Surface	LR	8	10	3	0	21	
A	Surface	GR	0	1	0	0	1	
A	Surface	QZ	1	0	0	1	2	
A	Surface	RED	0	1	0	0	1	
B	Surface	DR	2	9	9	3	23	
B	Surface	LR	8	4	14	0	26	
B	Surface	GR	0	0	2	0	2	

Table A.2 (Continued): Results of Free-Standing Typology Analysis

Unit	Level	Material	Complete	Broken	Flake	Debris	Total Debitage	Heat Treated
B	Surface	QZ	0	0	0	2	2	
C	Surface	DR	7	16	5	7	35	
C	Surface	LR	4	14	2	1	21	
C	Surface	GR	0	1	2	0	3	
C	Surface	CCS	1	1	0	0	2	
C	Surface	QZ	0	1	1	0	2	
C	Surface	RED	0	1	0	0	1	
C	Surface	QT	0	2	1	1	4	
D	Surface	DR	7	5	1	2	15	
D	Surface	LR	10	7	13	5	35	
D	Surface	CCS	0	0	1	0	1	
D	Surface	QZ	0	0	0	1	1	
E	Surface	DR	0	4	3	0	7	
E	Surface	LR	7	6	9	1	23	
E	Surface	GR	1	0	0	0	1	
E	Surface	CCS	0	0	1	0	1	
F	Surface	DR	0	0	0	0	0	
F	Surface	LR	0	0	0	0	0	
F	Surface	BS	0	0	0	0	0	
F	Surface	QZ	0	0	0	0	0	
G	Surface	DR	1	4	2	0	7	
G	Surface	LR	5	7	5	1	18	
G	Surface	BS	2	0	1	0	3	
H	Surface	DR	4	4	3	0	11	
H	Surface	LR	6	7	3	0	16	
H	Surface	GR	1	0	1	0	2	
H	Surface	CCS	0	0	1	0	1	

Table A.2 (Continued): Results of Free-Standing Typology Analysis

Unit	Level	Material	Complete	Broken	Flake	Debris	Total Debitage	Heat Treated
H	Surface	QZ	1	1	1	0	3	
H	Surface	GNR	0	1	0	0	1	
H	1	DR	10	2	8	5	25	
H	1	LR	18	11	23	11	63	
H	1	BS	0	0	0	1	1	
H	1	CCS	1	1	0	0	2	
H	1	RED	0	1	0	0	1	
H	1	QZ	3	1	1	1	6	
H	2	DR	3	3	8	0	14	
H	2	LR	3	2	2	1	8	
H	2	GR	0	0	0	0	0	
H	2	BS	1	2	2	1	6	
H	2	QZ	0	0	1	0	1	
H	2	RED	0	1	0	0	1	
H	2	AND	1	0	0	0	1	
H	3	DR	0	1	5	0	6	
H	3	LR	2	1	1	0	4	
H	3	QZ	0	0	1	2	3	
I	Surface	DR	4	9	3	3	19	
I	Surface	LR	8	14	14	6	42	
I	Surface	GR	1	0	0	0	1	
I	Surface	CCS	1	0	0	0	1	
I	Surface	QZ	0	1	5	1	7	
I	Surface	RED	0	1	0	0	1	
I	1	DR	6	5	7	2	20	
I	1	LR	16	15	25	9	65	
I	1	BS	1	3	0	0	4	

Table A.2 (Continued): Results of Free-Standing Typology Analysis

Unit	Level	Material	Complete	Broken	Flake	Debris	Total Debitage	Heat Treated
I	1	CCS	0	1	0	0	1	
I	1	QZ	0	2	1	0	3	
I	1	QT	1	0	0	0	1	
I	2	DR	6	2	1	2	11	
I	2	LR	8	4	9	2	23	
I	2	BS	2	0	1	0	3	
I	2	CCS	0	1	2	0	3	
I	2	QZ	0	0	0	3	3	
I	2	RED	0	1	0	0	1	
J	Surface	DR	2	6	6	0	14	
J	Surface	LR	4	5	7	0	16	1
J	Surface	GR	0	1	1	0	2	
J	Surface	BS	1	0	0	0	1	
J	Surface	CCS	0	0	1	0	1	
J	Surface	QZ	0	1	0	0	1	
J	1	DR	5	10	14	2	31	
J	1	LR	26	18	22	1	67	2
J	1	BS	1	1	0	0	2	
J	1	CCS	1	0	0	0	1	
J	1	AND	0	1	0	0	1	
J	1	QT	0	0	0	1	1	
J	2	DR	6	10	3	1	20	
J	2	LR	6	15	4	2	27	1
J	2	AND	0	0	1	0	1	
J	2	CCS	0	0	1	0	1	
J	2	QZ	0	0	1	0	1	
K	Surface	DR	0	2	0	1	3	

Table A.2 (Continued): Results of Free-Standing Typology Analysis

Unit	Level	Material	Complete	Broken	Flake	Debris	Total Debitage	Heat Treated
K	Surface	LR	4	7	11	1	23	
K	Surface	QZ	0	1	0	0	1	
K	Surface	QT	2	0	0	1	3	
L	Surface	DR	1	1	3	0	5	
L	Surface	LR	3	2	3	0	8	
L	Surface	CCS	1	1	0	0	2	
L	Surface	QZ	2	0	0	1	3	
M	Surface	DR	0	3	2	2	7	
M	Surface	LR	3	8	1	1	13	
M	Surface	GR	0	1	0	0	1	
M	Surface	BS	0	1	0	0	1	
M	Surface	QZ	0	0	1	0	1	
M	1	DR	21	29	27	5	82	
M	1	LR	23	27	26	5	81	
M	1	GR	4	0	1	0	5	
M	1	BS	0	0	0	0	0	
M	1	CCS	0	1	3	0	4	
M	1	QZ	0	4	4	1	9	
M	1	RED	1	0	6	1	8	
M	2	DR	2	0	3	3	8	
M	2	LR	6	3	5	0	14	
M	2	GR	0	0	0	1	1	
M	2	BS	1	1	0	0	2	
M	2	CCS	0	0	0	1	1	
M	2	QZ	1	0	0	0	1	
M	3	DR	1	2	0	0	3	
M	3	LR	0	0	2	0	2	

Table A.2 (Continued): Results of Free-Standing Typology Analysis

Unit	Level	Material	Complete	Broken	Flake	Debris	Total Debitage	Heat Treated
N	Surface	DR	3	3	7	4	17	
N	Surface	LR	17	10	15	11	53	
N	Surface	GR	0	0	0	1	1	
N	Surface	BS	0	1	0	0	1	
N	Surface	CCS	2	1	0	0	3	
N	Surface	QZ	2	2	1	1	6	
N	Surface	QT	0	1	1	0	2	
N	1	DR	1	12	5	5	23	
N	1	LR	4	31	13	2	50	
N	1	GR	0	1	0	0	1	
N	1	BS	2	3	2	0	7	
N	1	CCS	0	2	0	1	3	
N	1	QZ	1	1	1	0	3	
N	2	DR	8	3	4	0	15	
N	2	LR	11	6	19	2	38	
N	2	GR	1	0	2	1	4	
N	2	CCS	1	1	0	0	2	
N	2	QZ	2	1	1	0	4	
O	Surface	DR	0	2	1	0	3	
O	Surface	LR	1	2	7	1	11	
O	Surface	QT	0	0	2	1	3	
O	1	DR	7	36	9	8	60	
O	1	LR	16	70	10	9	105	
O	1	GR	1	1	0	5	7	
O	1	BS	4	3	0	0	7	
O	1	CCS	0	1	1	1	3	
O	1	QZ	0	4	3	0	7	

Table A.2 (Continued): Results of Free-Standing Typology Analysis

Unit	Level	Material	Complete	Broken	Flake	Debris	Total Debitage	Heat Treated
O	1	RED	0	1	0	0	1	
O	2	DR	2	1	1	0	4	
O	2	LR	3	9	6	1	19	
O	2	CCS	1	0	0	0	1	
O	2	QZ	0	1	1	0	2	
O	2	RED	0	1	0	0	1	
R	Surface	DR	2	8	7	2	19	
R	Surface	LR	17	16	18	4	55	
R	Surface	GR	0	0	1	0	1	
R	Surface	BS	0	2	2	0	4	
R	Surface	CCS	3	1	1	0	5	
R	Surface	QZ	1	0	2	0	3	
R	Surface	QT	0	1	0	0	1	
R	1	DR	15	8	22	3	48	
R	1	LR	23	16	26	1	66	
R	1	CCS	3	3	3	0	9	
R	1	QZ	0	4	2	1	7	
R	1	QT	1	0	0	0	1	
R	2	DR	6	9	8	3	26	
R	2	LR	9	20	8	5	42	
R	2	BS	0	0	1	1	2	
R	2	AND	0	1	0	0	1	
R	2	RED	0	0	0	1	1	
R	3	BS	0	1	0	0	1	
Feature	1	DR	1	0	0	0	1	
Feature	1	LR	1	1	0	0	2	
Feature	1	BS	0	1	0	0	1	

Table A.3: Results of Aggregate Size Analysis

Unit	Level	Material	1	2	3	4	5	6	7	Total Debitage
A	Surface	DR	0	1	3	2	2	0	1	10
A	Surface	LR	0	3	5	5	6	2	0	21
A	Surface	GR	0	0	0	0	1	0	0	1
A	Surface	RED	0	0	1	0	0	0	0	1
B	Surface	DR	1	3	5	5	4	1	3	22
B	Surface	LR	0	2	7	4	7	5	1	26
B	Surface	GR	0	0	1	0	0	0	0	1
B	Surface	QZ	0	1	0	1	0	0	0	2
C	Surface	DR	1	5	8	11	4	3	3	35
C	Surface	LR	0	3	6	7	2	3	0	21
C	Surface	GR	0	1	1	1	0	0	0	3
C	Surface	CCS	0	0	0	2	0	0	0	2
C	Surface	QZ	0	0	1	1	0	0	0	2
C	Surface	RED	0	1	0	0	0	0	0	1
C	Surface	QT	0	1	0	3	0	0	0	4
D	Surface	DR	3	4	5	1	2	0	0	15
D	Surface	LR	0	7	8	13	7	1	1	37
D	Surface	CCS	0	1	0	0	0	0	1	2
D	Surface	QZ	0	0	1	0	0	0	0	1
E	Surface	DR	0	1	1	5	0	0	0	7
E	Surface	LR	0	2	10	6	5	0	0	23
E	Surface	GR	0	0	1	0	0	0	0	1
E	Surface	CCS	0	0	0	1	0	0	0	1
F	Surface	DR	0	0	1	2	0	1	0	4
F	Surface	LR	2	4	3	4	1	1	0	15
F	Surface	QZ	0	0	1	0	0	0	0	1

Table A.3 (Continued): Results of Aggregate Size Analysis

Unit	Level	Material	1	2	3	4	5	6	7	Total Debitage
G	Surface	DR	0	1	2	1	1	2	0	7
G	Surface	LR	0	5	5	3	3	2	1	19
G	Surface	BS	0	1	0	0	0	0	0	1
G	Surface	CCS	0	0	0	1	0	0	0	1
H	Surface	DR	0	1	4	3	3	0	0	11
H	Surface	LR	0	1	3	4	3	4	0	15
H	Surface	GR	0	1	1	0	0	0	0	2
H	Surface	CCS	0	0	1	1	0	0	0	2
H	Surface	QZ	0	1	1	1	0	0	0	3
H	Surface	GNR	0	0	1	0	0	0	0	1
H	1	DR	0	3	8	7	1	2	2	23
H	1	LR	3	9	16	18	2	1	4	53
H	1	GR	0	1	0	0	0	0	0	1
H	1	BS	0	1	0	0	0	0	0	1
H	1	CCS	0	0	1	0	0	0	1	2
H	1	QZ	1	1	3	1	0	0	0	6
H	1	RED	0	0	2	0	0	0	0	2
H	2	DR	1	2	0	4	4	1	2	14
H	2	LR	0	1	2	1	1	0	2	7
H	2	BS	0	0	2	2	0	1	1	6
H	2	RED	0	0	0	0	1	0	0	1
H	2	AND	0	0	0	0	0	1	0	1
H	3	DR	0	1	1	1	1	0	2	6
H	3	LR	0	0	1	1	1	0	1	4
H	3	QZ	0	1	1	1	0	0	0	3
I	Surface	DR	0	2	4	6	4	1	0	17

Table A.3 (Continued): Results of Aggregate Size Analysis

Unit	Level	Material	1	2	3	4	5	6	7	Total Debitage
I	Surface	GR	1	1	0	0	0	0	0	2
I	Surface	CCS	0	0	1	0	0	0	0	1
I	Surface	QZ	0	4	1	2	0	0	0	7
I	1	DR	1	1	6	2	5	2	3	20
I	1	LR	2	8	13	18	13	8	2	64
I	1	BS	0	0	0	0	2	2	0	4
I	1	CCS	1	0	0	0	0	0	0	1
I	1	QZ	0	0	1	0	0	0	0	1
I	1	RED	0	1	0	0	0	0	0	1
I	1	QT	0	1	0	0	0	1	0	2
I	2	DR	0	1	3	0	3	1	3	11
I	2	LR	0	1	3	5	8	1	3	21
I	2	GR	0	1	0	0	0	0	0	1
I	2	BS	0	0	1	0	0	0	2	3
I	2	CCS	0	0	1	1	0	0	0	2
I	2	RED	0	0	1	0	0	0	0	1
I	2	QT	0	0	1	0	0	2	0	3
J	Surface	DR	0	0	5	6	1	0	1	13
J	Surface	LR	0	0	5	2	6	1	2	16
J	Surface	GR	0	0	1	1	0	0	0	2
J	Surface	BS	0	0	1	0	0	0	0	1
J	Surface	CCS	0	0	1	0	0	0	0	1
J	Surface	QZ	0	0	0	1	0	0	0	1
J	1	DR	0	1	3	7	9	9	1	30
J	1	LR	0	6	14	20	20	6	1	67
J	1	BS	0	0	0	1	1	0	0	2

Table A.3 (Continued): Results of Aggregate Size Analysis

Unit	Level	Material	1	2	3	4	5	6	7	Total Debitage
J	1	CCS	0	0	0	1	0	0	0	1
J	1	AND	0	0	0	1	0	0	0	1
J	1	QT	0	0	0	0	0	0	1	1
J	2	DR	0	4	3	7	4	1	1	20
J	2	LR	0	4	12	8	0	2	1	27
J	2	CCS	0	1	0	0	0	0	0	1
J	2	QZ	0	1	0	0	0	0	0	1
J	2	AND	0	0	0	1	0	0	0	1
K	Surface	DR	0	0	1	0	1	1	0	3
K	Surface	LR	0	0	4	10	6	2	1	23
K	Surface	QZ	0	0	1	2	0	0	0	3
L	Surface	DR	0	0	2	1	0	2	0	5
L	Surface	LR	0	1	2	3	2	0	0	8
L	Surface	QZ	0	0	1	1	1	0	0	3
L	Surface	QT	0	0	1	0	1	0	0	2
M	Surface	DR	0	0	2	4	1	0	0	7
M	Surface	LR	0	0	6	4	1	0	1	12
M	Surface	GR	0	0	1	1	0	0	0	2
M	Surface	BS	0	0	0	1	0	0	0	1
M	Surface	QT	0	0	0	0	1	0	0	1
M	1	DR	32	22	12	6	6	4	0	82
M	1	LR	7	22	21	8	12	8	2	80
M	1	GR	4	1	0	0	0	0	0	5
M	1	BS	0	0	0	0	0	0	1	1
M	1	CCS	3	0	1	0	0	0	0	4
M	1	QZ	2	3	4	0	0	0	0	9

Table A.3 (Continued): Results of Aggregate Size Analysis

Unit	Level	Material	1	2	3	4	5	6	7	Total Debitage
M	1	RED	2	5	1	0	0	0	0	8
M	2	DR	0	3	1	1	2	1	0	8
M	2	LR	1	2	2	2	2	3	1	13
M	2	GR	0	1	0	0	0	0	0	1
M	2	BS	0	1	1	0	0	0	0	2
M	2	CCS	0	0	1	0	0	0	0	1
M	2	QT	0	1	0	0	0	0	0	1
M	3	DR	0	1	2	0	0	0	0	3
M	3	LR	0	0	0	2	0	0	0	2
N	Surface	DR	1	6	4	3	2	0	1	17
N	Surface	LR	10	9	13	9	7	2	1	51
N	Surface	GR	0	0	0	1	0	0	0	1
N	Surface	BS	0	0	0	0	0	0	1	1
N	Surface	CCS	1	2	0	2	1	0	0	6
N	Surface	QZ	0	3	2	1	0	0	0	6
N	Surface	QT	0	1	1	0	0	0	1	3
N	1	DR	0	4	5	5	5	1	3	23
N	1	LR	0	2	10	19	16	6	3	56
N	1	GR	0	0	0	0	0	1	0	1
N	1	BS	0	1	0	0	2	2	2	7
N	1	CCS	0	0	2	0	1	1	0	4
N	1	QT	0	0	3	0	0	0	0	3
N	2	DR	0	1	5	2	1	1	0	10
N	2	LR	1	9	13	7	8	0	1	39
N	2	GR	2	1	0	1	0	0	0	4
N	2	CCS	0	0	0	2	0	0	0	2

Table A.3 (Continued): Results of Aggregate Size Analysis

Unit	Level	Material	1	2	3	4	5	6	7	Total Debitage
N	2	QT	0	2	0	2	0	0	0	4
O	Surface	DR	0	0	0	1	0	1	1	3
O	Surface	LR	0	0	1	7	2	0	0	10
O	Surface	QT	0	0	1	1	1	0	0	3
O	1	DR	2	10	11	19	11	4	3	60
O	1	LR	0	13	36	24	17	8	5	103
O	1	GR	1	1	3	1	1	0	0	7
O	1	BS	0	0	2	2	2	0	1	7
O	1	CCS	0	1	1	0	1	0	0	3
O	1	QZ	2	2	2	0	0	0	1	7
O	1	RED	0	0	1	0	0	0	0	1
O	2	DR	0	0	0	3	0	0	1	4
O	2	LR	3	8	3	3	1	2	0	20
O	2	BS	0	0	0	1	0	1	1	3
O	2	CCS	0	0	1	0	0	0	0	1
O	2	QT	0	1	1	0	0	0	0	2
O	2	RED	0	1	0	0	0	0	0	1
R	Surface	DR	0	3	5	5	2	1	2	18
R	Surface	LR	6	17	13	8	6	4	0	54
R	Surface	BS	0	0	0	1	0	1	1	3
R	Surface	CCS	0	0	1	0	0	0	0	1
R	Surface	RED	0	1	0	0	0	0	0	1
R	Surface	QT	0	1	1	0	0	0	0	2
R	1	DR	4	11	11	10	5	2	3	46
R	1	LR	4	12	18	8	17	5	1	65
R	1	GR	0	1	0	0	0	0	0	1

Table A.3 (Continued): Results of Aggregate Size Analysis

Unit	Level	Material	1	2	3	4	5	6	7	Total Debitage
R	1	CCS	0	5	2	1	1	0	0	9
R	1	QZ	0	3	2	0	0	0	0	5
R	1	QT	0	1	0	0	0	0	0	1
R	2	DR	0	1	5	2	3	4	2	17
R	2	LR	1	7	4	6	11	10	10	49
R	2	AND	0	0	0	1	0	0	0	1
R	3	DR	0	0	0	0	0	0	1	1
Feature	1	DR	0	0	0	0	0	0	1	1
Feature	1	LR	0	0	0	0	1	0	1	2
Feature	1	BS	0	0	0	0	0	0	1	1

Table A.4: Results of Aggregate Weight Analysis

Unit	Level	Material	0.1-0.2 g	0.3-0.4 g	0.5-0.6 g	0.7-0.8 g	0.9-1.0 g	1.1-1.2 g	1.3-1.4 g	1.5-1.6 g	1.7-1.8 g	1.9-2.0 g	2.1+ g	Total Debitage
A	Surface	GR	0	0	0	0	0	0	0	0	0	0	1	1
A	Surface	RED	0	0	0	0	0	0	0	0	0	0	1	1
A	Surface	QZ	1	0	1	0	0	0	0	0	0	0	0	2
A	Surface	DR	0	0	0	0	0	1	0	0	0	0	9	10
A	Surface	LR	0	1	1	1	0	0	1	0	0	0	17	21
B	Surface	GR	0	0	0	0	0	0	0	0	1	0	0	1
B	Surface	QZ	0	1	0	0	0	0	0	0	0	0	1	2
B	Surface	DR	1	1	0	0	1	0	0	0	0	1	19	23
B	Surface	LR	1	0	0	0	1	0	1	1	0	1	21	26
C	Surface	RED	0	0	0	0	1	0	0	0	0	0	0	1
C	Surface	CCS	0	0	0	0	0	0	0	0	0	0	2	2
C	Surface	QZ	0	0	0	0	0	0	0	0	0	0	2	2

Table A.4 (Continued): Results of Aggregate Weight Analysis

Unit	Level	Material	0.1-0.2 g	0.3-0.4 g	0.5-0.6 g	0.7-0.8 g	0.9-1.0 g	1.1-1.2 g	1.3-1.4 g	1.5-1.6 g	1.7-1.8 g	1.9-2.0 g	2.1+ g	Total Debitage
C	Surface	GR	0	0	0	0	0	1	0	0	1	0	1	3
C	Surface	QT	0	0	0	0	1	0	0	0	0	0	3	4
C	Surface	LR	0	1	0	2	0	1	0	1	0	1	15	21
C	Surface	DR	4	1	0	1	1	1	0	0	0	0	27	35
D	Surface	CCS	0	1	0	0	0	0	0	0	0	0	2	3
D	Surface	LR	1	5	0	0	2	0	0	0	0	3	36	47
D	Surface	DR	1	1	2	2	0	0	0	0	0	0	10	16
E	Surface	GR	0	0	0	0	0	0	0	0	0	0	1	1
E	Surface	CCS	0	0	0	0	0	0	0	0	0	0	1	1
E	Surface	DR	0	0	0	0	2	0	0	0	0	0	5	7
E	Surface	LR	0	1	1	0	0	0	0	2	1	1	17	23
F	Surface	QZ	0	0	0	0	0	0	0	0	0	0	1	1
F	Surface	DR	0	0	0	0	0	0	0	0	0	0	4	4
F	Surface	LR	0	0	1	0	1	1	1	0	0	0	11	15
G	Surface	BS	0	1	0	0	0	0	0	0	0	0	0	1
G	Surface	CCS	0	0	0	0	0	0	0	0	0	0	0	1
G	Surface	DR	0	0	1	0	0	0	0	0	0	0	6	7
G	Surface	LR	3	2	1	1	0	1	1	0	0	1	9	19
H	Surface	QZ	0	0	0	0	0	0	0	1	0	0	2	3
H	Surface	GR	0	0	0	0	0	1	0	0	0	0	1	2
H	Surface	CCS	0	0	0	0	0	0	0	0	0	0	2	2
H	Surface	DR	0	0	0	1	0	0	0	0	2	0	8	11
H	Surface	GNR	0	0	0	0	0	0	0	0	0	0	1	1
H	Surface	LR	0	0	0	0	0	1	0	0	0	0	14	15
H	1	DR	0	0	0	0	1	0	0	1	1	1	18	22
H	1	LR	4	0	3	0	1	2	3	3	0	2	43	61
H	1	GR	0	0	1	0	0	0	0	0	0	0	0	1

Table A.4 (Continued): Results of Aggregate Weight Analysis

Unit	Level	Material	0.1-0.2 g	0.3-0.4 g	0.5-0.6 g	0.7-0.8 g	0.9-1.0 g	1.1-1.2 g	1.3-1.4 g	1.5-1.6 g	1.7-1.8 g	1.9-2.0 g	2.1+ g	Total Debitage
H	1	CCS	0	0	0	0	0	0	0	0	0	0	2	2
H	1	RED	0	0	0	0	0	0	0	0	0	0	2	2
H	1	BS	0	0	0	0	1	0	0	0	0	0	0	1
H	1	QZ	1	0	0	0	0	0	0	1	1	0	3	6
H	2	BS	0	0	0	0	0	0	0	0	0	0	6	6
H	2	LR	0	0	1	0	0	0	0	0	0	0	6	7
H	2	DR	1	1	0	0	0	0	0	0	1	0	10	13
H	2	QZ	0	0	0	0	0	0	0	0	0	0	1	1
H	2	RED	0	0	0	0	0	0	0	0	0	0	1	1
H	2	AND	0	0	0	0	0	0	0	0	0	0	1	1
H	3	QZ	0	0	0	0	0	0	0	0	0	0	3	3
H	3	LR	0	0	1	0	0	0	0	0	0	0	3	4
H	3	DR	0	0	1	0	0	0	0	0	0	0	5	6
I	Surface	DR	1	0	1	0	0	0	0	1	0	0	14	17
I	Surface	QZ	1	1	0	0	2	0	0	0	0	1	2	7
I	Surface	CCS	0	0	0	0	0	0	0	0	0	0	1	1
I	Surface	GR	2	0	0	0	0	0	0	0	0	0	0	2
I	Surface	LR	2	0	1	1	0	0	0	1	1	0	37	43
I	1	DR	2	0	0	0	0	1	0	0	1	0	16	20
I	1	LR	6	0	2	3	1	0	0	0	0	0	51	63
I	1	BS	0	0	0	0	0	0	0	0	0	0	4	4
I	1	QT	0	1	0	0	0	0	0	0	0	0	1	2
I	1	CCS	1	0	0	0	0	0	0	0	0	0	0	1
I	1	QZ	0	0	0	0	0	0	0	0	0	0	1	1
I	1	RED	1	0	0	0	0	0	0	0	0	0	0	1

Table A.4 (Continued): Results of Aggregate Weight Analysis

Unit	Level	Material	0.1-0.2 g	0.3-0.4 g	0.5-0.6 g	0.7-0.8 g	0.9-1.0 g	1.1-1.2 g	1.3-1.4 g	1.5-1.6 g	1.7-1.8 g	1.9-2.0 g	2.1+ g	Total Debitage
I	2	GR	1	0	0	0	0	0	0	0	0	0		1
I	2	RED	0	0	0	0	0	0	0	0	0	0	1	1
I	2	CCS	0	0	0	0	0	0	1	0	0	0	1	2
I	2	BS	0	0	0	0	0	0	0	0	0	0	3	3
I	2	QT	0	0	0	0	0	0	0	0	0	0	3	3
I	2	DR	1	0	1	0	0	0	0	0	0	0	9	11
I	2	LR	0	1	0	0	0	1	0	0	0	1	18	21
J	Surface	DR	0	0	0	0	0	0	0	2	0	1	10	13
J	Surface	LR	0	0	0	1	0	0	1	1	0	2	11	16
J	Surface	BS	0	0	0	0	0	0	0	0	0	0	1	1
J	Surface	CCS	0	0	0	0	0	0	0	0	0	0	1	1
J	Surface	QZ	0	0	0	0	0	0	0	0	0	0	1	1
J	Surface	GR	0	0	0	0	0	0	0	0	0	0	2	2
J	1	DR	0	0	0	0	0	0	1	1	1	0	27	30
J	1	LR	0	1	0	1	2	2	2	2	0	2	55	67
J	1	BS	0	0	0	0	0	0	0	0	0	0	2	2
J	1	CCS	0	0	0	0	0	0	0	0	0	0	1	1
J	1	QT	0	0	0	0	0	0	0	0	0	0	1	1
J	1	AND	0	0	0	0	0	0	0	0	0	0	1	1
J	2	CCS	1	0	0	0	0	0	0	0	0	0	0	1
J	2	QZ	0	0	0	0	0	0	1	0	0	0	0	1
J	2	AND	0	0	0	0	0	0	0	0	0	0	0	1
J	2	DR	2	0	0	1	1	0	0	0	0	0	16	20
J	2	LR	0	1	0	2	4	0	0	1	2	1	15	26
K	Surface	LR	0	0	0	0	0	0	0	0	0	1	22	23
K	Surface	QT	0	0	0	0	0	0	0	0	0	0	2	2

Table A.4 (Continued): Results of Aggregate Weight Analysis

Unit	Level	Material	0.1-0.2 g	0.3-0.4 g	0.5-0.6 g	0.7-0.8 g	0.9-1.0 g	1.1-1.2 g	1.3-1.4 g	1.5-1.6 g	1.7-1.8 g	1.9-2.0 g	2.1+ g	Total Debitage
K	Surface	DR	0	0	0	0	0	0	0	0	0	0	3	3
K	Surface	QZ	0	0	0	0	0	1	0	0	0	0	0	1
L	Surface	QT	0	0	0	0	0	0	0	1	0	0	1	2
L	Surface	QZ	0	0	0	0	0	0	0	0	0	0	3	3
L	Surface	DR	0	0	0	0	0	1	0	0	0	0	4	5
L	Surface	LR	0	0	0	1	0	0	0	0	0	1	6	8
M	Surface	BS	0	0	0	0	0	0	0	0	0	0	1	1
M	Surface	QT	0	0	0	0	0	0	0	0	0	0	1	1
M	Surface	GR	0	0	0	0	0	0	0	0	0	0	2	2
M	Surface	DR	0	0	0	0	0	0	1	0	0	1	5	7
M	Surface	LR	0	0	0	0	0	0	0	1	0	0	12	13
M	1	DR	39	6	1	3	3	1	3	0	1	1	23	81
M	1	LR	18	9	2	0	0	3	3	3	1	1	41	81
M	1	QZ	3	1	0	0	1	0	0	0	0	1	1	7
M	1	RED	5	0	1	0	1	0	0	0	0	0	1	8
M	1	CCS	3	0	0	0	0	0	0	0	0	0	1	4
M	1	GR	4	1	0	0	0	0	0	0	0	0	0	5
M	1	BS	0	0	0	0	0	0	0	0	0	0	1	1
M	2	LR	2	1	0	0	0	0	0	1	0	3	7	14
M	2	DR	3	0	0	0	0	0	0	0	0	0	5	8
M	2	GR	0	1	0	0	0	0	0	0	0	0	0	1
M	2	CCS	0	0	0	0	0	0	0	0	0	0	1	1
M	2	QT	0	1	0	0	0	0	0	0	0	0	0	1
M	2	BS	0	0	1	0	0	0	0	0	0	0	1	2
M	3	LR	0	0	0	0	0	0	0	0	0	0	2	2
M	3	DR	1	0	0	0	0	0	0	0	0	0	2	3

Table A.4 (Continued): Results of Aggregate Weight Analysis

Unit	Level	Material	0.1-0.2 g	0.3-0.4 g	0.5-0.6 g	0.7-0.8 g	0.9-1.0 g	1.1-1.2 g	1.3-1.4 g	1.5-1.6 g	1.7-1.8 g	1.9-2.0 g	2.1+ g	Total Debitage
N	Surface	GR	0	0	0	0	0	0	0	0	0	0	1	1
N	Surface	BS	0	0	0	0	0	0	0	0	0	0	1	1
N	Surface	QT	1	0	0	0	0	0	1	0	0	0	1	3
N	Surface	CCS	3	0	0	0	0	0	0	0	0	0	3	6
N	Surface	QZ	0	2	0	1	0	0	0	0	0	1	2	6
N	Surface	DR	3	1	1	0	1	1	0	0	0	2	9	18
N	Surface	LR	12	2	3	2	0	0	2	0	2	1	23	47
N	1	LR	1	0	1	0	0	0	2	0	0	2	50	56
N	1	DR	0	2	1	0	0	1	0	1	1	0	17	23
N	1	BS	0	0	0	0	0	1	0	0	0	0	6	7
N	1	CCS	0	0	0	0	0	0	0	0	0	0	4	4
N	1	GR	0	0	0	0	0	0	0	0	0	0	1	1
N	1	QT	0	0	0	0	0	0	0	0	0	0	3	3
N	2	CCS	0	0	0	0	0	0	0	0	0	0	2	2
N	2	GR	3	0	0	0	0	0	0	0	0	0	1	4
N	2	QT	2	0	0	0	0	0	0	0	0	0	2	4
N	2	DR	6	0	0	0	0	0	1	0	0	1	7	15
N	2	LR	4	2	2	3	1	0	0	1	2	1	23	39
O	Surface	DR	0	0	0	0	0	0	0	0	0	0	3	3
O	Surface	LR	0	0	0	0	0	0	0	0	0	0	10	10
O	Surface	QT	0	0	0	0	0	0	0	0	0	1	2	3
O	1	DR	4	1	4	1	1	4	1	0	0	0	44	60
O	1	LR	5	3	2	5	3	2	2	2	0	4	75	103
O	1	QZ	2	1	0	0	0	0	0	0	0	0	4	7
O	1	GR	1	0	0	0	2	0	0	0	1	0	3	7
O	1	BS	0	0	0	0	0	0	0	0	0	0	7	7
O	1	CCS	0	0	0	0	0	0	0	0	0	0	3	3

Table A.4 (Continued): Results of Aggregate Weight Analysis

Unit	Level	Material	0.1-0.2 g	0.3-0.4 g	0.5-0.6 g	0.7-0.8 g	0.9-1.0 g	1.1-1.2 g	1.3-1.4 g	1.5-1.6 g	1.7-1.8 g	1.9-2.0 g	2.1+ g	Total Debitage
O	1	RED	0	0	0	0	0	0	0	0	0	0	1	1
O	2	CCS	0	0	0	0	0	0	0	0	0	0	1	1
O	2	RED	0	1	0	0	0	0	0	0	0	0	0	1
O	2	QT	0	0	0	1	0	0	0	0	1	0	0	2
O	2	BS	0	0	0	0	0	0	0	0	0	0	3	3
O	2	DR	0	0	0	0	0	0	0	0	0	0	4	4
O	2	LR	3	1	3	0	2	1	1	1	1	0	7	20
R	Surface	GR	0	0	0	0	0	0	0	0	0	0	1	1
R	Surface	QZ	0	0	0	0	0	0	0	0	0	1	2	3
R	Surface	BS	1	1	1	0	0	0	0	0	0	0	1	4
R	Surface	QT	0	0	0	0	0	0	0	0	0	0	4	4
R	Surface	CCS	2	0	0	0	1	0	0	0	0	0	2	5
R	Surface	DR	0	0	0	1	1	1	0	0	0	1	15	19
R	Surface	LR	9	4	6	3	1	1	0	0	2	0	28	54
R	1	QZ	0	1	0	0	0	0	0	1	0	1	2	5
R	1	CCS	4	0	1	0	0	0	0	0	0	0	4	9
R	1	LR	5	1	4	1	3	1	6	1	0	1	43	65
R	1	DR	6	1	2	1	0	7	1	1	2	1	26	48
R	1	GR	0	0	0	0	1	0	0	0	0	0	0	1
R	1	QT	0	0	0	1	0	0	0	0	0	0	0	1
R	2	LR	3	1	3	1	0	0	0	0	0	0	41	49
R	2	BS	0	0	0	0	0	0	0	0	0	0	1	1
R	2	AND	0	0	0	0	0	0	0	0	0	0	1	1
R	2	DR	0	0	1	0	0	0	1	0	1	0	14	17
R	3	BS	0	0	0	0	0	0	0	0	0	0	1	1

Lithic Tool Data and Results of Analysis

Table A.5: Results of Core Analysis

Catalog Number	Unit	Level	Length	Width	Thickness	Weight	Direction	Cortex	Platform Grinding	Material
J69E-0172	A	Surface	46.4	40	32.8	51.8	multiple	5%	x	LR
J69E-0173	G	Surface	40	51.2	38	48.6	uni	50+%		LR
J69E-0174	H	Surface	42	28.7	27.7	34.4	uni	20%		LR
J69E-0175	H	1	39.9	33.5	22	26.3	uni	10%	x	LR
J69E-0176	H	1	60	50.8	41.2	99.4	uni	50+%	x	LR
J69E-0178	H	1	78	60.2	45.6	199	uni	30%	x	DR
J69E-0179	H	1	49	52.7	45	125.2	multiple	5%		DR
J69E-0180	H	1	57.4	48.4	39.3	82.7	uni	20%		LR
J69E-0181	H	2	60.9	38.4	37.8	69.7	uni	5%	x	LR
J69E-0183	H	2	54.5	50.7	25.6	91.3	uni	50+%	x	DR
J69E-0184	I	Surface	54.3	41	38	59.7	multiple	<5%		LR
J69E-0185	I	1	43.3	38	33.4	54.5	multiple	<5%	x	LR
J69E-0186	I	1	65.9	64.4	37.5	142.3	uni	50+%		QT
J69E-0187	I	2	55	38	37.5	65.2	uni	15%		DR
J69E-0189	J	1	42.2	36.8	22.4	57.4	uni	50+%	x	DR
J69E-0190	J	1	53.2	37.7	24	52	multiple	<5%	x	DR
J69E-0191	J	1	67	52.6	43	121.8	uni	50+%	x	LR
J69E-0192	J	2	52.1	29.1	28.7	43.6	uni	30%	x	LR
J69E-0193	J	2	50.2	34	35	57.2	uni	30%	x	DR
J69E-0194	M	1	50.8	42.4	46	106	multiple	30%	x	DR
J69E-0195	M	2	49.8	52	30.6	97.6	uni	10%	x	DR
J69E-0196	M	2	54.6	45.2	36	82.9	uni	50+%		LR
J69E-0197	M	2	128.8	85.1	43.3	200+	uni	<5%	x	LR
J69E-0198	N	Surface	44.6	47.4	21.6	32.9	uni	50+%	x	LR
J69E-0199	N	Surface	57.7	41.2	28.4	92.1	uni	50+%		DR

Table A.5 (Continued): Results of Core Analysis

Catalog Number	Unit	Level	Length	Width	Thickness	Weight	Direction	Cortex	Platform Grinding	Material
J69E-0200	N	Surface	50.9	37.6	25.7	46.7	uni	<5%		LR
J69E-0201	N	1	54.5	53.4	47	84.8	multiple	<5%	x	LR
J69E-0202	N	2	35.9	40	41.8	51.4	uni	<5%		LR
J69E-0203	O	1	69.2	54.9	48.8	134	uni	50+%		DR
J69E-0205	R	1	86	66.6	46	200+	uni	<5%		BS
J69E-0207	R	2	43.1	36.4	31.6	39.6	uni	10%		GR
J69E-0208	R	3	64.5	47.8	42	85.3	uni	<5%	x	GR
J69E-0209	Feature	1	50.2	47.6	35	60.1	uni	50+%		LR
J69E-0210	Feature	1	69.4	51.7	37.4	116	uni	<5%	x	RED
J69E-0211	Feature	1	25.9	25.9	19.5	18.8	uni	<5%		QZ

Table A.6: Results of Tested Pebble Analysis

Catalog Number	Unit	Level	Length	Width	Thickness	Weight	Material
J69E-0212	J	1	67.4	50.9	38.5	177.8	DR
J69E-0213	M	2	47.8	43	34.7	80.4	GR
J69E-0214	R	1	72.2	52.4	30.8	153	GR
J69E-0215	Feature	1	56.8	44.6	37.7	87.1	DR
J69E-0216	Feature	1	65	52	34.9	147.1	GR

Table A.7: Results of Groundstone Analysis

Catalog Number	Unit	Level	Length	Width	Thickness	Weight	Material	Notes
J69E-0217	B	Surface	64.9	51.6	32.4	129.9	DR	Smoothed end, Flattened, Flake Removed
J69E-0218	C	Surface	64.3	54.1	27.2	133.2	LR	Battered on opposite ends
J69E-0219	H	1	51.8	62	32.9	104.1	LR	Smoothed end, Flattened
J69E-0220	H	2	106	58	32.6	200+	LR	Smoothed end, Flattened, and Shaped
J69E-0221	H	2	72.9	59.8	40	199.8	BS	Battered corner of end, Discoloration
J69E-0247	H	2	58.1	31.6	36.2	83.3	BS	Smooth and Discolored end
J69E-0248	I	2	87.8	59.8	36.7	200	LR	Crushing on corner
J69E-0222	M	2	61.9	48.8	33.6	138.1	LR	Smoothed end, Flattened
J69E-0226	M	1	125.5	85	104	200+	BS	Smoothed surface on the face, Discoloration, Shapped
J69E-0249	M	2	74.8	38.7	31.8	115.1	LR	Crushing, Shapped on one end, Smooth shaping, Discoloration on other end
J69E-0223	N	1	66.1	39.8	32.5	106.6	GR	Battered end on one side
J69E-0246	N	1	78.7	39.2	29.9	118	LR	Discoloration, Crushing on end
J69E-0274	N	1	74.6	55.5	30	159.9	LR	Crushed on end
J69E-0244	R	2	106.3	39.7	32	169.3	DR	Crushing on opposite ends
J69E-0245	R	2	64	32.5	34.2	103.7	BS	Crushing on end
J69E-0251	R	2	76.2	43.7	32.8	134.4	LR	Edge Modification (wear)
J69E-0224	Feature	1	61.7	26	16.6	46.2	LR	Battered on end, Discoloration
J69E-0225	Feature	1	89.3	47	16.2	125.6	DR	Battered on side and on end, Bifacially utilized
J69E-0250	Feature	1	64.5	52.4	38.2	173.5	LR	Smoothed surface on end

Table A.8: Results of Uniface Analysis

Catalog Number	Unit	Level	Length	Width	Thickness	Weight	(0-90)	Matherial	Notes
J69E-0177	H	1	60.3	51.5	25.6	56.9	65-75	LR	Random patterning, grinding , thick cross section
J69E-0154	J	2	53	41.9	16.4	39.6	62-75	DR	Random patterning, grinding on broken edge
J69E-0155	R	1	64.3	17.3	11.1	13.6	75-85	CCS	Collateral patterning, slight grinding, no breakage
J69E-0206	R	2	47.4	37.6	20	29.9	45-60	LR	Collateral, thick cross section grinding

Table A.9: Results of Biface Analysis

Type	Catalog Number	Unit	Level	Length	Width	Thickness	Weight	Material	Angle	Notes
Preform1	J69E-0158	B	Surface	52.2	39	22.1	36.8	DR	45-75	grinding, break near center, cortex present
Blank	J69E-0171	F	Surface	42.5	25.5	11.4	10.4	LR	50-60	Thick cross section, collateral, broken in center
Blank	J69E-0159	I	2	52	42.4	20.5	35.7	LR	60-70	no grinding, multiple small flakes on one side
Blank	J69E-0162	M	1	54.7	30.7	14.2	22	LR	60-70	no grinding, step fractures on one side, cortex, collateral
Blank	J69E-0163	M	1	58.6	47.2	21.5	62.7	LR	75-85	no grinding, collateral
Blank	J69E-0164	M	2	47.5	31.8	19.9	20	RED	45-55	grinding, collateral
Preform 2	J69E-0165	R	1	60.2	31.5	8.6	12.6	LR	45-55	grinding, collateral, notch in center, thin cross section

Table A.10: Results of Modified Flake Analysis

Catalog Number	Unit	Level	Length	Width	Thickness	Weight	Cortex	Freestand	# of Edges	Location	T.E. Char	T.E. Disc	(0-90)	RT Dist.	Material	Comments
J69E-0111	B	S	34.4	24	8.1	7.5	T	Fragment	1	Rt Lateral	Convex	uni-marg	70	Cont	LR	
J69E-0112	E	S	38.3	34.4	17.7	29	T	Fragment	3	Rt/Lt Lat/Dis	St/CC/CC	tri-marg	45-70	Cont	LR	3 worked edges on broken piece
J69E-0113	E	S	31	37.3	14.3	15.1	S	Broken	1	Rt Prox	St	uni-marg	33	Cont	LR	
J69E-0114	G	S	66.6	42	24	53.5	P	Broken	1	Lt Lateral	St	uni-marg	60	Cont	DR	
J69E-0115	H	1	30	36.8	12.6	11.6	T	Complete	1	Distal	Concave	uni-marg	77	Cont	LR	
J69E-0116	H	1	46.8	32	11.6	15.7	P	Complete	1	Lt Lateral	St	uni-marg	38	Cluster	CCS	
J69E-0117	H	2	36.1	23	7	5.5	T	Fragment	1	Rt Lateral	Concave	uni-marg	69	Cont	DR	
J69E-0118	H	2	26.5	34.4	10	7.3	S	Fragment	1	Rt Distal	St	uni-marg	64	Cont	DR	
J69E-0141	H	2	39.1	17	9.3	5.4	T	Complete	2	Distal/Rt Lateral	CC/St	bi-marg	29/71	Cont	LR	
J69E-0142	H	1	41.2	37.5	20.3	32.1	S	Broken	1	Rt Lateral	St-CV	uni-marg	65	Cont	LR	
J69E-0143	H	2	39.7	32.2	10.7	10.5	T	Fragment	1	Lt Lateral	St	uni-marg	55	Cont	DR	
J69E-0160	H	1	65.8	31.2	13.6	22	T	Broken	1	Rt Lateral	Concave	uni-marg	67	Cont	LR	Bificially utilized
J69E-0182	H	2	37	34.2	22.4	17.4	T	Fragment	1	Lt Lateral	St	uni-marg	82	Cont	DR	
J69E-0119	I	S	36	49	19.9	25.4	T	Fragment	1	Lt Lateral	St	uni-marg	67	Cont	LR	
J69E-0120	I	2	50	28.6	16.6	13.8	T	Complete	1	Rt Lateral	St	uni-marg	79	Cont	DR	
J69E-0156	I	1	44	34.7	12.5	18.5	T	Broken	1	Proximal	Concave	uni-marg	79	Cont	LR	
J69E-0157	I	1	55.6	37.9	11.3	23.9	S	Broken	1	Distal	Concave	uni-marg	48	Cont	LR	
J69E-0188	I	2	53.2	59	21.8	69.8	P	Broken	1	Rt Lateral	St	uni-marg	65	Cont	DR	
J69E-0121	J	S	58	37.1	22.2	36.4	T	Broken	1	Lt Lateral	Concave	uni-marg	70	Cont	LR	

Table A.10 (Continued): Results of Modified Flake Analysis

Catalog Number	Unit	Level	Length	Width	Thickness	Weight	Cortex	Freestand	# of Edges	Location	T.E. Char	T.E. Disc	(0-90)	RT Dist.	Material	Comments
J69E-0122	J	1	35.6	31.2	10	10.4	S	Broken	1	Lt Lateral	Concave	uni-marg	56	Cont	CCS	
J69E-0123	J	1	42.2	61	14.2	26.5	P	Broken	1	Lt Lateral	Concave	uni-marg	64	Cont	LR	
J69E-0161	K	S	67.6	20.1	15	12.4	T	Broken	1	Rt Lateral	Concave	uni-marg	61	Cont	DR	Bificially utilized
J69E-0124	M	S	53.4	44.3	11.7	25	T	Fragment	1	Rt Lateral	Concave	uni-marg	45	Cont	DR	
J69E-0125	M	S	53	36	24	39.8	T	Fragment	1	Distal	Concave	uni-marg	55	Cont	LR	
J69E-0126	M	1	28	18	6.4	2.9	T	Fragment	1	Distal	Concave	uni-marg	64	Cont	LR	Polish on microfractures
J69E-0127	M	1	42.5	30.5	17	20.9	S	Fragment	1	Rt Lateral	Concave	uni-marg	60	Cont	LR	
J69E-0128	M	1	45	36	13	17.8	T	Broken	1	Proximal	Concave	uni-marg	62	Cont	LR	
J69E-0129	M	2	43	75	20.5	62.6	S	Fragment	1	Lt Lateral	Convex	uni-marg	72	Cont	LR	
J69E-0144	M	3	42.5	39.5	25.9	53	P	Fragment	1	Proximal	St	uni-marg	25	Cont	RED	Rounded rock w/utilized area
J69E-0130	N	S	53	50.9	17.4	37.6	T	Broken	1	Distal	Concave	uni-marg	48	Cont	DR	
J69E-0131	N	S	42.3	24	12.7	12	T	Broken	1	Distal	St	uni-marg	49	Cont	DR	
J69E-0132	N	S	24	16.5	9.4	4.3	S	Fragment	1	Rt Lateral	Concave	uni-marg	64	Cont	QZ	
J69E-0133	N	2	46.5	26	12.2	12.2	T	Fragment	2	Rt&Lt Lateral	Concave	bi-marg	47/50	Cont	LR	
J69E-0166	N	1	64.6	54.3	19	59.9	P	Fragment	1	Rt Lateral	Concave	uni-marg	60	Cont	LR	Bificially utilized
J69E-0167	N	1	57.5	42.7	26.3	57.5	S	Fragment	1	Rt Lateral	Concave	uni-marg	70	Cont	LR	Bificially utilized
J69E-0145	O	S	37	39.2	10.2	15.8	T	Fragment	1	Lt Lateral	St	uni-marg	84	Cont	LR	
J69E-0146	O	S	42.3	21.6	14.2	15.5	S	Fragment	1	Distal	Concave	uni-marg	67	Cont	LR	

Table A.10 (Continued): Results of Modified Flake Analysis

Catalog Number	Unit	Level	Length	Width	Thickness	Weight	Cortex	Freestand	# of Edges	Location	T.E. Char	T.E. Disc	(0-90)	RT Dist.	Material	Comments
J69E-0168	O	1	37.6	49.1	35.4	55.1	P	Fragment	1	Rt Distal	Concave	uni-marg	74	Cont	LR	Bificially utilized
J69E-0134	R	S	36	33.8	7.4	10.8	T	Fragment	1	Proximal	Concave	uni-marg	30	Cont	DR	
J69E-0135	R	S	33	32.8	12	7.9	T	Fragment	1	Rt Lateral	Concave	uni-marg	60	Cont	LR	
J69E-0136	R	S	32.3	55	9.6	18.6	T	Broken	2	Proximal/Rt Lateral	St	bi-marg	57/30	Cluster	LR	
J69E-0137	R	1	32.2	22	14	11.2	T	Fragment	1	Rt Lateral	Convex	uni-marg	71	Cont	LR	
J69E-0138	R	2	46.1	67	17	47.9	S	Broken	1	Rt Lateral	St	uni-marg	52	Cont	DR	
J69E-0139	R	2	27.7	10.1	5.7	1.5	T	Complete	1	Lt Lateral	St	uni-marg	57	Cont	DR	
J69E-0140	R	3	48	47	23.4	43.3	P	Fragment	1	Distal	Convex	uni-marg	53	Cont	GR	
J69E-0147	R	S	54.4	41.4	22	45.4	T	Broken	1	Rt Lateral	Concave	uni-marg	35	Cont	DR	
J69E-0148	R	S	56.8	38	16.7	24.8	S	Complete	1	Rt Lateral	St	uni-marg	72	Cont	LR	
J69E-0149	R	1	22.2	49	13.6	9.6	T	Broken	1	Lt Lateral	St	uni-marg	54	Cont	LR	
J69E-0150	R	1	33.6	21.5	7.8	4.2	T	Fragment	1	Proximal	St	uni-marg	40	Cont	LR	
J69E-0151	R	1	29	18.3	9	3.6	S	Broken	1	Lt Lateral	St	uni-marg	64	Cont	LR	
J69E-0152	R	1	30.9	58.8	12.2	17	T	Fragment	2	Proximal/Distal	CC/CV	bi-marg	61	Cont	LR	
J69E-0153	R	1	55	30.7	10.5	16.1	T	Broken	2	Rt Lateral/Proximal	St/St	bi-marg	56/52	Cont	LR	
J69E-0169	R	2	45.5	52.4	12.8	31.9	T	Broken	1	Distal	Concave	uni-marg	40	Cont	DR	Bificially utilized
J69E-0170	R	2	69.1	40.8	15.9	53.9	T	Fragment	1	Rt Distal	Concave	uni-marg	55	Cont	DR	Bificially utilized
J69E-0204	R	S	45	38	25.2	39.6	S	Broken	1	Lt Lateral	Concave	uni-marg	79	Cont	DR	

APPENDIX B

Images of formal tools found at site J69E.

Figure B.1: Uniface J69E-0154

Figure B.2: Uniface J69E-0155

Figure B.3: Uniface J69E-0177

Figure B.4: Biface Preform I J69E-0158

Figure B.5: Biface Blank J69E-0159

Figure B.6: Biface Blank J69E-0162

Figure B.7: Biface Blank J69E-0163

Figure B.8: Biface Blank J69E-0164

Figure B.9: Biface Preform II J69E-0165

Figure B.10: Biface Blank J69E-0171

Figure B.11: Metate 1

Figure B.12: Metate 2

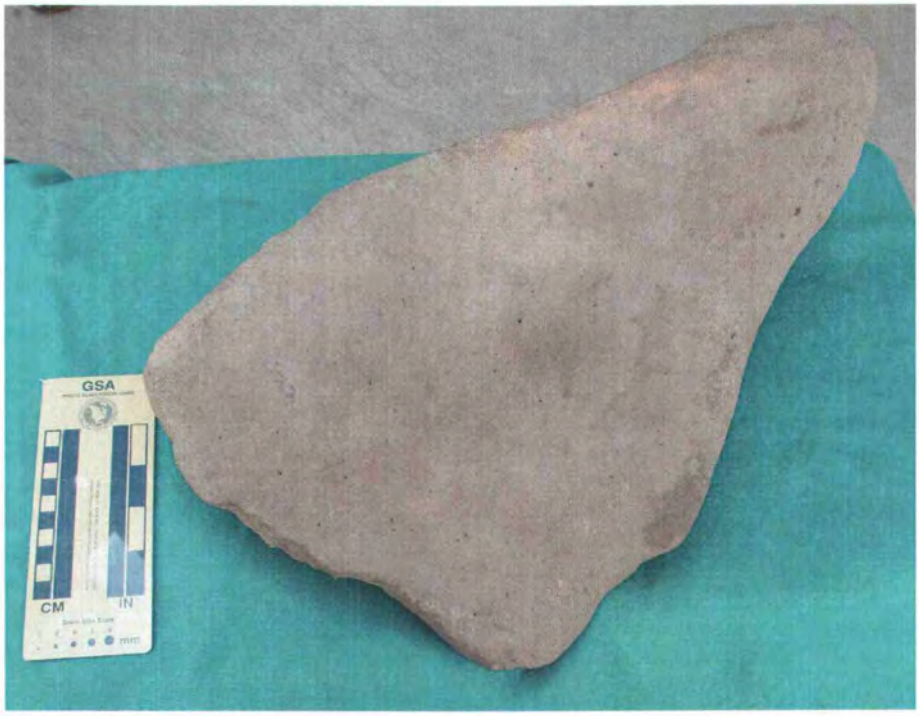

Figure B.13: Metate 3

Figure B.14: Metate 4

Figure B.15: Core J69E-0198

Figure B.16: Core J69E-0200

Figure B.17: Core J69E-0175

Figure B.18: Core J69E-0191

Figure B.19: Core J69E-0194

Figure B.20: Core J69E-0186

Figure B.21: Core J69E-0189

Figure B.22: Core J69E-0185

Figure B.23: Core J69E-0190

Figure B.24: Core J69E-0187

Figure B.25: Core J69E-0181

Figure B.26: Core J69E-0183

Figure B.27: Core J69E-0178

Figure B.28: Core J69E-0180

Figure B.29: Core J69E-0176

Figure B.30: Core J69E-0179

Figure B.31: Core J69E-0172

Figure B.32: Core J69E-0174

Figure B.33: Core J69E-0209

Figure B.34: Core J69E-0211

Figure B.35: Core J69E-0210

Figure B.36: Core J69E-0203

Figure B.37: Core J69E-0205

Figure B.38: Core J69E-0208

Figure B.39: Core J69E-0202

Figure B.40: Core J69E-0207

Figure B.41: Core J69E-0192

Figure B.42: Core J69E-0193

Figure B.43: Core J69E-0195

Figure B.44: Core J69E-0201

Figure B.45: Core J69E-0184

Figure B.46: Core J69E-0199

Figure B.47: Core J69E-0196

Figure B.48: Core J69E-0173

Figure B.49: Core J69E-0197

Figure B.50: Tested Pebble J69E-0212

Figure B.51: Tested Pebble J69E-0213

Figure B.52: Tested Pebble J69E-0214

Figure B.53: Tested Pebble J69E-0215

Figure B.54: Tested Pebble J69E-0216

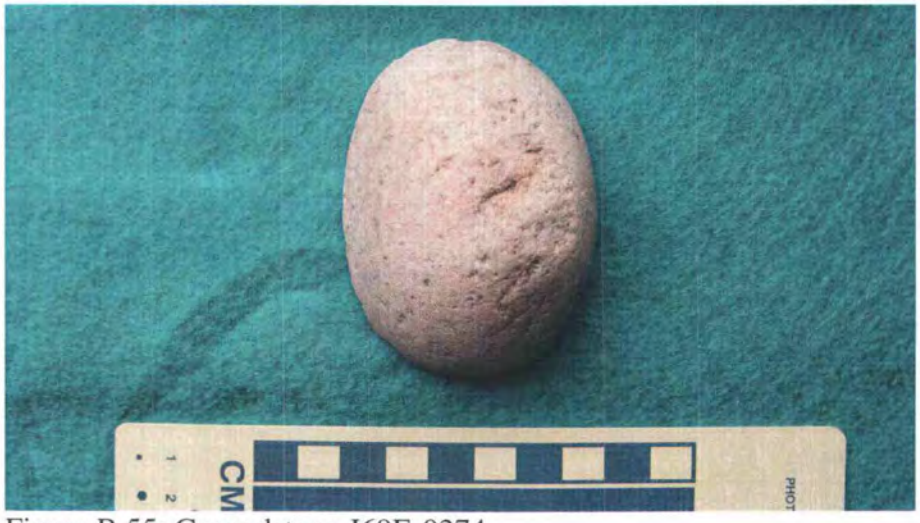

Figure B.55: Groundstone J69E-0274

Figure B.56: Groundstone J69E-0251

Figure B.57: Groundstone J69E-0250

Figure B.58: Groundstone J69E-0249

Figure B.59: Groundstone J69E-0248

Figure B.60: Groundstone J69E-0247

Figure B.61: Groundstone J69E-0245

Figure B.62: Groundstone J69E-0246

Figure B.63: Groundstone J69E-0244

Figure B.64: Groundstone J69E-0226

Figure B.65: Groundstone J69E-0225

Figure B.66: Groundstone J69E-0223